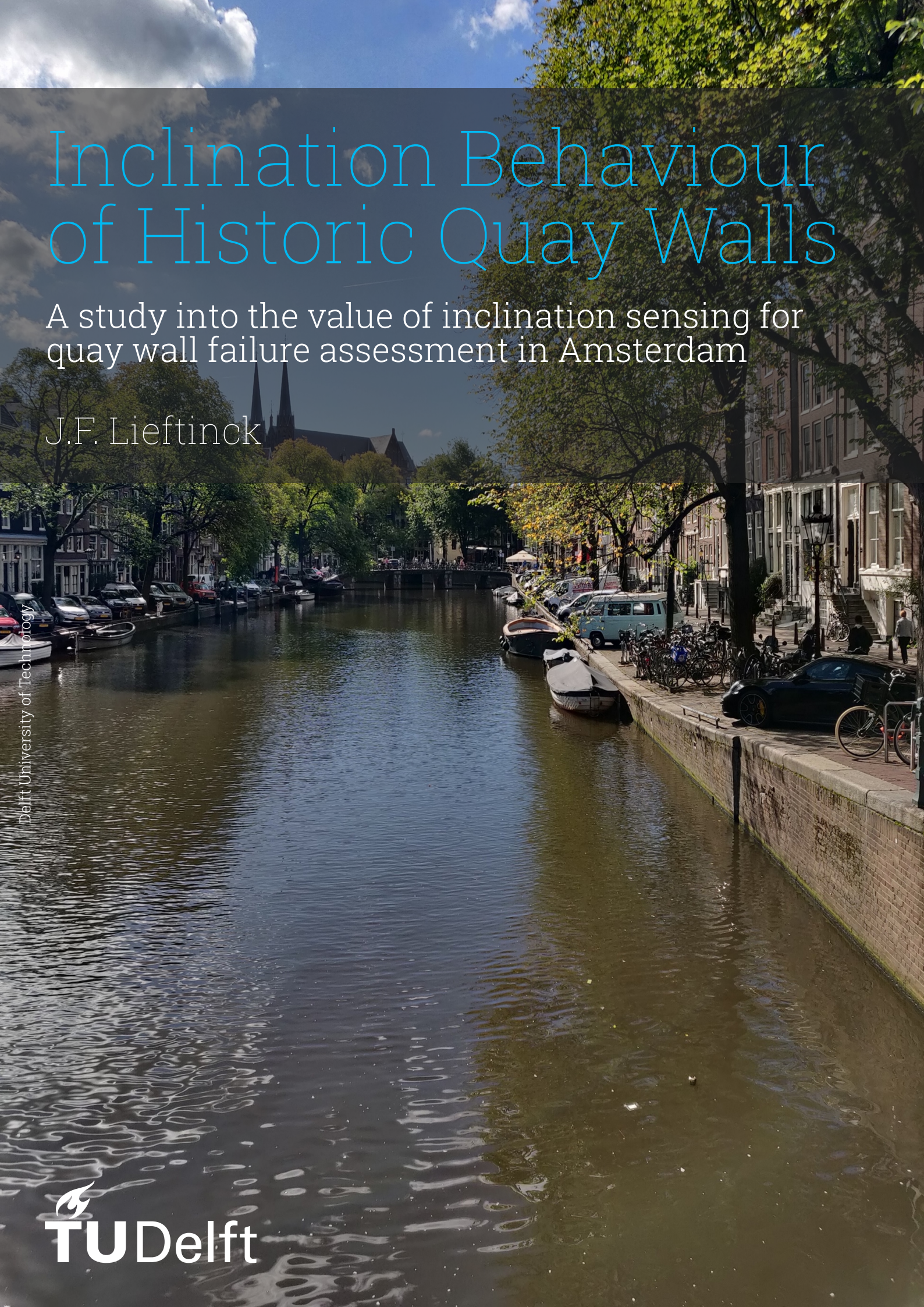

Inclination Behaviour of Historic Quay Walls

A study into the value of inclination sensing for quay wall failure assessment in Amsterdam

J.F. Lieftinck

Delft University of Technology

TU Delft

Inclination Behaviour of Historic Quay Walls

A study into the value of inclination sensing for quay wall failure assessment in Amsterdam

by

J.F. (Joris) Lieftinck

to obtain the degree of Master of Science in
Applied Earth Sciences, track Geo-Engineering
at the Delft University of Technology

Defended publicly on Thursday January 19, 2022

Student number:	4544137	
Project duration:	May 2022 - January 2023	
Thesis committee:	Dr. ir. M. (Mandy) Korff *(Chair)*	TU Delft, Geo-Engineering
	Dr. ir. C. (Cong) Mai Van,	TU Delft, Hydraulic Engineering
	Ir. B. (Bernd) Rietberg	Althen Sensors and Controls
	Ir. R. (Robbin) Wesstein	Arcadis
	Dr. ir. K. (Kamchai) Choosrithong	TU Delft, Hydraulic Engineering

An electronic version of this thesis is available at `https://repository.tudelft.nl/`
Cover image by Joris Lieftinck
Back cover image by Althen Sensors & Controls

TU Delft Delft University of Technology

ALTHEN SENSORS & CONTROLS

ARCADIS Design & Consultancy for natural and built assets

Preface

This thesis is written to conclude the master track Geo-Engineering for the study Applied Earth Sciences at the Delft University of Technology. The work has been done in cooperation with the company Althen Sensors and Controls, Arcadis, and the TU Delft.

The quay walls in Amsterdam are currently a hot topic for further research and inspection in the 'Programma Bruggen en Kademuren'. I was very excited to have found a graduation subject in geotechnical engineering related to this program in Amsterdam. As a response to the vulnerable conditions of the quay walls in Amsterdam, insight into the behaviour of the masonry quay wall tilt towards quay wall failure proves to be useful. This thesis uses PLAXIS 2D in combination with monitoring data from SmartBrick to evaluate the value of inclination sensing towards failure. This helps to detect and monitor quay wall failure indications for quicker mitigating measures. It proved useful for Althen, as a sensor company, to cooperate with Geo-Engineering and provide an explanation for the behaviour that is currently being monitored.

I am happy to have been introduced to the process and enthusiasm in Althen behind making and applying the monitoring sensors for geotechnical purposes. Additionally, the company Arcadis gave me access to their expertise in modelling quay walls in Amsterdam and I was allowed to use data and participate in the 'Programma Bruggen en Kademuren'. I am grateful for the help and discussions together with Bernd Rietberg and Robbin Wesstein as daily supervisors. They helped me to see the importance and relevance of the work that I have been doing and introduced me to the world as a geotechnical- and sales engineer in IoT.

On top of that, I would like to thank my TU supervisors Mandy Korff and Cong Mai Van for their feedback during the process meetings, their guidance during the project and for setting up the cooperation between Althen, Arcadis and the TU Delft.

Last but not least, I would like to thank my parents and family for their continuous support and care throughout my thesis and my entire study period.

J.F. (Joris) Lieftinck
Delft, January 11, 2023

Abstract

The inner-city of Amsterdam contains a large network of vulnerable, historic quay walls. Most of these quay walls consist out of masonry gravity walls placed on wooden relieving floors and wooden foundation piles. Due to the changing surface loading conditions behind the wall and the degradation of the masonry and wooden structures over the last century, the safety of the quay walls is in critical condition. Insight into the behaviour of the masonry wall tilt and its relationship with several failure mechanisms is still limited. Therefore, the objective of this thesis is to provide this insight into the behaviour of historic quay walls and the tilting they experience approaching failure in the center of Amsterdam. Additionally, the use of monitoring data from SmartBrick devices (an inclination monitoring device developed by Althen) is analyzed to assess the value of quay wall inclination monitoring.

Using PLAXIS 2D, quay wall models are made aimed to create a sensitivity analysis towards the wall tilt using multiple variations in quay structure dimensions and parameters. These variations investigate the wall height, wall thickness, floor length (and the amount of pile rows), the canal depth and the pile diameters based on a typical Amsterdam soil profile.

For the tested geometry variations, there is a linear relationship seen between the wall tilt and the horizontal wall displacement towards the canal, during the addition of the surcharge load behind the wall. The relationship between the wall tilt and the surcharge load is predominately linear at lower/realistic surface loads, at higher loads, towards failure, the wall tilt becomes exponentially larger, this is also seen by setting the varied dimensions towards failure scenarios. The most sensitive variations for inclination are the change in the masonry wall height and thickness, the pile distribution underneath the floor and the addition of a surcharge load directly behind the masonry wall.

The failure mechanism describing the horizontal displacement of the masonry wall and the piles is recognized by increasing the height of the masonry wall and by decreasing the pile diameters (pile degradation). By increasing the wall height, the quay structure also settles vertically, which in combination with the horizontal displacement, initiates wall tilt. During the addition of the surcharge load, the crossbeam (kesp) and the piles can deform, and their bending moments can exceed their bending capacity, indicating another failure mechanism with initiates wall tilt. The failure mechanism describing rotation of the masonry wall on the floor towards the canal is activated by decreasing the wall thickness and therefore decreasing its lateral capacity. This causes the masonry wall to fall over.

Damage to the foundation elements has an important impact on the tilt of the wall, due extensive axial displacements of the front pile row or cracks in the masonry wall. This could cause the wall tilt to be five times higher than predicted in the PLAXIS models over the lifespan of the structure.

To compare the SmartBrick inclination and PLAXIS inclination, it is important to know the exact degradation, erosion and loading conditions during the time between two SmartBrick measurements. The linear relation between the wall inclination and the wall displacement is useful for SmartBrick because it shows that monitoring the inclination also predicts the wall displacement and the state of the quay wall.

Pile degradation and canal erosion only give a small wall tilt increase, but a larger increase in horizontal displacement of the wall is seen. These lateral displacement changes are often in decimeters towards failure compared to the 0.1 degrees in wall inclination changes. Therefore, high measuring accuracy and resolution are necessary to monitor only the wall tilt.

To conclude, approaching quay wall failure shows that wall tilt in combination with horizontal displacement is expected, this behaviour can be monitored using SmartBrick. High wall tilt is often a first consequence of the exceedance of the bending capacities in the wooden elements.

Contents

List of Figures

List of Tables

1

Introduction

1.1. Problem definition

The municipality of Amsterdam contains roughly 600 km of quay walls under its responsibility in the city center. Most of these structures are historic quay walls older than one hundred years supported by a wooden piled foundation. During the construction and design of the quay walls, the traffic conditions consisted of light carriages and small temporary carts. Today, the quay structures have to endure an increase in heavy vehicles and permanent loads, for which they were not initially designed. Additionally, an increase in groundwater pumping around the subsiding polders near Amsterdam cause the wooden foundations to become susceptible to bacteria, which causes the wood to rot and degrade.

Due to these changes over the last century and also due to the lack of available, detailed archive drawings and documents, from about two hundred kilometers of the quay walls in Amsterdam the structural state, timber degradation, safety, and the amount of load it can manage is unclear. City councils avoided research into the quay walls and only conducted repairs when the walls were threatened to collapse or when it was already too late, figure 1.1.

A change in the policy regarding the bridges and quay structures caused more active monitoring, research, and risk analysis regarding quay wall deformations of the quay structures and bridges in Amsterdam and imposed more traffic restrictions, de Cleen (2021). This resulted in the municipality of Amsterdam initiating the program 'Aanpak bruggen en kademuren' (Gemeente Amsterdam, 2020) to monitor and assess the quay walls and bridges and maintain a safe and accessible inner-city, Jaeger (2020). This program raised more awareness to the need for more information about the soil, foundations, and the entire quay structure, which can give insight into the current state of the quay walls and the amount of load it can manage.

According to the municipality of Amsterdam and the TU Delft, the insight into historic quay wall failure mechanisms is still limited. Some failure mechanisms start with tilting and horizontal movement of the masonry quay wall, which could therefore be recognized before the full failure occurs. This horizontal displacement and tilt/inclination (both terms will be used as synonyms in this research) can already be seen in some quay walls, figure 1.1. It is still unclear how much inclination occurs during various failure mechanisms of these inner-city quay walls. Therefore, monitoring could be helpful. Current inclination measurements are available but it is uncertain what should be done with this data and if/how it can be linked to failure. By means of a combination between active monitoring and numerical modelling it could be possible to examine which monitoring signs give insight into different failure mechanisms of quay walls, including the tilting of the wall.

(a) Extensive horizontal displacement of the quay wall at the Prinsengracht

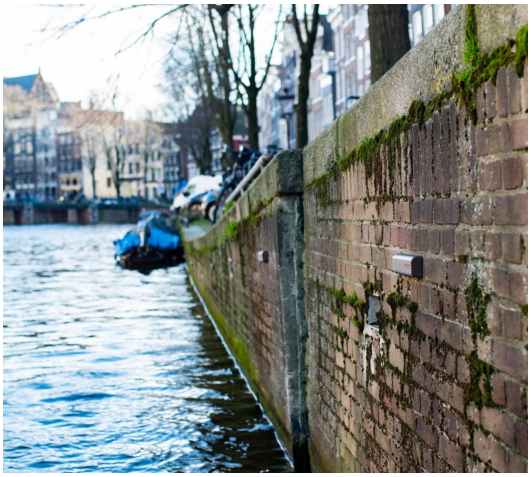

(b) Forward tilt of the quay wall at the Singel, Althen Sensors

(c) Collapsed quay wall at Grimburgwal, (Korff et al., 2022)

Figure 1.1: Critical state of quay walls in Amsterdam

In the majority of the known failure mechanisms, inclination of the quay wall should be seen, which can be monitored. To monitor this inclination in a cheap, innovative, and effective way, SmartBrick is developed by Althen Sensors and Controls. SmartBrick is a new IoT-sensor for affordable, precise monitoring for civil infrastructure. In this application, it monitors the inclination and other physical parameters of the quay walls daily, in order to describe the state of quay walls and detect early, potential failure mechanisms in combination with numerical studies. The concept of SmartBrick currently has to be validated before it can be used on a large scale. This gives potential for a two-way validation for both SmartBrick and numerical models done by means of finite element simulations.

1.2. Research objective and questions

The objective of this thesis is to gain insight into the behaviour of the historic quay walls and the tilting they experience in the center of Amsterdam. Could the amount of tilt and the corresponding horizontal displacement of the wall be an indication for possible failure mechanisms? For the SmartBrick monitoring data it is necessary to gain insight into the value of this inclination sensing to give insight into the current state of the quay wall, to predict more unstable quay walls in the area of Amsterdam, so that quick precautionary measures can be taken.
(Note: both the word tilt and inclination are used to describe the angle of the masonry wall)

This divides the project into two sub-questions related to the main question. The first part aims to answer the numerical modelling elements for quay walls and the second parts discusses the added value of inclination monitoring. From this objective the following main research question is defined:

What is the relationship between the tilt of the masonry quay wall and the state of the quay wall structure approaching failure?

To answer this main research question, the following sub-questions are discussed:

1. How can the link between quay wall tilt and failure mechanisms be predicted in finite element modelling as seen in Amsterdam's city center?
    - What are typical quay wall geometries in Amsterdam that are sensitive to wall inclination?
    - What is the displacement pattern of the front quay wall before failure?
2. To what extent is inclination monitoring using SmartBrick able to give insight and recommendations to predict the state of the quay wall?
    - How should the finite element model results be interpreted as a tool to proof the concept of inclination sensing in SmartBrick as an indication for further inspection?
    - What is the uncertainty of inclination monitoring with SmartBrick?

1.3. Research method

In this study the finite element software PLAXIS 2D will be used for the numerical simulations. The SmartBrick monitoring data is used at Althen using their expertise and online dashboard. The PLAXIS 2D simulations are based on a sensitivity analysis for typical quay wall geometries, soil information and the environment in the Amsterdam city center. The quay wall models will be compared with an actual case study quay wall and available SmartBrick inclination data on existing quay walls. It is valuable for numerical models to be validated to obtain an accurate representation of the reality, and for the SmartBrick data it is necessary to gain insight into which failure mechanisms can be accurately measured by the inclination data. An overview of the research structure and objective is shown in figure 1.2.

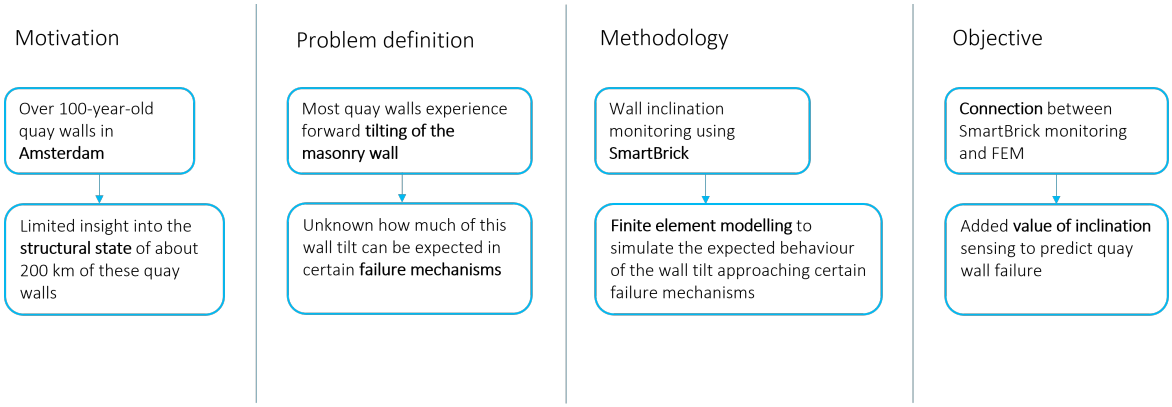

Figure 1.2: Objective flow diagram

1.3.1. Scope and Limitations

This study is mainly focused on masonry brick quay walls and soil conditions in the center of Amsterdam, this is the location where currently the SmartBrick monitoring sensors are placed. The results of this project will therefore mainly be applicable for masonry gravity walls with a relieving platform and foundation piles.

To perform a numerical analysis, information about the behaviour of the structures needs to be known. The quay walls consist out of masonry bricks, which react differently to displacement than concrete L-walls. Other factors that play a role in making a realistic model are knowledge about the geometry of the quay wall structure, the subsurface and structural properties. Modelling always aims to be as close to reality as possible but is not feasible to include every detail in practical numerical models projects, therefore some simplifications and assumptions have to be made about, for example, the material models, material parameters and the soil-structure interactions (Ma et al., 2006).

1.3.2. Research flow diagram

The approach to answering the main- and sub-questions is elaborated by the following chapter overview. The report consists out of four main parts. In the first part the theoretical framework and background knowledge for quay wall modelling is explained by a literature analysis. Thereafter, the setup of the PLAXIS 2D model with the used soil and structural parameters is elaborated, followed by the methodology for answering the research questions. Next, the application of the PLAXIS simulations is shown, and the results of different cases are presented in a sensitivity analysis for both the monitoring data and PLAXIS data. An extra model is made regarding a real quay wall, the case study. These results are evaluated based on their applicability for failure mechanisms in the discussion. In the conclusion, the research questions are answered related to the problem definition. This thesis lay-out is visualized in a flow diagram, figure 1.3.

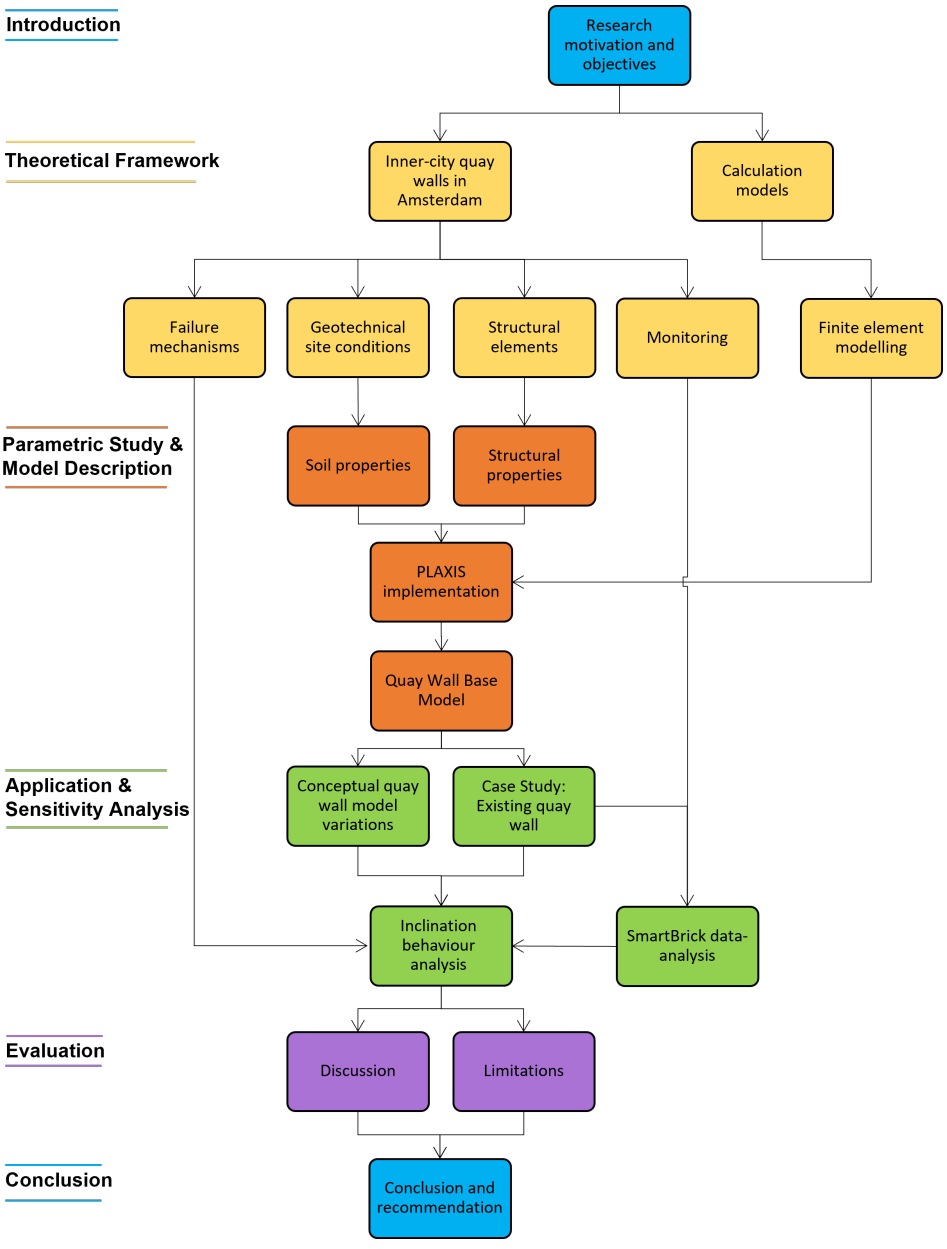

Figure 1.3: Research flow diagram

2

Theoretical Framework For Quay Wall Modelling

In this chapter the purpose and the theoretical framework for the project is described. This is done by means of a literature analysis related to the structural and geotechnical elements of quay structures, calculation methods and monitoring availability.

2.1. Quay walls in Amsterdam's city center

Amsterdam is famously known for its large, narrow network of canals within the city center contained by their quay walls. These historic, masonry quay walls can be over one hundred years old and are therefore primarily build according to past conditions and usage. In the present-day, more vehicles drive through the city center, large construction machines are located along the canals and heavier storage units are placed in top of the quay walls. This results in larger surcharge loads on the quay structure.

Additionally, the historic quay foundations are made of wooden elements, such as piles and crossbeams. These wooden elements can lose their bearing capacity and degrade over a span of one hundred years, due to varying water levels, rotting, bacteria, overloading and due to negative skin frictions (SBRCURnet, 2012). As a result of these changes over time, the state of the structural conditions of about two hundred kilometers of quay walls in Amsterdam is uncertain and needs further research or inspection. This research can be aimed towards simulations for loads and typical quay dimensions, to predict the state of the quay walls in real-life.

The quay wall structures in the city center are designed for several key functions. The main function is to retain the soil and water pressure on both sides of the wall, the retaining function. Additionally, the vertical surcharge loads, caused by permanent and variable loads such as traffic and storage, should be safely transferred from the ground level to the subsurface, the supporting, traffic, and storage function. Furthermore, the ships should be able the moor along the quay wall without causing failure, a mooring function. Lastly, the historic quay walls play a significant role in conserving the image of the city of Amsterdam and its monumental value, the surrounding function.

Over the years, four main types of quay walls have been designed to fulfill the mentioned functions of the quay walls, namely: gravity walls, sheet pile walls, structures with relieving platforms and open berth quays. An adaptation of these main types is made to distinguish four classes of quay wall structures which are present in Amsterdam, SBRCURnet (2014). These structures are divided into the following classes:

1. Gravity wall on a shallow foundation.
2. Gravity wall on pile foundations.
3. L-wall on pile foundations.
4. Steel or concrete sheet pile walls.

The most common and currently most unstable class in Amsterdam is class 2, where the gravity wall consists out of brick masonry. A typical cross section of this design in Amsterdam is shown in figure 2.1. The most important parts consist out of:

1. Masonry wall with a capstone
2. Timber foundation piles
3. Timber crossbeam
4. Wooden floor
5. Soil backfill

The more detailed properties and functions of these elements will be further discussed in section 2.5.

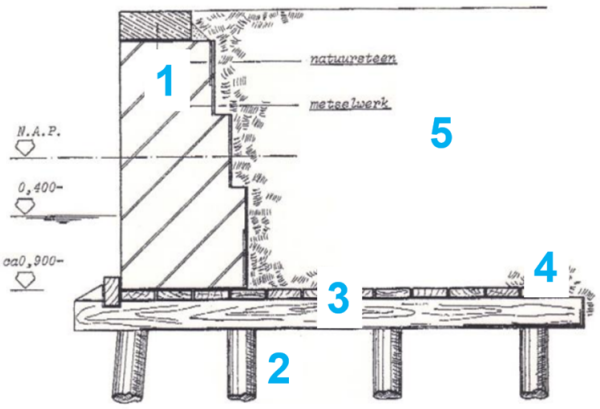

Figure 2.1: Typical quay wall in Amsterdam. (Gemeente Amsterdam, 2021c)

2.2. Failure mechanisms for quay walls

The uncertain physical state of the inner-city quay walls can over time lead to the collapse of the structure. An analysis to which factors correspond to this failure is useful to identify possible failure mechanisms of quay walls. Knowledge of the types of failure mechanisms will give insight in potential early triggers, which indicate the start of failure. As an example, in a study about the collapse of the Grimburgwal (Korff et al., 2022), the local deepening of the canal and the increase in surcharge load due to street renewal caused the wooden quay piles to break. This gives therefore one of the likely triggers to model for a failure mechanism, namely the horizontal bending of the piles. The behaviour of these failure indications can be modelled in simulations and detected using monitoring equipment.

Following the CUR211, the handbook of quay walls (SBRCURnet, 2013), the failure modes for a gravity wall on piled foundations are distinguished based on geotechnical (GEO), structural (STR) and hydraulic aspects (HYD). The municipality of Amsterdam has made ten sketches of known failure mechanisms specific for their typical masonry wall on wooden piles in 'Toetskader Amsterdamse Kademuren' (Gemeente Amsterdam, 2021c). A combination of the failure categories according to SBRCURnet (2013) and the municipality of Amsterdam is listed and shown in figure 2.2, sub listed with elements to check for its initiation:

1. Exceedance of the geotechnical bearing capacity of the structure (GEO)
    - Subsidence of weak soil
2. Horizontal displacement of the masonry wall from the crossbeam (STR)
    - Failure of the connection between the crossbeam and the wall
3. Structural failure of the masonry wall (STR)

4. Structural failure of the timber foundation piles (STR)
    - Bending moment or shear force capacity exceeded
    - Tension or compression strength exceedance (Van Tilborg, 2016)
    - Failure of entire pile rows
5. Tilting of the masonry wall (STR)
    - Positive tilt (towards the waterside) of the masonry wall and floor, also in combination with failure mode ten
6. Exceedance of the general stability (GEO)
    - Occurrence of a circular sliding plane
    - Soil heave underneath the water, failure of the passive soil wedge (Van Tilborg, 2016)
    - Negative tilt (towards the streetside) of the structure
7. Structural failure of the crossbeam (STR)
8. Failure caused by internal erosion or piping (HYD)
9. Structural failure of the floor (STR)
10. Horizontal displacement of the masonry wall and failure of the soil due to lateral pressures (GEO)
    - Extensive horizontal displacement of the floor and the masonry wall (negative displacement is towards the waterside)
    - Extensive deformation of the foundation pile
    - In combination with positive tilt, failure mode five

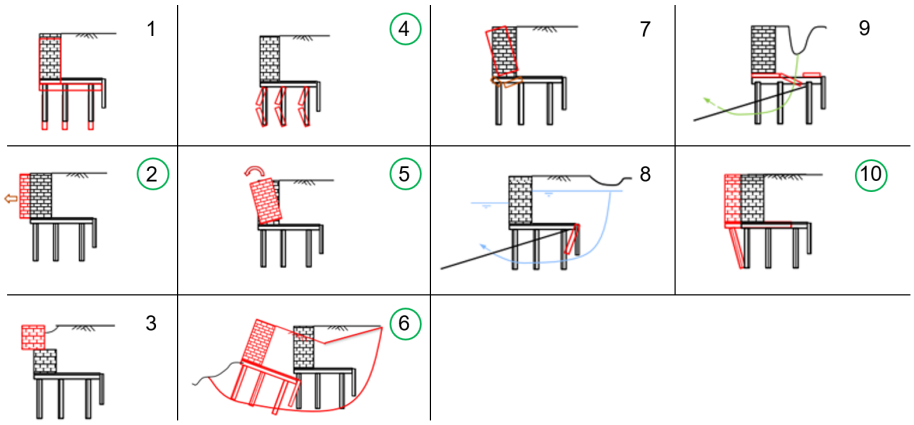

Figure 2.2: Cross-sections of typical failure mechanisms in Amsterdam. (Gemeente Amsterdam, 2021c)

In reality, multiple failure mechanisms can be active at the same time for quay wall failure. Within the framework of this project in the center of Amsterdam, a selection is made out of the ten failure mechanisms. This is done to select only the ones which are most critical to occur according to past failure reports (Kuiper et al., 2020) and are expected to experience tilt of the masonry wall as failure indication. These mechanisms are labeled with a green circle in figure 2.2 and will be analyzed through monitoring and numerical modelling in this project. Based on initial site inspections and research, van Hulten (2021), the selected failure modes are accompanied by horizontal movement of the structure towards the water side due lateral forces caused by the soil pressures.

This selection is chosen because of their relationship between failure and inclination of the wall (which can be monitored by inclination sensing), the feasibility to model the mechanism in PLAXIS 2D and current available calculation/monitoring methods to evaluate the state of these elements (which is not available for floor and retaining screen failure and for the connection between the pile and the crossbeam).

Due to the surcharge load increase over the last one hundred years in Amsterdam, more quay wall failure has occurred. Therefore, it is expected that the quay wall structure is not always able to redistribute the increase in vertical load on the surface in a safe way, namely the resulting lateral forces and axial forces. Depending on the geometry and material properties of the quay wall structure and the soil conditions, this surcharge load will be an important driving force for movement and inclination in the failure mechanisms. The other important time-dependent driving factor is the degradation of the timber elements. This can be simulated by a change in pile diameter and strength, giving larger deformations. The methodology for creating the triggers in activating a failure mechanism resulting in tilt of the wall is further discussed in section 4.

2.3. Calculation methods for quay walls

The theoretical behaviour of quay walls can be calculated using several methods with relation to the soil-structure interaction. The three main methods; analytical models, spring models and finite element modelling, are described in this section. Within the framework of this project, finite element modelling in PLAXIS 2D will be used.

2.3.1. Analytical model

The most used analytical model for retaining walls is the method of Blum (Blum, 1931). Blum uses the concept related to the beam theory, schematizing a retaining wall and surrounding soil. This gives a statically defined system and a calculation method which assumes equilibrium around the retaining wall.

The equilibrium of the retaining wall is defined by the straight failure surfaces of the active and passive zones. In the active zones the retaining wall is being pushed by the soil, and in the passive zones the soil is pushed by the structure. The acting earth pressures of both these zones are determined by Coulomb's theory. Displacement and deflection of the wall is governed by the lateral active and passive earth pressure distribution, which results in a bending moment distribution or rotation around the toe. Based on this distribution the minimum depth of soil penetration can be calculated to ensure a stable structure.

The advantages of using Blum's method is that it is easy to use, and it has been validated during 70 years of usage. It is a good method to understand the mechanics of the retaining wall and to perform fast, simple initial calculations to give a rough estimation of the penetration depth. Its disadvantages are that it does not give realistic or accurate predictions of the displacement and deformations. The effect of the construction phases is not taken into account and there is no solution for more than two anchors. Therefore, it is not typically used for the final design. With the use of more sophisticated calculation methods, more factors could be taken into account and the designs can be further optimized.

2.3.2. Spring models

Spring supported beam methods are mainly used for simple quay walls. The model describes the soil behaviour by uncoupled (non)-linear springs. As such, piles are modelled as beams on springs, according to Winkler spring models (Hetényi and Hetbenyi, 1946). These models are based on the following formula:

$$\frac{EId^4w}{dx^4} + k(x,w) * w = f(x)$$

This formula relates the lateral deflection and position of the structure to the beam rigidity (bending stiffness), the elastic foundation or soil response (modulus of subgrade reaction and spring supports (earth springs and elastic anchors)) and external loads.

A schematization is depicted in figure 2.3. Non-linear behaviour and heterogeneous soil are modelled using the p-y curve. In this curve, p is the soil reaction per unit length and y is the pile-soil displacement. Each spring has its own p-y curve which depends on the soil properties, depth, and pile dimensions, Hemel et al. (2022).

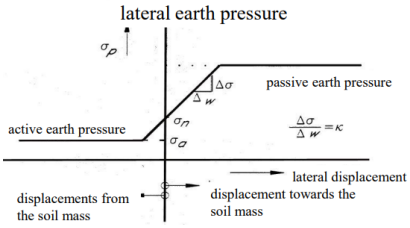

(a) Soil-Spring graph

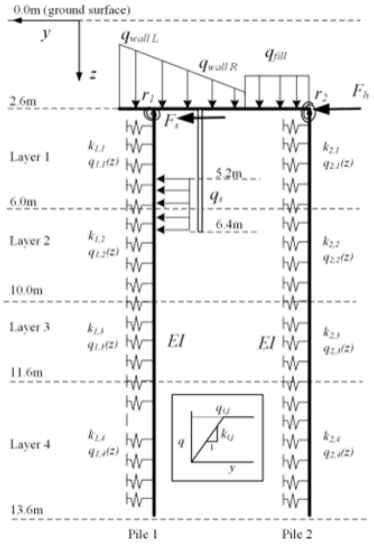

(b) Schematized spring calculation model. (Korff et al., 2021)

Figure 2.3: Spring model

The main advantages (SBRCURnet, 2013) using this method are shorter calculation times, a simple interface, well adjustable for draft designs, a fully incorporated safety approach, clear soil schematization and easily verifiable results. Moreover, it is possible to include the building phases of the structure, include multiple anchors, give the normal forces in the retaining wall and it shows a more realistic relation between the soil reaction and the pile displacement, EAU (2004). The disadvantages related to quay walls are that the method provides only a rough estimate of deformations, no surface deformation and no displacements included behind the wall, the impact of inclined surfaces and walls is overestimated or not included, only the soil-structure interaction of the front wall can be covered, undrained behaviour is usually not included, and the severe soil simplifications may give large differences in results.

2.3.3. Finite Element Modelling (FEM)

With 2D finite element modelling, more complex, coupled geometries can be modelled. It is used to investigate the combination of soil stress/strain distribution and structural elements. In the context of quay structures, it is primarily done for quay walls with relieving platforms. This method integrates complex pile-soil interaction, advanced soil behaviour, structural elements, and the stress history during installation in one model.

The soil is described by the equilibrium of the stress-strain-deformation relationship and forces, in a system of partial and ordinary differential equations. The deformation in structural elements, such as the wooden elements in a quay structure, are expressed by equations concerning their bending behaviour and axial and lateral forces. In the interface between the soil and the structural elements, the sliding behaviour can be defined. All these equations are connected, which creates a system of equations with unknown node displacement. This can be solved numerically which results in the displacement field, the stress envelope in the soil, and the bending moments and forces in the structural elements, Korff (2018).

A widely used finite element software for solving these sets of equations in geotechnical applications is PLAXIS (2D/3D). Using such software, it is therefore possible to calculate deformations and stresses in both the structural elements and geotechnical sections to solve for the global stability of the structure and soil mass.

The finite elements typically consist out of triangles or rectangles connected by corner nodes, dividing the soil mass in small sections called elements. Together, these elements create a mesh which represents the soil. The displacement of the nodes with respect to each other describes the stress/strain situation inside an element, based on the material properties. The behaviour of the soil is non-linear and can be described by choosing between constitutive models, which each define a set of soil parameters, section 3.

The results of the simulations are effected by the geometry and dimensions of the soil/structure model, the schematization of the construction stages, the constitutive models with its soil parameters and the magnitude and discretization of the mesh. A finer mesh usually gives more accurate results; however, this implies a longer calculation time.

The main advantages (SBRCURnet, 2013) by using this method are its fundamental approach, no geometry limitations, extensive soil-structure interactions of all elements, consolidation analysis, undrained/drained soil behaviour and deformation behind and in front of the retaining walls. Moreover, it is able to analyze geotechnical failure mechanisms, sectional forces in structural elements and global stability and deformations of a quay wall, Korff (2018). The results from finite element modelling are reliable and show accurate deformations of soil and the effects on piles and all stability verifications are performed in one calculation.

The disadvantages consist mainly of needing higher knowledge of the soil behaviour and verification methods and the incorporation of safety approaches is less straightforward. Also, the computation time can be long if a fine mesh, with high accuracy is adapted. Therefore, an optimal mesh size for the needed accuracy should be determined.

When comparing a PLAXIS finite element model with analytic calculation methods such as Blum (1931), bending moments and anchor forces are typically more overestimated with these analytical methods. This is due to Blum not taking the vertical arching into account and it neglects the structural rigidity of the wall and the backfilling of the soil, Roubos (2019).

The advantage of using PLAXIS 2D is that the soil displacement around the masonry wall, crossbeams/floors and the foundation piles can be calculated during the multiple construction phases of the quay structure. These objects are sensitive to the soil deformation and can be linked to the tilt of the masonry wall, which is calculated from the results, (Mourillon et al., 2017).

2.3.3.1. Embedded beam row

Using FEM in PLAXIS allows the timber foundation piles to be modelled as embedded beam rows. The embedded beam row interaction in PLAXIS 2D has been developed to model a more realistic pile-soil interaction compared to other methods such as plates or node-to-node anchors. It combines the advantages of these traditional methods by separating the pile from the soil. This allows for soil movement along and in between the pile rows and the addition of lateral soil properties, these are not simulated in node-to-node anchors. The piles are modelled as rows by using spacing factors. Embedded beam rows can only be solved with finite elements software due to their high degree of freedom.

This beam element describes infinite, equally spaced embedded pile rows out-of-plane on top of the 2D mesh, creating a 2.5D model. This means that the embedded beam is connected to the mesh but not present in the mesh. Therefore, the embedded beam rows create a simplified method to take the 3D stress state and deformation around piles into account. According to Sluis et al. (2013) and Bentley (2022), the horizontal forces along the shaft of the pile are more realistic than at the top of the pile.

In PLAXIS, the embedded beam rows create both a geometry line and the embedded pile itself. The mesh elements are generated around the geometry line, duplicated, and connected with interface elements. This connection is represented by horizontal and vertical springs to interact with the soil, as presented in figure 2.4. Pile properties can be assigned to these beams and springs, such as the stiffness, diameter, base capacity, and axial/lateral resistance values. The simulated deformation behaviour between the soil and the pile is described by the interaction between the pile stiffness, soil stiffness and the interface stiffness, Sluis et al. (2013).

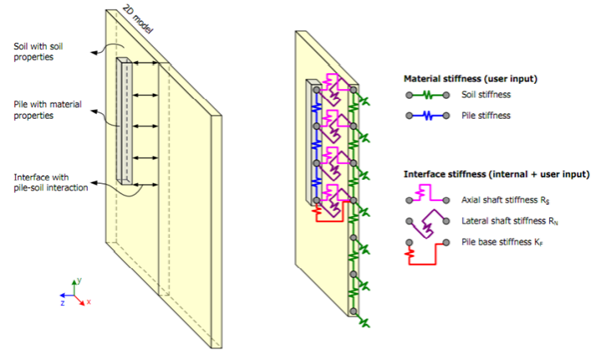

Figure 2.4: Schematization of the Embedded Beam Model. (Sluis et al., 2013)

2.4. Geotechnical site conditions in the inner-city of Amsterdam

This section describes the typical soil profile, water levels and surcharge load by use of available geotechnical measurements.

The most probable lithology classes underneath the city center of Amsterdam, according to borehole information and CPTs in DINOloket (2022a), is shown in figure 2.5 and 2.6 respectively. From this cross-section and CPT can be seen that the top part of the subsurface consist out of a fill layer, followed by a peat layer. This fill layer consists out of sand and pavement. Following the peat layer, an alternation between two clay and two sand layers is present. Based on this data, a simplified soil profile around a quay wall, near the Ceintuurbaan, is shown in figure 2.6, with the Dutch names of the layers. The detailed soil profile and parameters used for modelling is given in chapter 4.

For historic buildings and quay walls in Amsterdam, it was typical to drive the piled foundation into the first sand layer around NAP -10 meters. For modern buildings, the second sand layer, starting around NAP -20 meters is used for the piled foundations, de Gans (2011). The water level in the canals is typically NAP -0.40 meters, according to the 'Toetskader Amsterdamse Kademuren (TAK)' (Gemeente Amsterdam, 2021c). The canal depth can vary for each quay wall group, but it is usually around NAP -2.4 meters with a 1:2 slope towards the landside.

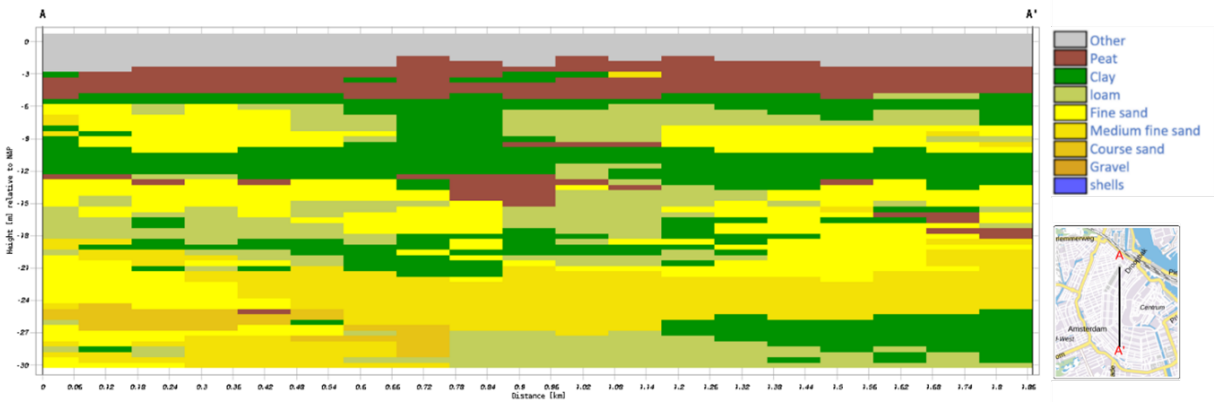

Figure 2.5: Subsurface cross-section in the center of Amsterdam. (DINOloket, 2022b)

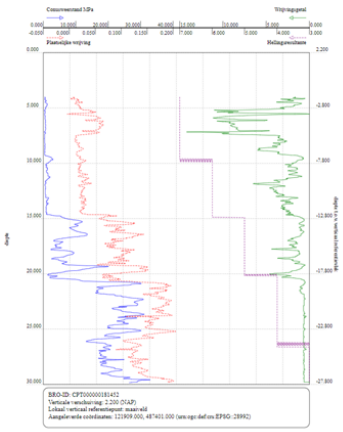

(a) CPT results within the inner-city of Amsterdam, CPT000000181452. (DINOloket, 2022a)

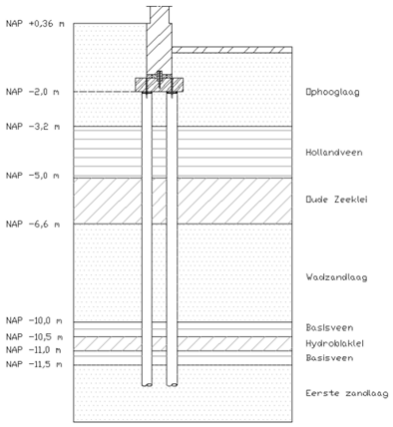

(b) Simplified soil model based on the CPT and cross-section. (Frankenmolen, 2006)

Figure 2.6: Soil lithology in Amsterdam

2.4.1. Surcharge loads

Since a quay wall is constructed near existing infrastructure, multiple surface loads on top of and near a quay wall can be present. These surcharge loads can be divided into permanent loads and variable loads. Permanent loads are the self-weight of the quay wall, ground/water loads and parking/storage loads. Variable loads could be the traffic loads and wind/tree loads, Voortman (2021).

A representative value for permanent loads (storage and parking) and variable loads (traffic loads) is between the 5-10 kPa and 10-20 kPa respectively, according to CUR166 (CURNET, 2008) and the TAK (Gemeente Amsterdam, 2021c).

2.5. Structural elements of masonry quay walls

The most critical structural elements and their function in the quay structures are discussed in this section. These elements of the structure can be divided into timber foundation elements and the brick masonry wall.

2.5.1. Masonry wall

The masonry wall consists out of stacked bricks held together by mortar. It is the most clearly visible part of the quay wall structure and will therefore give the first indication about the state of the entire structure. The main function is to retain the water and soil on both sides. Additionally, it has a structural bearing and aesthetical function, SBRCURnet (2012). The bricks typically do not degrade as much as the timber elements in the structure, but they do show more brittle behaviour. Therefore, cracks such as dilation joints can be observed over time, which result in a lack of cohesion. In the longitudinal direction, the masonry wall carries most of its own weight due to arching effects, Sas (2006). The weight of the wall is transferred through the floor and crossbeam to the foundation piles.

2.5.2. Wooden elements

The other elements of the quay wall structure are made out of wood which are most of the time fully submerged. The crossbeam (kesp) provides the connection between the piles and the rest of the structure and creates an even distribution of the forces, Sas (2006). Moreover, it gives stability during the construction phases.

The wooden foundation piles support the crossbeam and provide geotechnical bearing capacity. These piles are in longitudinal rows with a defined center-to-center distance. Usually, the number of piles in a cross section is between three to four. The piles penetrate the soil through the soil layers into a suitable deep sand layer to provide the bearing capacity. Depending on the canal depth, the piles are subjected to material degradation, therefore losing their structural capacity, such as their bending capacity.

The function of the wooden floor is to distribute the weight of the soil and the loads over the crossbeam. From quay wall inspections the dimensions and state of the floor are most of the time unknown, therefore this element is not modelled in PLAXIS, within PLAXIS the crossbeam can take over this role. The 'sloof'

(horizontal beam) in front of the masonry wall gives the wall horizontal constraint, this element has lost a lot of it structural capacity or is completely gone over the years (Jaeger, 2020), therefore this element is not taken into account in PLAXIS. If the sloof is present, it would prevent the wall from sliding into the water from the crossbeam, this can also be simulated by using a friction interface between the wall and the crossbeam.

A wooden scour protection screen is sometimes present after the first pile row or after the last pile row. From quay wall inspections this screen is often broken, allowing erosion underneath the floor and water intrusion. Moreover, the properties and connection type between this screen and the floor are uncertain, which gave reason to not model it in PLAXIS and use an eroded water gap underneath the quay floor.

2.6. Monitoring of quay structures in Amsterdam

This section gives a description of the current ways of monitoring the quay structures in Amsterdam and the reason for SmartBrick.

In the past, the deformation rate of quay walls has been determined by levelling of markings on the building facades. Over time (at least two years) this gives a time series with can predict the deformation of the structure, Venmans et al. (2020)

The municipality of Amsterdam is encouraging innovative techniques to monitor their quay walls to determine their current state. These innovations are assessed on their robustness, scalability, accuracy, reliability, convenience, and financial feasibility (Wolfert, 2019). The monitoring methods are used to evaluate which quay walls should be repaired and to determine the cause of failure. A widely used monitoring technique currently is tachymetry. With this technique, reference points in the quay structure are bored and these are measured once a month using infrared light. The data shows the movement and deformation of the quay wall in the defined x-y-z planes (Jaeger, 2020). These are manual measurements which require a lot of surveying equipment and are therefore slow and expensive.

One of the new techniques is using satellite images with InSAR data (Permanent Scatterer Interferometric Synthetic Aperture Radar), SkyGEO (2022). With this technique, large areas can be monitored for quay wall displacement over an already existing considerable time span, with millimeter accuracy. This technique is however only capable of measuring the horizontal displacement and settlement of the quay walls. A case study done by Venmans et al. (2020) showed that the deformation rate of structures using InSAR measurements are significantly higher than measurements using levelling. Moreover, the standard deviation of this deformation rate is much lower due to the higher number of satellite measurements with respect to levelling methods.

The purpose of this project is to predict the state of the quay wall by its current inclination. For most failure modes, it is still uncertain how much inclination of the quay wall occurs. The occurrence of tilting has been observed in a test location in Overamstel and several quay walls in the inner-city. This quay wall tilt can be measured in real-life using inclination sensors. Such an inclination sensor is SmartBrick (AlthenSensors, 2022) developed by Althen Sensors and Controls, and is used in this project as an addition to numerical modelling. SmartBrick is a cost effective, highly scalable, and easy to implement system for quay and bridge monitoring. An example of two SmartBricks installed on an unstable quay wall is shown in figure 2.7.

By allowing improved monitoring measurements, more insight into the quay wall limits can be set. These limits can indicate when the displacement or inclination is too much, so that safety measures have to be taken. These measures could be the closure of parking spots or traffic, removal of trees, placing an emergency structure and quay wall renewal. This means that better risk analyses can be performed, giving an overview of the unwanted events and their probability.

Figure 2.7: Installed SmartBricks around a displaced quay wall in Amsterdam

3

Modelling Methodology - Parameters Implementation

This chapter gives an overview of both the geotechnical and structural best estimate parameters needed to represent the subsurface of Amsterdam and implement them in a PLAXIS model.

3.1. Geotechnical properties

This section discusses and shows the methodology to obtain the needed soil and water properties for the study. Additionally, it will show the used best estimates parameters that will be applied in the PLAXIS model.

3.1.1. Constitutive model

As has been mentioned in section 2.3.3, the soil behaviour in PLAXIS can be described by various constitutive models. Such models consider the effect of change in stress state on the soil stiffness. A widely used model is the Mohr-Coulomb model, which is linear elastic perfectly-plastic. This model is mainly used for a first order approximation calculation, it does not take different stiffness moduli into account. To consider more moduli for different soil stress states and stiffness, the Hardening-Soil (HS) model is developed.

In this model the soil stiffness is described more accurately by using different input stiffness parameters such as E_{50}, E_{ur} and E_{oed}. In relation to the normal Harding Soil model, two additional parameters, namely the small-strain shear modulus and the strain level at which the shear modulus has reduced to seventy percent of the small-strain shear modulus are introduced in the Hardening Soil with small strain stiffness (HS-small) model, Vakili et al. (2013). Therefore, the HS-small includes increased stiffness at small strains, which results in more reliable deformations, SBRCURnet (2013). It does however not include creep and gradual softening during cycling loading. This creep can occur in the wooden foundations and in the soil since the wall deformations happens over a long time period, giving extra deformations. However, for this study the creep behaviour has been neglected. The behaviour of creep in the timber foundation has been analyzed by the work of Spannenburg (2020). Failure in the HS-small model is according to the Mohr-Coulomb criterion:

$$\tau_{max} = c' cos(\phi') + psin(\phi')$$

Using this model, results in more accurate results, but more knowledge about the conditions is needed. Stiffness parameters need extensive laboratory tests to be accurately determined. For this project, values are taken according to available literature in the study area and have been adapted to use in the HS-small model.

Figure 3.1, includes an overview of all the existing material models and their application. From this, it shows that the HS-small model is a reliable choice for retaining structures such as quay wall modelling. The HS-small model is useful for a second-order approach of soil behaviour in general and is most suitable for retaining structures. Compared to the Mohr-Coulomb model (Brinkgreve, 2021), it has better non-linear formulation of the soil behaviour, distinction between primary loading and unloading, memory of pre-consolidation stress, and it is well suited for unloading simulations in excavation, such as quay wall structures. An overview of the model parameters for the HS-small model are presented in 3.1.

Model	Foundation	Excavation	Tunnel	Embankment	Slope	Dam	Offshore	Other
Soft Soil Creep model	B	B	B	A	A	B	B	B
Soft Soil model	B	B	B	A	A	B	B	B
Jointed Rock model	B	B	B	B	B	B	B	B
Modified Cam-Clay model	C	C	C	C	C	C	C	C
NGI-ADP model	B	B	B	A	A	B	A	B
UDCAM-S model*							A	
Hoek-Brown model	B	B	B	B	B	B	B	B
Concrete model	A	A	A	A	A	A	A	A
A : The best standard model in PLAXIS for this application								
B : Reasonable modelling								
C : First order (crude) approximation								
* : UDCAM-S model for cyclic analysis, in case only undrained strength is known; UBC3D-PLM model for dynamics analysis of sandy soils involving undrained cyclic loading								
* : As an alternative PM4Sand is available as a user-defined soil model under [GSE]								

Figure 3.1: Comparison of different constitutive model applications. (PLAXIS Material Models Manual Bentley (2022))

Table 3.1: Soil parameters for the HSsmall material model. (Brinkgreve, 2019) and (SBRCURnet, 2013)

Parameter symbol	Description
E_{50}^{ref}	Secant soil stiffness for a reference stress in triaxial test
E_{oed}^{ref}	Tangent stiffness for a reference stress in oedometer test
E_{ur}^{ref}	Unloading-reloading stiffness for a reference stress
$\gamma_{0.7}$	Shear strain level at which the shear modulus has reduced to seventy percent compared to its small-strain value
G_0^{ref}	Shear stiffness at small strains
m	Rate of stress dependency in stiffness behaviour
v_{ur}	Poisson's ratio in unloading/reloading
c'	Effective cohesion
ϕ'	Effective friction angle
ψ	Dilatancy angle
γ_{sat}	Saturated soil weight
γ_{unsat}	Unsaturated soil weight
R_{int}	Interface strength ratio

3.1.2. Soil profile

Typical soil profiles for Amsterdam haves been elaborated in section 2.4. The subsurface near the Rechtboomsloot in Amsterdam, shows the most similarities for the general subsurface of Amsterdam. Therefore, this soil profile is taken as a reference (De Boer et al., 2022) and it has been adapted using parameters and layers from Frankenmolen (2006), figure 3.2. An overview of the relevant soil parameters corresponding to the HS-Small material model are given in table 3.2. The values of these soil parameters have been adapted from a study along the Noord-Zuidlijn in Amsterdam, Frankenmolen (2006), with help from Arcadis (De Boer et al., 2022) and with reference to table 2b in NEN9997 with general geotechnical soil parameters, appendix figure C.1.

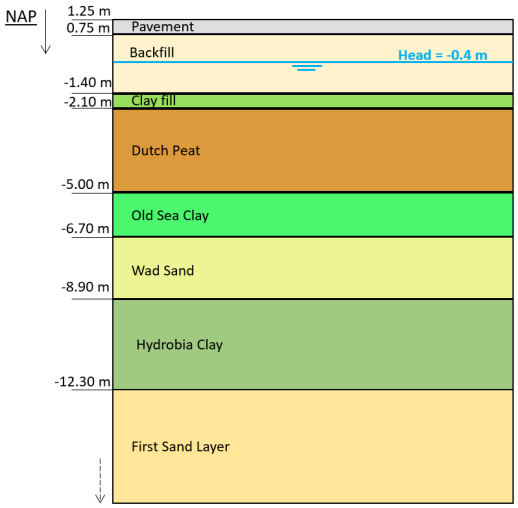

Figure 3.2: PLAXIS soil profile

Table 3.2: General soil parameters for Amsterdam

Layer	Top [m NAP]	γ_d[kN/m^3]	γ_w[kN/m^3]	c' $[kN/m^2]$	ϕ'[°]	E_{50}^{ref} $[kN/m^2]$	E_{oed}^{ref} $[kN/m^2]$	E_{ur}^{ref} $[kN/m^2]$	$\gamma_{0.7}$ [-]	G_0^{ref} $[kN/m^2]$
Pavement	1.25	18	20	0.5	32.5	20000	20000	60000	0.0001	89500
Deposited sand (backfill)	0.75	17	19	1	30	17134	15000	50000	0.0001	81000
Clay fill	-1.40	13.9	13.9	7.1	20	4284	2200	15000	0.0002	15000
Dutch peat	-2.10	10.5	10.5	3.6	18	2000	1085	7000	0.0002	7000
Old sea clay (Clay deposit)	-5.00	16.5	16.5	5	26	7500	3780	20000	0.0002	47000
Wad sand (Clayey sand)	-6.70	17.9	17.9	1.4	27	10000	5890	25000	0.0001	53500
Hydrobia clay (Sandy clay)	-8.90	15.2	15.2	5.7	27	5000	2850	10000	0.0002	33000
First sand layer	-12.30	16.6	19.7	0.1	33	35000	20000	100000	0.0001	121500

3.1.3. Ground and water level

The surface level near the inner-city canals of Amsterdam should be determined using average values in 'Actueel Hoogtebestand Nederland' (AHN, 2019). The water level in the canals is −0.4 meters below NAP, according to the TAK (Gemeente Amsterdam, 2021c). The groundwater level is around −0.35 meters below NAP and the phreatic groundwater height of the first sand layer is between the $-2.0mNAP$ and $-2.5mNAP$, this is estimated using groundwater monitoring wells, figure 3.3a and a contour map of the phreatic height in the first sand layer, figure 3.3b. The depth of the canals in Amsterdam is on average between the $-2.4mNAP$ and $-3.0mNAP$.

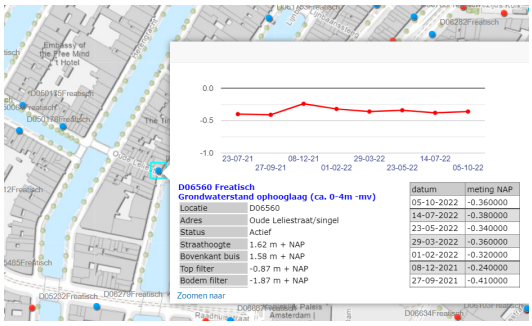

(a) Typical groundwater monitoring well in Amsterdam, Waternet (2022)

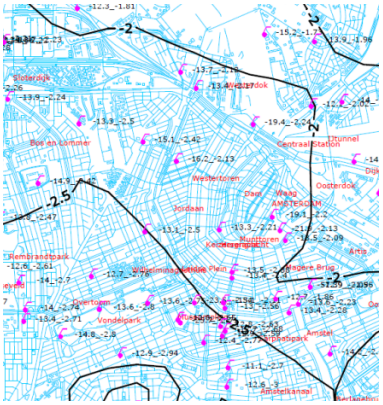

(b) Contour lines of the phreatic groundwater level of the first sand layer in Amsterdam, Waternet (2005)

Figure 3.3: Groundwater levels in Amsterdam

3.2. Structural properties

This section describes the material properties and the implementation into PLAXIS of the elements that have been used for the quay wall base model. The structural elements consist out of the masonry wall, the wooden crossbeam and wooden foundation piles, the floor/pile connection, and the interfaces. The properties of the elements have been compared with a study done concerning the Grimburgwal (Korff et al., 2022), the Overamstel (Kuiper et al., 2020), the project of Voortman (2021) and with Arcadis (De Boer et al., 2022).

3.2.1. Masonry Wall

The masonry wall is modelled as a linear elastic soil polygon with non-porous characteristics, its properties are shown in table 3.3. It is a gravity wall on piled foundations with the crossbeam acting as relieving platform. A typical height is chosen according to the average surface level and archive drawings (Gemeente Amsterdam, 1902). The corresponding thickness is estimated using the rule of thumb values provided in the TAK (Gemeente Amsterdam, 2021c) which depends on the surface level and the wall height.

Table 3.3: Parameters for the masonry wall

γ_d[kN/m^3]	Stiffness (E_m) [kN/m^2]	Height [m]	Thickness [m]	Poisson's ratio (ν) [-]	Material type	Drainage type
20.0	$8.0 * 10^6$	2.35	0.8	0.2	Linear elastic (Mohr coulomb for tension cut-off interface)	Non-porous

3.2.2. Wooden Crossbeam (Kesp)

The crossbeam is modelled as an elastic plate. The properties are shown in table 3.4. The plate has been set to elastic behaviour; this means that the bending moments can exceed the bending capacity while still being elastic. This is done to reduce to computation time and to see the full conceptual effect of the geotechnical behaviour and the maximum values before structural failure, a manual check is done to see if the bending moment is exceeded.

Table 3.4: Parameters for the crossbeam

γ[kN/m^2]	Stiffness (E_m) [kN/m^2]	Height [m]	Width [m]	Area [m^2]	Inertia [m^4]	Poisson's ratio (ν) [-]	Material type	Wood class
0.187	$11.0 * 10^6$	0.2	0.22	$5.0 * 10^{-2}$	$1.67 * 10^{-2}$	0.35	Elastic	C24

3.2.3. Wooden foundation piles

The wooden foundation piles are modelled as embedded beam rows. For the wooden piles, C24 timber is applied. This has a bending capacity of 24 N/mm^2 with a stiffness of 11000N/mm^2. The centre-to-centre spacing between the piles in the out-of-plane direction is set to 1 meter. Table 3.5 shows the material properties of the wooden piles. The figure in appendix C.2 shows the typical timber properties for different wood strengths, these values have been adapted with some modifications in discussion with Arcadis.

The wooden piles do not have a constant diameter over their length, they show a tapered form. Diving inspections regarding the pile diameter have been performed near the top of the piles. The maximum bending moment and shear forces along the pile occur above 3/4 of the pile length in the base model (De Boer et al., 2022). Therefore, an average pile diameter above this depth of the pile length has been chosen using the pile taper table, figure 3.4, of wooden piles in Amsterdam. For the same reasons as the wooden plates, the embedded beam rows have also been set to elastic behaviour.

kopdiameter	280	270	260	250	240	230	220	210	200	190	180	170	160	mm
gem. tapsheid/m bij 11 m	11,8	11,4	11,0	10,6	10,2	9,8	9,4	9,0	8,6	8,2	7,8	7,4	7,1	mm/m
gem. tapsheid/m bij 16 m	10,5	10,1	9,8	9,4	9,1	8,7	8,4	8,0	7,7	7,3	7,0	6,6	6,3	mm/m

Figure 3.4: Taper progression of wooden piles in Amsterdam. (De Boer et al., 2022)

Table 3.5: Parameters for the wooden piles (Embedded beam rows)

γ[kN/m^3]	Stiffness (E_m) [kN/m^2]	Diameter [m]	Spacing [m]	Area [m^2]	Inertia [m^4]	Poisson's ratio (ν) [-]	Material type	Wood class
4.25	$11.0 * 10^6$	0.221	1.0	$3.84 * 10^{-2}$	$1.17 * 10^{-4}$	0.35	Elastic	C24

3.2.3.1. Axial/Lateral resistance

The axial and lateral skin resistance along the pile length should be defined in the material set. The deformation of the pile depends on lateral and axial behaviour. This is governed by the resistance of the pile to the soil. As a result of axial pile deformation, soil settlement and negative skin friction can be triggered (Korff et al., 2016). Using a multi-linear resistance, a table of skin resistance is made where the shaft capacity can be related to the strength properties of the surrounding soils over the length of the pile (Wang, 2019).

Within PLAXIS, a multi-linear resistance is opted where the axial skin resistance is calculated using Koppejan's method for the part of the pile within the first sand layer. In this equation, the maximum pile shaft friction is calculated using the pile installation factor (α_s), the cone resistance (q_c) and the area of the pile tip (A_{tip}).

$$p_{shaft} = \alpha_s * q_c * A_{tip}$$

The lateral resistance is calculated over the length of the pile using Brinch-Hansen's method for the ultimate lateral capacity. This is calculated using the earth pressure coefficients (K_q and K_c), the vertical soil pressure (σ'_v) and the cohesion (c).

$$\sigma_p = K_q * \sigma'_v + K_c * c$$

The detailed calculations, with the intermediate steps, for these methods is shown in appendix C.3, based on available CPT data. For the base resistance a value of $100 kN/pile$ is applied, as recommended by the TAK (Gemeente Amsterdam, 2021c), this value is usually not reached in the PLAXIS calculations.

3.2.4. Soil-Structure Interfaces

Using interfaces between structures and the soil in the PLAXIS geometry allows to model the soil-structure interaction. This creates a transition zone which transfers the displacements and forces from the stiff structure to the weaker or stronger soil. This can be done by using a strength reduction factor for the adjacent soil or another material. The reduced interface value (Rinter) gives reduced friction (wall frictions) and interface cohesion (adhesion) compared to the friction angle and the cohesion in the adjacent soil. The interface is weaker and more flexible than the surrounding soil giving the Rinter a value less than 1.

Interfaces have been placed between:

- The masonry wall and the soil
- The masonry wall and the crossbeam
  - This introduces a tension cut-off between the wall and the wooden floor. This means that the wall is able to tilt freely from the floor, so it is not stuck to the floor.
  - Also, to ensure that the wall does not slide of the crossbeam/floor. This represents the wooden 'sloof'.
- The crossbeam and the backfill
- The crossbeam and the clay fill layer
- An extra interface, acting as a fictive soil retaining wall, is placed at the end of the floor. This is done to improve the mesh and increase the computational behaviour

3.2.5. Pile-crossbeam connection

The connection between the piles and the crossbeam is modelled as an elastic spring, with a spring constant of 400 kN m/m/rad. This stiffness corresponds to a connection between a fixed connection and a free hinge. This behaviour is often seen and recommended in quay wall calculations according to the TAK (Gemeente Amsterdam, 2021c).

4

Modelling Methodology - Quay Wall Model Description

4.1. Base model setup

This section gives a visualization of the base model in PLAXIS 2D with all the construction phases, table 4.1 and figure 4.1.

The detailed geometry of the base model in PLAXIS is shown in figure 4.2. The dimensions for this model are shown in table 4.2. The base model represents a typical cross-section for a quay wall in Amsterdam, this cross-section is based on the sketches made by the municipality of Amsterdam (figure 2.2) in the TAK (Gemeente Amsterdam, 2021c), diving inspections (Nebest Duikinspectie B.V., 2021b), Arcadis safety inspection (De Boer et al., 2022) and a combination of quay wall specifications in archive documents from the municipality of Amsterdam (Gemeente Amsterdam, 1887) (this includes specifications around, among others, the RechtBoomsloot street (Gemeente Amsterdam, 1988) and the Singel street in Amsterdam (Gemeente Amsterdam, 2021a)). Quay walls in Amsterdam have usually around three to four pile rows underneath the floor. For the base model three pile rows have been chosen to see the impact of the wall tilt better, since four piles usually give a more stable structure.

Table 4.1: Staged construction phases for the base quay wall model

Phase 0	Initial phase (K0 procedure)
Phase 1	Lowering groundwater table
Phase 2	Excavating of the building pit and canal
Phase 3-4	Installation of the piles, wall, and the crossbeam
Phase 5-6	Final backfill and rising of the (ground)water table
Phase 7	Canal erosion (dredge profile)
Phase 7.5	Degradation of the piles (only for the sensitivity analysis)
Phase 8	Activation of the surcharge loads

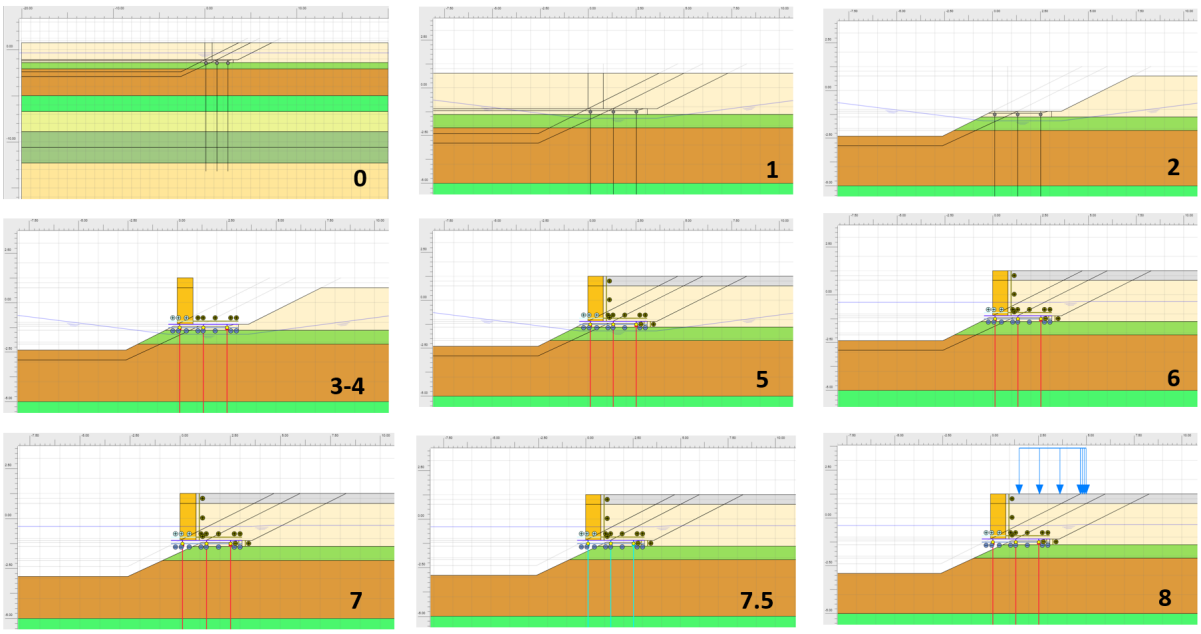

Figure 4.1: Step by step phases in PLAXIS 2D for the base quay wall model

Table 4.2: Base model geometry

Base model	
Dimension	Value
W_t (Wall thickness)	0.8 [m]
W_h (Wall height)	2.35 [m]
CB_l (Crossbeam length)	3.55 [m]
Z (Canal depth)	-2.5 [m]
P_d (Pile diameter)	0.221 [m]
Amount of piles	3 [-]
Pile spacing	1.2 [m]
Surcharge load	20 [kPa]

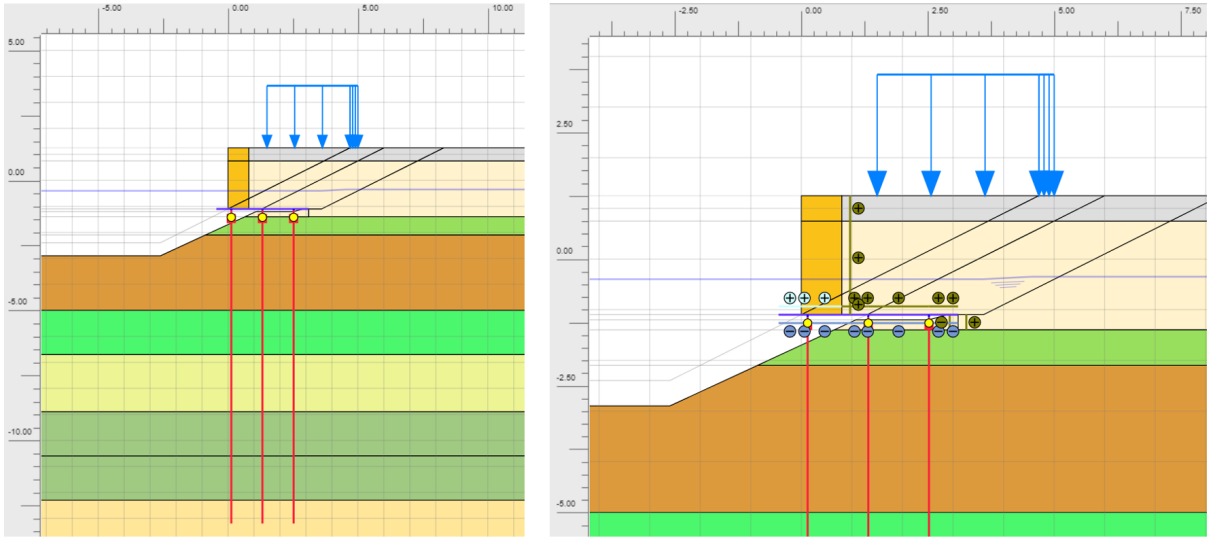

Figure 4.2: Geometry of the base model in PLAXIS

4.2. Inclination Sensitivity Setup

This section explains the sensitivity variations with respect to the base model. These geometries are chosen to simulate potential quay wall failures where high inclination or horizontal displacements occur.

4.2.1. Geometrical analysis

Figure 4.3 gives an overview of the quay structure elements for which certain dimensions can be altered. From these elements, five sensitivity analyses, table 4.3, have been made which will be modelled in PLAXIS to compare their impact towards inclination and failure. For each case, the values that are not changed are kept the same as in the base model, table 4.2. In table 4.3, a description of the cases is also briefly elaborated.

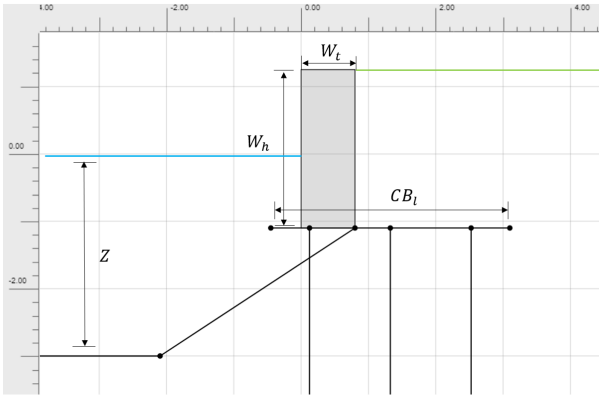

Figure 4.3: Geometry parameters to vary in the analysis

Table 4.3: Concept cases

Conceptual cases		
Case	Varied dimension	Comment
1	W_h (Wall height)	Together with the height of the sand backfill (surface level)
2	CB_l (Crossbeam length)	Together with the number of piles
3	Z (Canal depth)	The slope is kept the same
4	P_d (Pile diameter)	Diameter reduction to simulate pile degradation
5	W_t (Wall thickness)	To better analyze the tipping over of the wall and the wall height/thickness ratio

4.2.2. Surcharge load

The surcharge load is assumed to be 20 kPa at a distance between 1.5 to 5 meters behind the quay wall. This is usually the largest surcharge load near the quay wall, which therefore gives a complete picture of the potential failure mechanisms. This load is activated in the last phase of the construction. Tree loads have been ignored for this project. They could have an impact due to the wind force on the tree, causing a horizontal force on the quay wall through the roots. This wind effect is most of the time not that large due to the buildings blocking the wind. In the quay wall safety study done by Arcadis (De Boer et al., 2022) the tree loads did not have a significant impact on the wall tilt.

5

Inclination Sensitivity Analysis

This chapter gives the results of the analysis done with the base model and sensitivity models, to see the effect of the wall inclination and the relation to the failure mechanisms for each case. This is done by plotting the wall tilt against the top horizontal displacement of the quay wall and against the surcharge load development. A positive tilt means an inclination towards to canal. A negative horizontal displacement means horizontal movement towards the canal. In the discussion, chapter 8, the sensitivity analysis is compared and the underlying behaviour for the inclination is discussed.

5.1. Base model: Inclination behaviour

The base model is the start model from which all the other cases and applications in PLAXIS are built. It follows the construction phases and dimensions mentioned in section 4.1.

In figure 5.1, the relation between the wall tilt and the horizontal displacement of the top of the wall is plotted. After the construction of the quay structure (after rising the water level), the wall already experiences a small tilt and displacement. During the addition of the surcharge load behind the wall, this tilt linearly increases together with the horizontal displacement. In figure 5.1 can be seen that for high surface loads, the tilt and displacement become exponentially more.

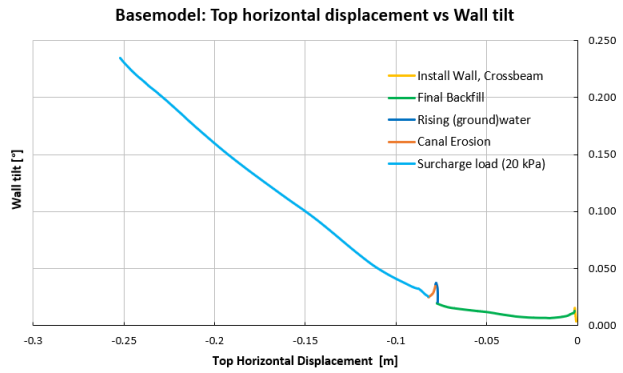

(a) Top wall horizontal displacement against the wall tilt

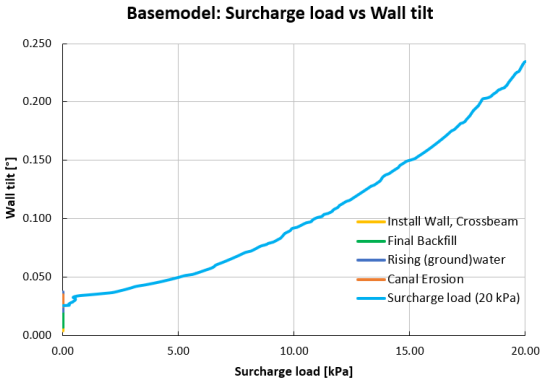

(b) Surcharge load (20 kPa) against the wall tilt

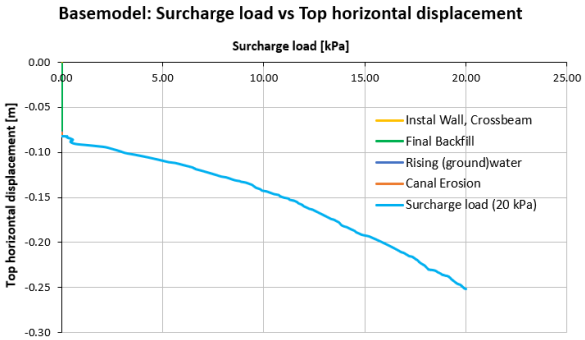

(c) Surcharge load (20 kPa) against the top wall horizontal displacement

Figure 5.1: PLAXIS output for the base model

In the base model, failure of the quay structure is not reached. This means that the displacements are still stable. In figure 5.2 can be seen that most of the displacement around the quay structure occurs behind the masonry wall and underneath the floor. The top of the piles shows the largest displacement towards the canal, which also moves the floor and the masonry wall. The floor/crossbeam bends downward (figure 5.4), this displacement is the largest underneath the masonry wall, which partially causes the wall to tilt forward, in addition to the lateral pressure behind the wall.

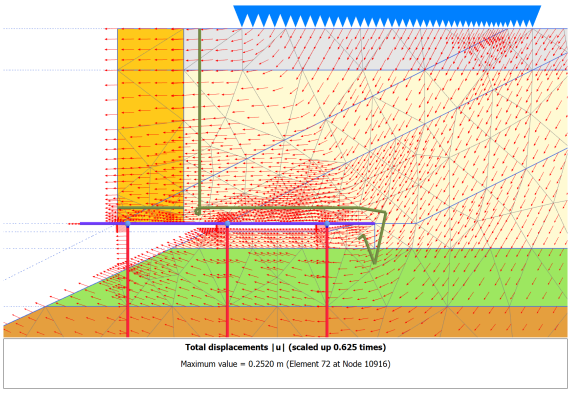

(a) Total displacement of the soil around the quay wall

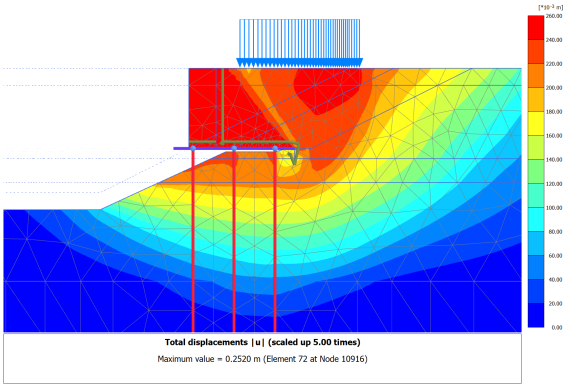

(b) Total displacement behaviour of the quay wall structure

Figure 5.2: Quay structure displacement during the final phase

The maximum value of the bending moments (figure 5.3) occur in the sea clay layer, and the minimum (negative) bending moments at the connection between the piles and the floor. This connection is not hinged; therefore, a bending moment can accumulate. The bending moment in the piles and in the crossbeam (figure 5.4) do not exceed their bending capacity, so no structural failure is expected. The more detailed effect of different connection types is shown in appendix figure A.3.

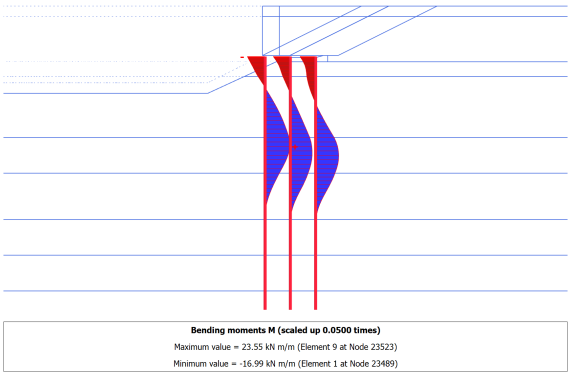

(a) Bending moment distribution during the final phase

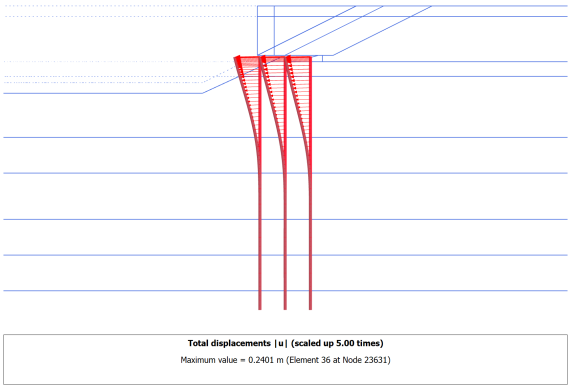

(b) Total displacement during the final phase

Figure 5.3: PLAXIS output for the foundation piles

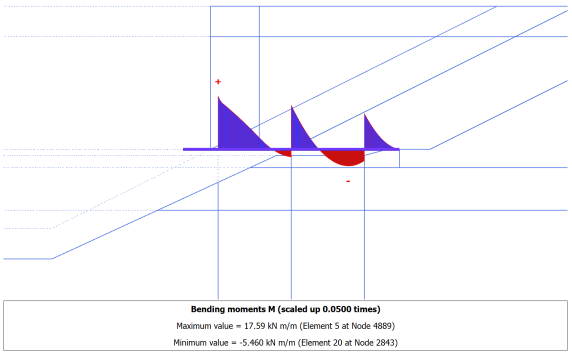

(a) Bending moment distribution during the final phase

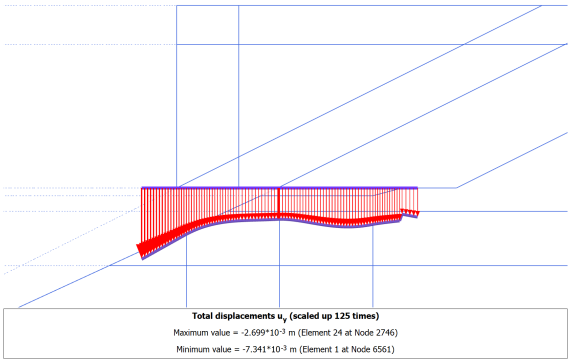

(b) Total displacement during the final phase

Figure 5.4: PLAXIS output for the crossbeam

5.2. Geometrical Variations: Inclination behaviour

The results of the analysis by generating a sensitivity cases are given in this section. These plots include the tilt of the quay wall against the horizontal displacement for multiple loads and geometries. The red points, lines and values in the tables and graphs show that failure has been reached before or at 20 kPa, which can indicate that the wall falls over.

The table for each case shows the varied dimension and if for that case the maximum bending capacity in the pile or crossbeam has been reached before the maximum surcharge load is applied, this point is also marked for some variations in the load-tilt curves (star-shaped points). The development of this bending moment in a few piles is shown in appendix figure A.4, where the amount of load active during the exceedance of the bending capacity is seen. A more detailed effect of the implementation of a maximum bending capacity (elastoplastic behaviour) is shown in figure A.5 in the appendix

For some of the sensitivity models, the results of noticeable soil and structural behaviour as seen in PLAXIS 2D is presented, which help to understand and explain the inclination behaviour. These are images such as the displacement and bending stiffness in the piles, floor, and soil body.

5.2.1. Case 1: Wall Height

The masonry wall height is increased together with the height of the soil backfill. The thickness of the wall is kept the same, resulting in a ratio between the wall height and wall thickness, table 5.1. The results for the first geometry case are shown in figure 5.5 and 5.6. The development of the bending moments in the piles for wall height 2.6 meters and 2.9 meters is shown in appendix figure A.4.

Table 5.1: Case 1: Wall height variation

Case 1: Wall height variation			
W_h (Wall height)	Ratio W_h/W_t	Pile Bending capacity reached	Crossbeam bending capacity reached
1.0 [m]	1.3 [-]	No	No
1.6 [m]	2.0 [-]	No	No
1.95[m]	2.4 [-]	No	No
2.35 [m]	2.9 [-]	No	No
2.6 [m]	3.3 [-]	Yes	No
2.9 [m]	3.6 [-]	Yes	Yes
3.1 [m]	3.9 [-]	Yes	Yes
3.2 [m]	4.0 [-]	Yes	Yes

The relationship between the height of the wall and the maximum wall tilt (figure 5.5) shows that by setting a height closer to failure, the tilt becomes exponentially more until the wall falls over or the entire quay structure collapses. The behaviour between the wall tilt and the wall displacement is linear for all height variations, figure 5.6. Most of this tilt is activated during the loading phase. For a wall height reaching its maximum height before failure, a larger increase in wall tilt per loading step is seen, showing a more plastic behaviour.

For a wall height of 3.2 meters or a W_h/W_t ratio of 4.0, the PLAXIS model indicated failure. In figure 5.6 only a small part of this curve has been shown. In appendix figure A.6 the entire development of the curve for a W_h/W_t ratio of 4.0 during failure is shown. These graphs indicate that at a certain surcharge load, the tilt rapidly increases, and the horizontal displacement approaches a constant value, indicating that the wall falls over.

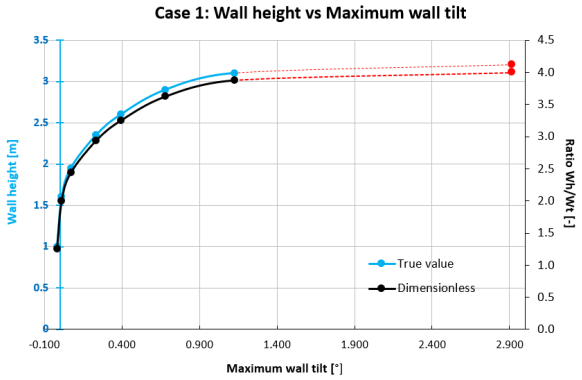

Figure 5.5: Wall height versus wall inclination, also shown as ratio (W_h / W_t) with the wall thickness of 0.8 meters.

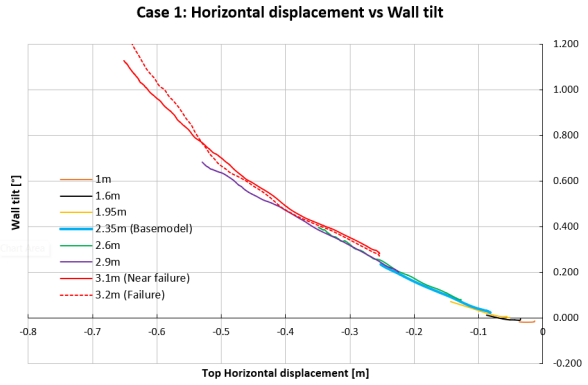

(a) Wall inclination versus the horizontal displacement for different wall heights

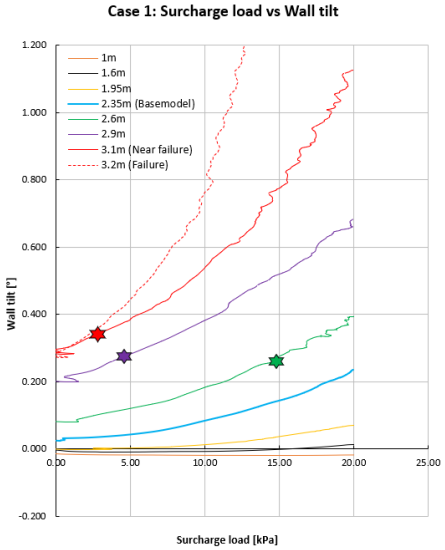

(b) Surcharge load versus the wall tilt for different wall heights. The star-shaped dots indicate the points when the bending capacity in the piles is exceeded

Figure 5.6: Inclination output for case 1

5.2.1.1. Crossbeam behaviour

Figure 5.7, shows the scaled-up crossbeam structure deformation for two different wall heights. The masonry wall typically follows and rotates due to this curvature, causing the wall tilt. In case 1-4, more vertical deformation in the crossbeam gives more wall tilt. By increasing the vertical load on top of the crossbeam and by erosion, this vertical displacement increases. This effect is also seen in the other sensitivity models.

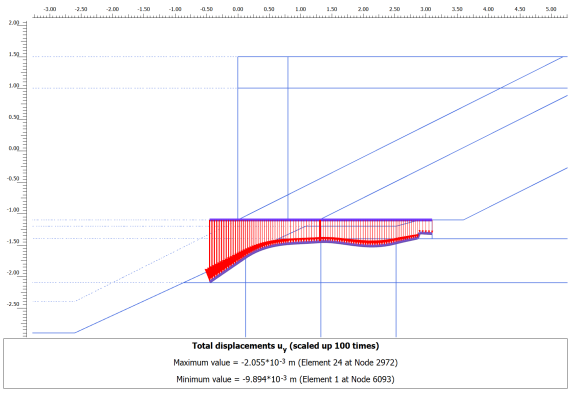

(a) Crossbeam deformation for a wall height of 2.6 meters ($W_h/W_t = 3.3[-]$)

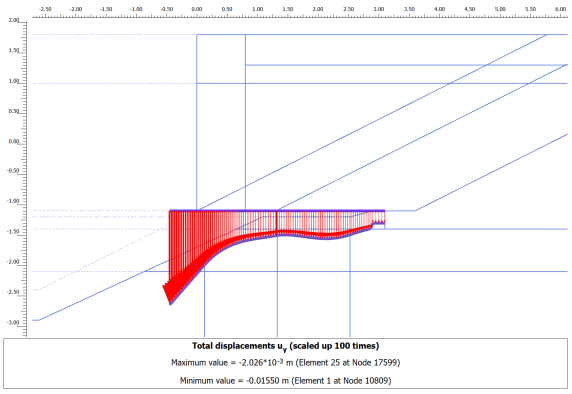

(b) Crossbeam deformation for a wall height of 2.9 meters ($W_h/W_t = 3.6[-]$)

Figure 5.7: Crossbeam deformation for different quay wall height, in case 1-4, more vertical displacement gives more wall tilt

5.2.2. Case 2: Crossbeam length

This section presents the results of the second geometry case. In this case the crossbeam length is changed and in doing so, the amount of piles is also increased or decreased, table 5.2 and table 5.3. In the graphs, green lines/points mean 2 pile rows, black lines/points mean 3 pile rows and orange line/points are 4 pile rows underneath the floor. A symmetric pile distribution means that the piles have an even distance to each other and to the front and end of the crossbeam. An asymmetric distribution means that the distance from the last pile to the end of the crossbeam is different from the distance from the first pile to the start of the crossbeam, figure 5.8, or the piles are placed at different spacing, so out of balance.

A CB_l/W_t ratio less than 2 also gives an unrealistic quay wall configuration, where the wall is almost as long as the crossbeam. This would already result in failure during the construction of the quay wall.

Table 5.2: Case 2: Crossbeam length variation symmetric pile distribution below the crossbeam

Case 2: Crossbeam length variation (Symmetric)					
CB_l (Crossbeam length)	Ratio CB_l/W_t	Pile Bending capacity reached	Crossbeam bending capacity reached	Pile spacing	Number of piles
1.85 [m]	2.31 [-]	Yes	Yes	0.75 [m]	2
2.17 [m]	2.71 [-]	Yes	Yes	1.03 [m]	2
2.35 [m]	2.94 [-]	Yes	Yes	1.2 [m]	2
2.95 [m]	3.69 [-]	Yes	Yes	1.5 [m]	2
3.55 [m]	4.44 [-]	No	No	1.2 [m]	3
4.75 [m]	5.94 [-]	No	No	1.2 [m]	4

Table 5.3: Case 2: Crossbeam length variation asymmetric pile distribution below the crossbeam

Case 2: Crossbeam length variation (Asymmetric)					
CB_l (Crossbeam length)	Ratio CB_l/W_t	Pile Bending capacity reached	Crossbeam bending capacity reached	Number of pile rows	Comment
2.65 [m]	3.31 [-]	Yes	Yes	2	Longer distance between the last pile and end of the crossbeam
2.95 [m]	3.69 [-]	Yes	Yes	2	Longer distance between the last pile and end of the crossbeam
3.55 [m]	4.44 [-]	No	No	3	Two piles directly underneath the wall, third pile further away
4.15 [m]	5.19 [-]	No	No	3	Longer distance between the last pile and end of the crossbeam
3.55 [m]	4.44 [-]	No	No	4	Extra pile for the base model

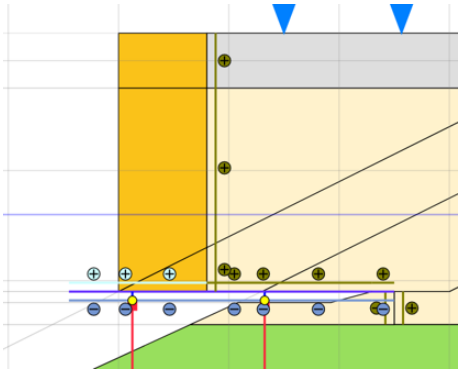

Figure 5.8: Asymmetric distribution of the piles along the crossbeam

Figure 5.9 shows the maximum wall inclination for different crossbeam lengths. A larger crossbeam length results in more piles and a more stable quay wall. Reaching a CB_l/W_t ratio around 2 rapidly increases the maximum wall tilt. Any ratio higher than this, gradually and linearly decreases the wall tilt towards a stable quay structure configuration. For the crossbeams with only two pile rows, the bending capacity in the wooden elements is already reached before the maximum surcharge load could be added. This would result in failure of the structure before the predicted wall tilt is reached. An asymmetric distribution of the piles underneath the floor gives a higher wall tilt for the same ratio's. Only when more piles are placed directly underneath the wall, the maximum tilt becomes lower.

Figure 5.10 shows a similar behaviour to case 1 (wall height variation), namely a linear relation between the wall displacement and wall tilt. Not only is the tilt more for shorter crossbeams with less piles, but also the horizontal displacement of the wall becomes more. A long crossbeam with four piles shows the most stable configuration, with only 10 cm of displacement and 0.1 degrees of tilt. For a crossbeam length reaching its shortest length before an unrealistic configuration is made, a larger increase in wall tilt per loading step is seen, showing a more plastic behaviour. This tilt increase per loading step is smaller and more constant compared to the wall height variations.

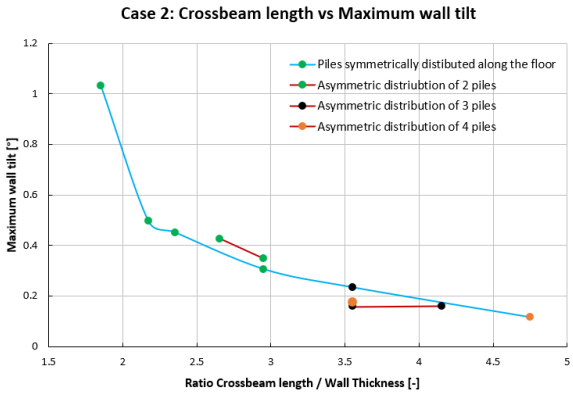

Figure 5.9: Ratio crossbeam length over wall thickness (0.8 meters) (CB_l/W_t) against the maximum wall inclination

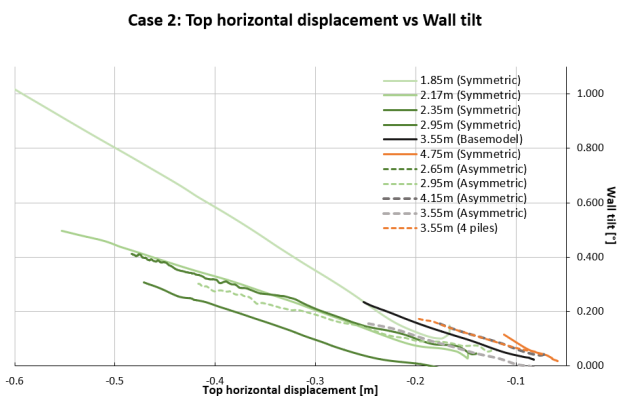

(a) Wall inclination versus the horizontal displacement (ux) for different floor lengths

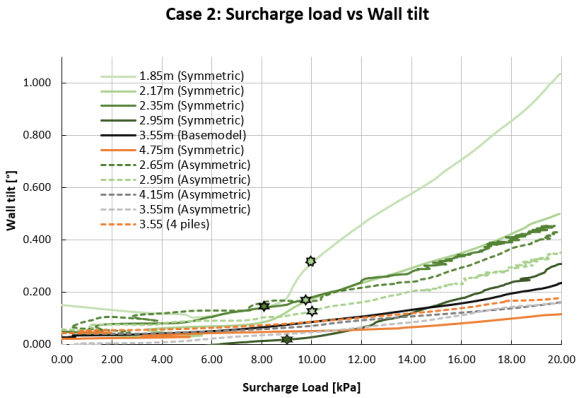

(b) Surcharge load versus the wall tilt for different floor lengths. The star-shaped dots indicate the points when the bending capacity in the piles is exceeded

Figure 5.10: Inclination output for case 2

5.2.2.1. Effect of pile rows on the quay wall stability

Figure 5.12 and 5.12 show the scaled-up quay wall structure deformation and the corresponding bending moment for two different crossbeam lengths. In these graphs can be seen that four pile rows give a more stable quay wall structure, with less horizontal displacement, wall inclination and less bending moments. In appendix figure A.2 the effect of the removal of the front pile row is plotted. This increases the wall tilt significantly, but it gives an unrealistic representation of reality.

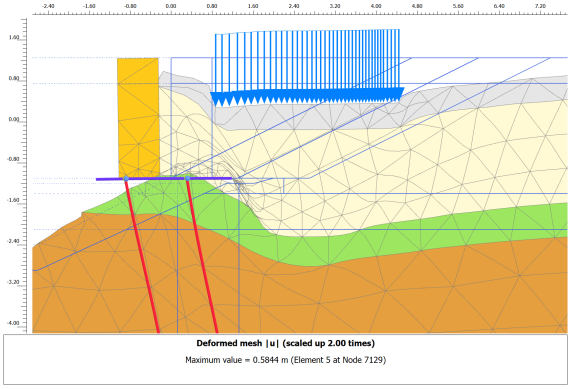

(a) Quay wall deformation for a crossbeam length of 2.65 meters ($CB_l/W_t = 3.31[-]$)

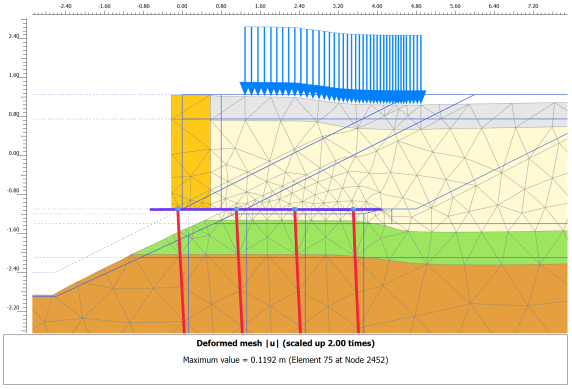

(b) Quay wall deformation for a crossbeam length of 4.75 meters ($CB_l/W_t = 5.94[-]$)

Figure 5.11: Deformation of the quay wall with different crossbeam length

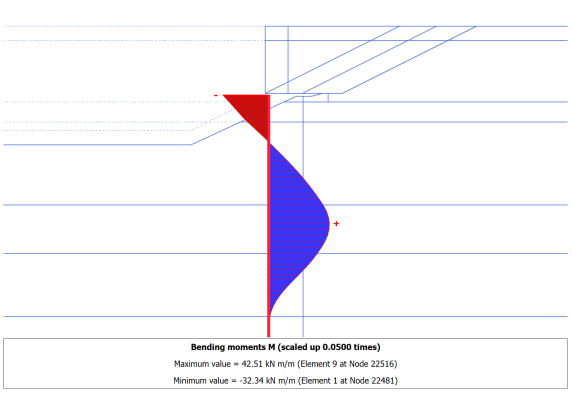

(a) Front pile bending moment for a crossbeam length of 2.65 meters ($CB_l/W_t = 3.31[-]$)

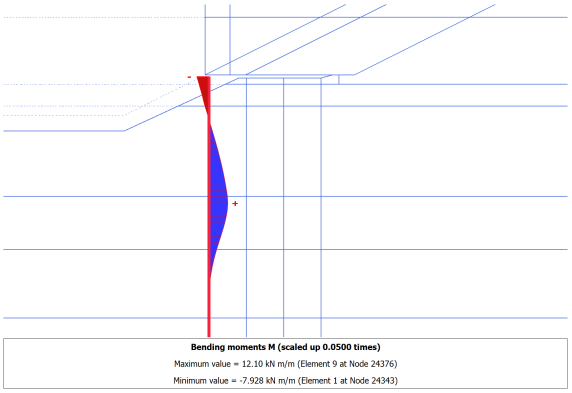

(b) Front pile bending moment for a crossbeam length of 4.75 meters ($CB_l/W_t = 5.94[-]$)

Figure 5.12: Front pile bending moment of a quay wall with different crossbeam length

5.2.3. Case 3: Canal Depth

In the third case the depth of the canal is increased. This simulates the time-dependent effect of canal bottom erosion, table 5.4. The slope from the quay wall towards the bottom of the canal is kept the same in the variations. This means that for a deeper canal the slope starts more towards the end of the crossbeam, exposing more piles. Eroding the canal with 1.6 meters gives an increase in wall tilt of 0.243 degrees, however the exact time span during which this inclination occurs is not known.

Table 5.4: Case 3: Canal depth variation

Case 3: Canal depth variation				
Z (Canal Depth)	Ratio Z/CB_l	Depth increase	Pile Bending capacity reached	Crossbeam bending capacity reached
-2.4 [m]	0.68 [-]	0 [m]	No	No
-2.65 [m]	0.75 [-]	0.25 [m]	No	No
-2.9 [m]	0.82 [-]	0.50 [m]	No	No
-3.15 [m]	0.89 [-]	0.75 [m]	No	No
-3.4 [m]	0.96 [-]	1.00 [m]	Yes	No
-3.55 [m]	1.00 [-]	1.15 [m]	Yes	No
-3.8 [m]	1.07 [-]	1.40 [m]	Yes	Yes
-4 [m]	1.13 [-]	1.60 [m]	Yes	Yes

The relation between the canal depth increase (and therefore also the starting point of the slope) and the difference in maximum wall tilt for each of the steps, is shown in in figure 5.13. This relation is shown for erosion happening when the maximum surcharge load is already active and erosion before the addition of the surcharge load. As seen in the plot, this does not change much in the maximum wall tilt. Typically, an increase in depth results in more wall tilt. This wall tilt is not as high when reaching failure compared to the other cases. This means that for observing the wall inclination during erosion, small values can be expected.

Again, linear behaviour between the horizontal displacement of the wall and the wall tilt is predicted in the PLAXIS model and this tilt exponentially increases during the addition of the surcharge load, as seen in figure 5.14. For deeper canals, the bending capacities are reached in the piles before the wall reaches its maximum inclination.

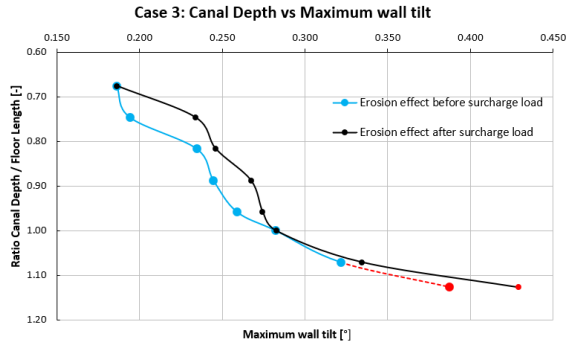

(a) Ratio canal depth over floor length (3.55 meters) (Z/CB_l) against the maximum wall tilt

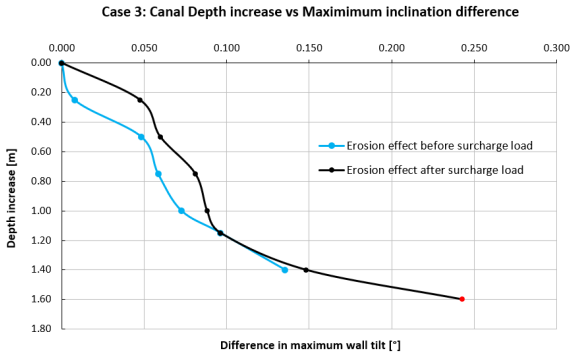

(b) Increase in wall tilt per canal erosion step

Figure 5.13: Inclination output for case 3: Canal Erosion

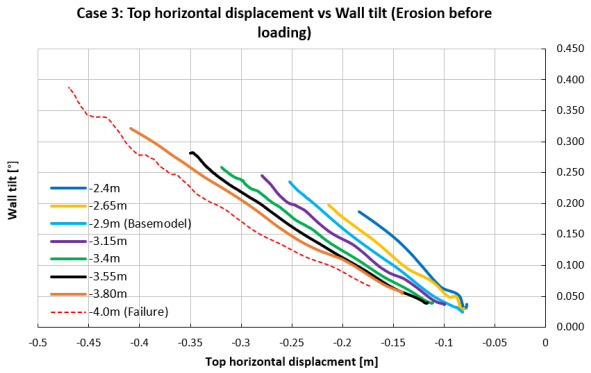

(a) Top wall horizontal displacement against the wall tilt during the loading phase

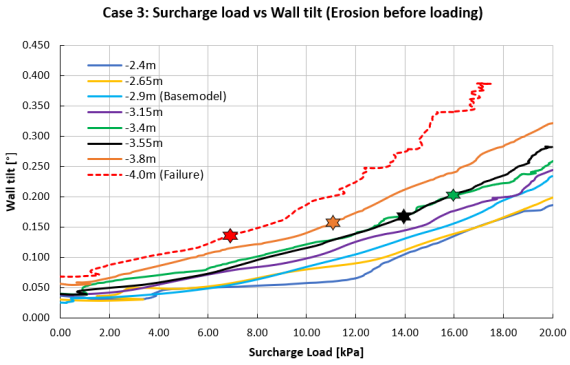

(b) Surcharge load (20 kPa) against the wall tilt. The star-shaped dots indicate the points when the bending capacity in the piles is exceeded

Figure 5.14: Inclination output for case 3

In figure 5.15, the increase/decrease of the wall tilt is plotted without any surface load active. These graphs show that during the erosion phase, the wall only tilts and moves slightly forward. For shallow canals, the wall tends to tilt slightly towards the street side. This shows that the surcharge load has an important impact on the final wall displacement.

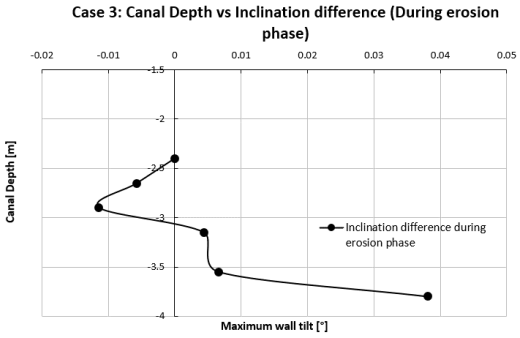

(a) The canal depth against the inclination difference wall tilt with respect to the initial depth of -2.4m

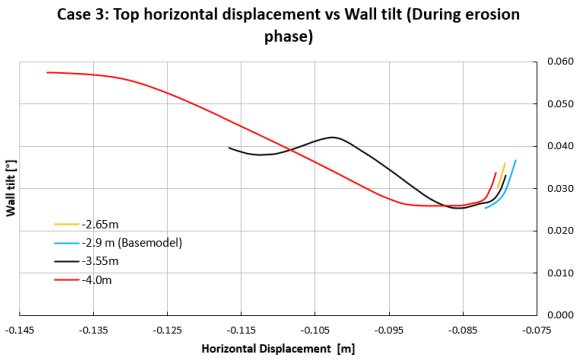

(b) Top wall horizontal displacement against the maximum wall tilt for several depths

Figure 5.15: Displacements during deepening of the canal for PLAXIS output case 3

5.2.3.1. Soil displacement underneath the floor

The effect of the movement of the slope towards the end of the crossbeams is shown in figure 5.16. For a deeper slope, the amount of soil pushing up along the piles is less, resulting in more forward tilt, more about this in chapter 8.

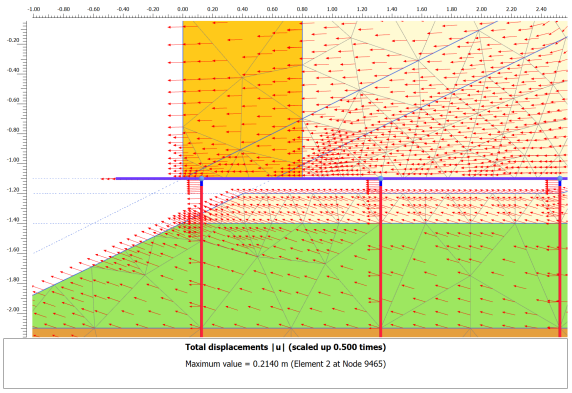

(a) Soil deformation along the piles and the crossbeam for a canal depth of -2.65 meters ($Z/CB_l = 0.75[-]$)

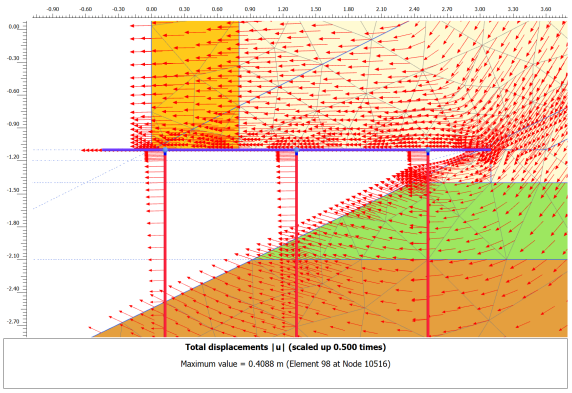

(b) Soil deformation along the piles and the crossbeam for a canal depth of -3.80 meters ($Z/CB_l = 1.07[-]$)

Figure 5.16: Soil deformation along the piles and the crossbeam for different canal depths

5.2.4. Case 4: Pile degradation

The pile degradation is a time-dependent analysis where the pile diameters reduce over time, table 5.5. It is assumed that the volume of the wooden piles stays the same after degradation, the reduction in diameter only has an impact on the moment of inertia of the wooden piles. This is because the outer shell of the piles loses its structural strength, but it does not disappear, it becomes a soft outer shell. It has also been assumed that the bending capacity for the degraded piles stays constant at 24 kN m/m, therefore no structural failure is seen in this analysis.

Table 5.5: Case 4: Pile diameter variation

Case 4: Pile degradation (diameter variation)			
P_d (Pile diameter)	Percentage of original P_d	Pile Bending capacity reached	Crossbeam bending capacity reached
0.221 [m]	100 [%]	No	No
0.175 [m]	79 [%]	No	No
0.150 [m]	68 [%]	No	No
0.125 [m]	57 [%]	No	No
0.100 [m]	45 [%]	Yes	No

Figure 5.17 shows the maximum wall tilt and maximum horizontal displacement for different degradation percentages. It also shows the difference in wall tilt for each step where the displacement is set to zero after the final surcharge load. The relation between the degradation and the tilt and displacement is nearly linear for the first 30% reduction, whereafter a more significant increase in the wall tilt and displacement is seen towards failure. Degrading the piles to a stable 56% of its original diameter gives an increase in wall tilt of 0.095 degrees and towards failure, when 45% of its diameter is left, an increase in wall tilt of 0.25 degrees is seen.

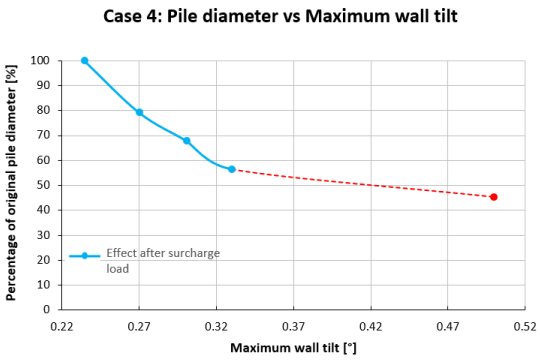

(a) Pile diameter reduction against the maximum wall tilt

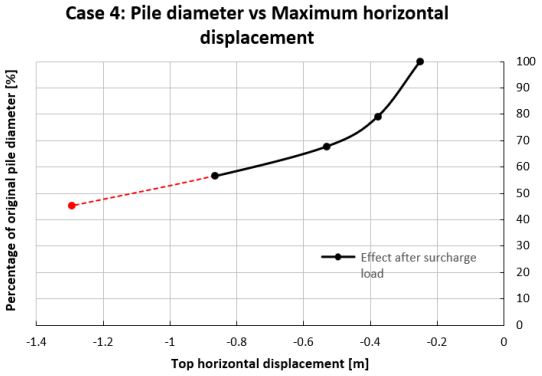

(b) Pile diameter reduction against the maximum top wall displacement

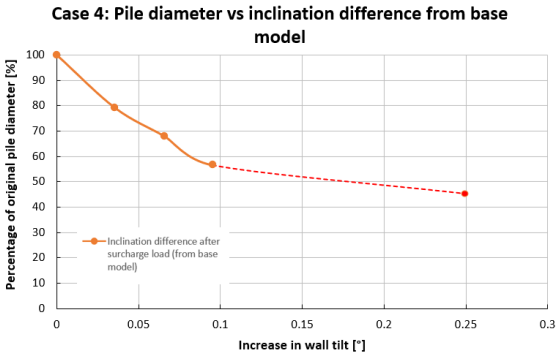

(c) Difference in pile diameter reduction steps before adding the load

Figure 5.17: Inclination output case 4: Wall reaction to different pile diameter reductions

The behaviour of the wall tilt during the pile degradation phase, before the addition of the surcharge load, is shown in figure 5.19. It shows that the pile degradation of all piles has little to no effect on the wall tilt. The exact time span during which this occurs is not certain. These are very small and hard to measure accurately. More difference is seen in the horizontal displacement of the wall during the pile degradation, this reaches values towards the 1-meter displacement.

The linear relationship between the wall tilt and wall displacement is again observed in figure 5.18. The addition of surcharge load has a more noticeable effect on the horizontal wall displacement than on the wall tilt and increases exponentially.

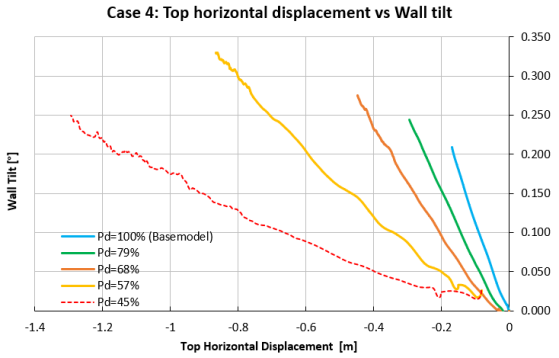

(a) Top wall horizontal displacement against the wall tilt for different pile diameter reductions

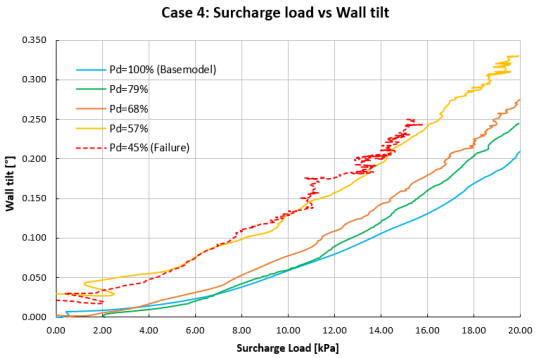

(b) Surcharge loads against the wall tilt for different pile diameter reductions

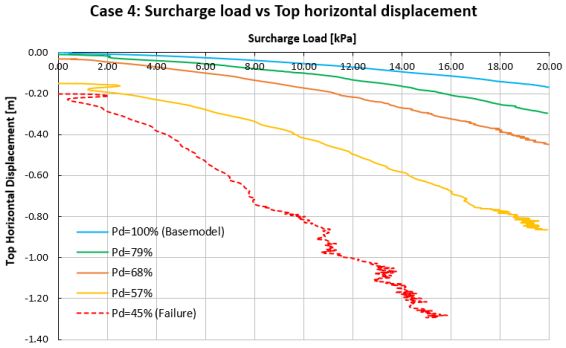

(c) Surcharge loads against the wall horizontal displacement for different pile diameter reductions

Figure 5.18: Horizontal displacement and tilt behaviour during loading

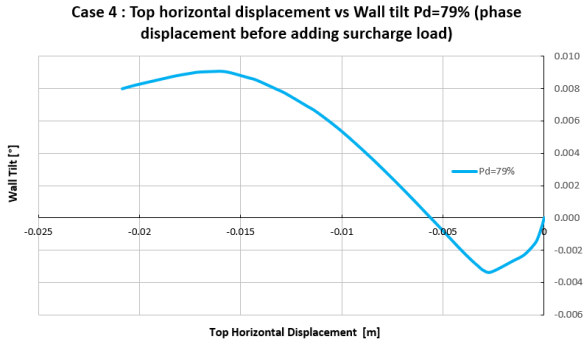

Figure 5.19: Phase displacement of the wall during the pile degradation phase (before the surcharge load)

5.2.5. Case 5: Wall thickness

In case five, only the thickness of the wall is varied, keeping the same height as the base model. From table 5.6, it can be seen that no bending capacity is reached. This means that failure happens due to the soil pressures on the quay wall, so at 0.5 meters thickness or 4.7 W_h/W_t ratio, the wall tips over on its own.

The ratio between the wall height and wall thickness is shown in figure 5.20. These ratio's approach the same ratio values towards failure compared to case 1. Decreasing the wall thickness, relates nearly linear to the increase in wall tilt before failure. At failure, the wall tips over and high inclination values are observed.

Table 5.6: Case 5: Wall thickness variation

Case 5: Wall thickness variation			
W_t (Wall thickness)	Ratio W_h/W_t	Pile Bending capacity reached	Crossbeam bending capacity reached
1.2 [m]	2.0 [-]	No	No
1.0 [m]	2.4 [-]	No	No
0.8 [m]	2.9 [-]	No	No
0.65 [m]	3.6 [-]	No	No
0.575 [m]	4.1 [-]	No	No
0.535 [m]	4.4 [-]	No	No
0.5 [m]	4.7 [-]	No	No

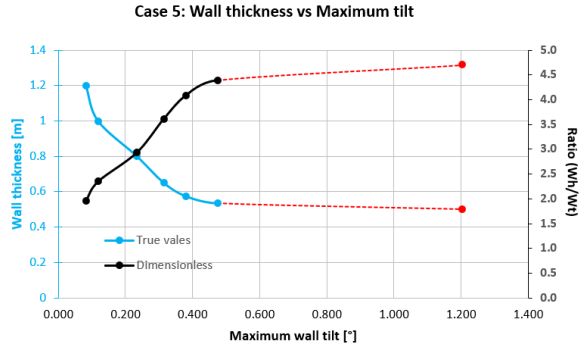

Figure 5.20: Wall thickness against the maximum wall tilt, for a wall height of 2.35 meters (W_h/W_t)

Figure 5.21 shows that when the wall reaches failure by increasing the surcharge load, the tilt rapidly increases in a more plastic way, without much more horizontal displacement. In this case the wall tilt is more noticeable than the wall displacement. For more stable quay wall configurations, the wall tilt and the horizontal displacement behave linearly with each other. From figure 5.21a can be seen that by varying the thickness, the horizontal displacement stays roughly constant at about -0.25 meters. Therefore, the horizontal displacement of the wall is less sensitive to the wall thickness, compared to the other sensitivity cases, where a larger change has been noticed in the variations.

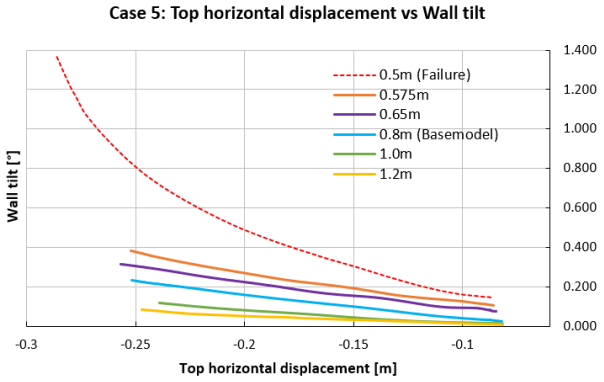

(a) Top wall horizontal displacement against the wall tilt for different wall thickness

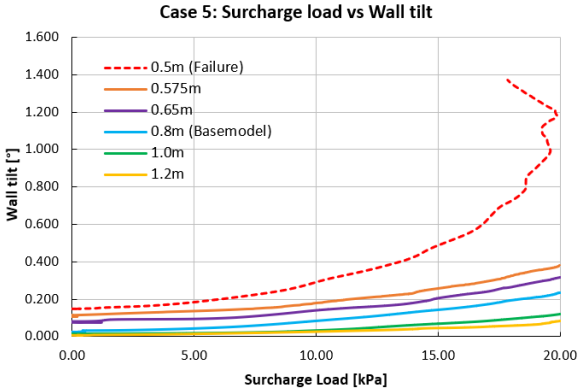

(b) Surcharge load (20 kPa) against the wall tilt for different wall thickness

Figure 5.21: Inclination output for case 5

5.2.5.1. Wall tilting

In figure 5.22 can be seen that a thin wall tips over on top of the crossbeam. It does this without exceeding the bending capacity in the crossbeam or in the piles. The vertical displacement in the crossbeam is not the main driving factor for the wall tilt, which is different from the rest of the cases, figure 5.23. This indicates that the wall independently rotates on top of the crossbeam due to the stress behind the wall, not predominately due to the vertical deformation of the crossbeam, figure A.8.

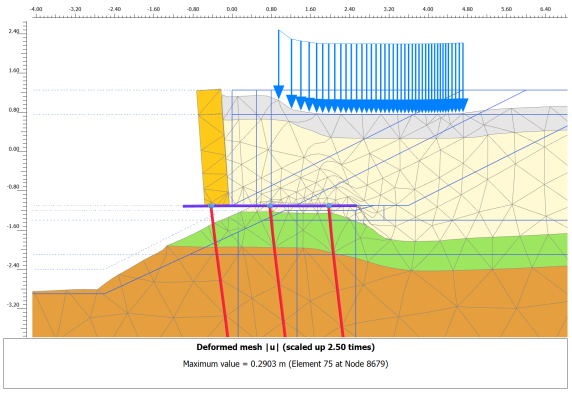

(a) Wall tilt and displacement of a 0.5 meters thick wall ($W_h/W_t = 4.7[-]$)

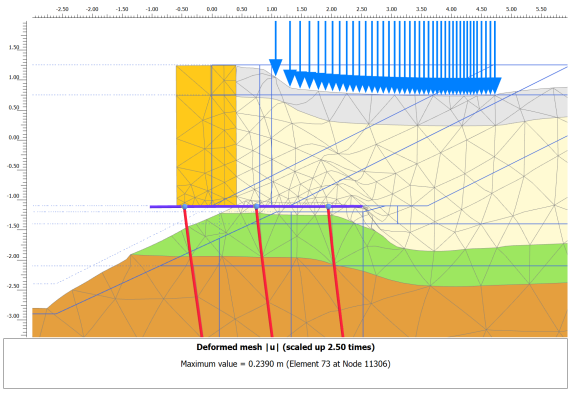

(b) Wall tilt and displacement of a 1.0 meters thick wall ($W_h/W_t = 2.4[-]$)

Figure 5.22: Wall tilt and displacement for different wall thickness

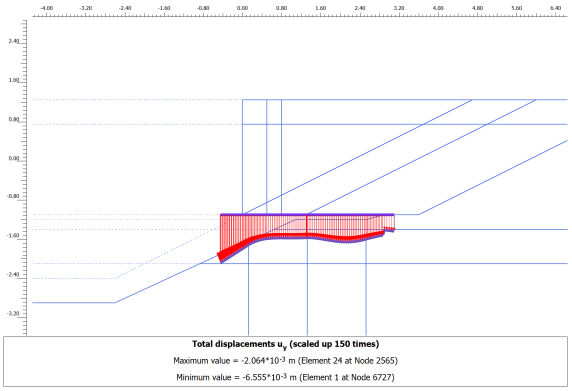

(a) Crossbeam vertical deformation for a wall thickness of 0.5 meters ($W_h/W_t = 4.7[-]$)

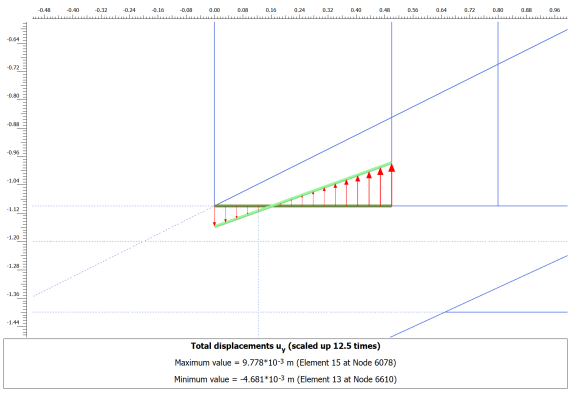

(b) Wall tilt of a 0.5 meters thick wall ($W_h/W_t = 4.7[-]$)

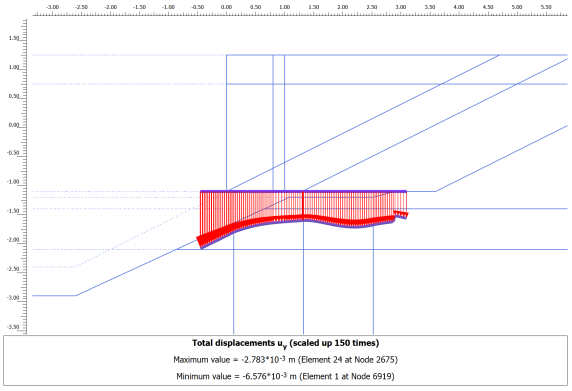

(c) Crossbeam vertical deformation for a wall thickness of 1.0 meters ($W_h/W_t = 2.4[-]$)

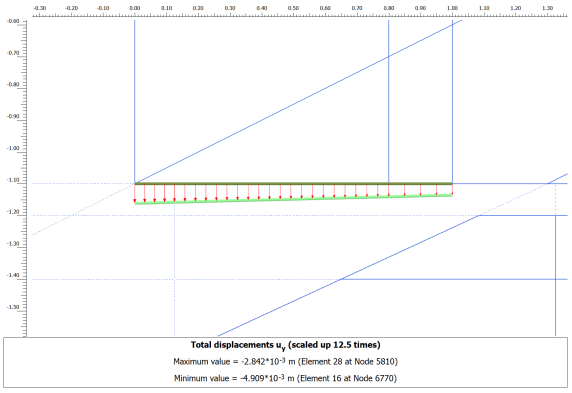

(d) Wall tilt of a 1.0 meters thick wall ($W_h/W_t = 2.4[-]$)

Figure 5.23: Relation between the crossbeam deformation and the wall tilt. Only in case 5 (wall thickness), for a higher crossbeam vertical deformation, a lower wall tilt is seen, meaning that the tilt is due to the lateral pressure behind the wall

5.3. Inclination Sensitivity Conclusions

The following key findings have been gained from the PLAXIS inclination sensitivity analysis in the base model and the geometrical variations:

- The activation of the surcharge load is the predominate factor in increasing the wall predominately tilt and top horizontal wall displacement and shows an exponential increase in tilt.
- The relationship between the wall tilt and the top horizontal wall displacement is linear in all geometrical variations.
- The changes in top horizontal wall displacement are in the order of decimeters, while the wall tilt is often less than one degree.
- The dimension changes in most sensitivity cases give both a notable change in horizontal displacement and in wall tilt. Only for the wall thickness, this horizontal displacement stays roughly constant in the variations and shows more increase in wall tilt.
- In most cases, the bending capacities in the wooden elements are exceeded before the maximum wall tilt is reached.
- The vertical deformation of the crossbeam plays a key role in the wall tilt.
- By decreasing the wall thickness, the wall tips over on the floor, without exceeding bending capacities in the wooden elements.
- The canal erosion and pile degradation only show a slight increase in wall inclination towards failure.
- Towards failure, the wall tilt becomes significantly larger compared to stable configurations.
- Manual measurements of the quay wall show that over the full lifespan of the structure, the wall tilt is five times higher than predicted in the numerical models, further elaborated in chapter 6 and chapter 7.

6

SmartBrick Application

This chapter describes the workflow for using and applying the SmartBrick data. It discusses how the data is analyzed, what corrections have to be done to make it usable for actual predictive applications, how it is presented in a dashboard, and it introduces the location and data for the case study.

6.1. Inclination Monitoring using SmartBrick

This section gives an explanation of the functionality, accuracy, and purpose of SmartBrick, their advantages and limitations and their relation to this project.

The SmartBrick contains, amongst other things, an inclination sensor with can be glued on the water side of the masonry quay wall. From that point on it measures the change in tilt of the wall over a specified time interval. The zero measurement is the tilt of the wall at the time of placement. This initial tilt mainly depends on the orientation of the individual masonry bricks and is not representative for the entire masonry wall. The inclination measurements have an accuracy of 0.05 degrees (Althen Sensors and Controls, 2022). This data is directly and wirelessly sent to the online SmartBrick platform, where an inclination versus time curve is produced. Currently, it measures four times each day and has a life span of ten years.

In addition, it also measures the temperature of the sensor. Since the measured wall inclination correlates to the current temperature, this needs to be compensated for, because it could be due to the sensor itself or natural wall movement due to the temperature. This natural movement can be noticed if one uses a very high accuracy and high-resolution sensor. An automatic way to compensate for the temperature is still being developed by Althen. For the time being, a manual compensation can be done by comparing measurement points with the same temperature.

6.1.1. Amsterdam's city center SmartBricks

A manual analysis has been done to check the data for inclination change in quay walls over time. This has been done using the same temperature method to remove the effect of temperature. The first results are shown in figure 6.1, which gives the monitored quay walls in Amsterdam and their inclination change. These values can be used to determine a suitable location to make a real-life numerical model of a certain quay wall. Most of these values have been obtained during 6 months of measuring. Most values of SmartBrick reach the edge of measuring the background noise, large inclination over time give more accurate results.

SmartBrick	Date 1	Date 2	Inclination 1	Inclination 2	Temperature 1	Temperature 2	Inclination change	Months	Link	Location
148042	12-apr	16-sep	-1.459	-1.91	14.1	14.1	0.451	5.1	https://app.bloc	Singel 300
148094	21-apr	18-sep	-4.962	-5.188	13.8	14	0.226	4.9	https://app.bloc	Nieuwe Herengracht 95 - 105
148102	13-apr	16-sep	-6.165	-5.957	16.4	16.6	0.208	5.1	https://app.bloc	Nieuwe Herengracht 65 - 69
148067	24-mei	26-aug	-2.576	-2.386	23.2	23.3	0.190	3.1	https://app.bloc	Da Costakade 118-122
147376	25-mrt	11-sep	-2.759	-2.924	17.3	17.3	0.165	5.6	https://app.bloc	Singel 112
148056	7-mei	5-sep	1.782	1.935	20.2	20	0.153	4.0	https://app.bloc	Da Costakade 118-122
148073	28-mrt	6-sep	-2.051	-1.904	21.7	21.7	0.147	5.3	https://app.bloc	Singel 354
148045	14-apr	19-sep	-4.144	-4.004	12.8	12.7	0.140	5.2	https://app.bloc	Kromboomsloot 36
148063	10-mei	16-sep	-1.831	-1.971	16.2	16.4	0.140	4.2	https://app.bloc	Bildijkkade
148066	17-mei	1-sep	1.184	1.324	23	23.1	0.140	3.5	https://app.bloc	Da Costakade 118-122
148077	22-mrt	12-sep	-0.562	-0.433	18.8	18.8	0.129	5.7	https://app.bloc	Nieuwe Herengracht 65 - 69
148064	23-apr	12-sep	-1.709	-1.605	19.7	19.9	0.104	4.7	https://app.bloc	Da Costakade 91-93
148082	23-apr	16-sep	-3.87	-3.967	15.2	15.4	0.097	4.8	https://app.bloc	Nieuwe Herengracht 95 - 105
148060	14-apr	19-sep	-2.252	-2.155	14.1	14.2	0.097	5.2	https://app.bloc	Singel 347
148079	22-apr	15-sep	-0.861	-0.769	19.4	19.5	0.092	4.8	https://app.bloc	Nieuwe Herengracht 95 - 105
148059	22-apr	13-sep	-3.43	-3.339	18.5	18.6	0.091	4.7	https://app.bloc	Bildijkkade
148053	10-mei	7-sep	-4.926	-4.84	19.9	19.9	0.086	3.9	https://app.bloc	Da Costakade 91-93
148054	16-mei	10-sep	-1.898	-1.813	18.6	18.5	0.085	3.8	https://app.bloc	Kromboomsloot 36
147366	10-mei	2-sep	0.134	0.214	20.2	20.2	0.080	3.8	https://app.bloc	Dommersbrug
147356	18-mei	7-aug	0.287	0.366	20.7	20.7	0.079	2.7	https://app.bloc	Oranjebrug
148071	21-mei	31-aug	0.037	0.11	15.3	15.2	0.073	3.3	https://app.bloc	Da Costakade 91-93
147352	25-mei	7-sep	2.148	2.216	19	19.1	0.068	3.4	https://app.bloc	Geldersekade 105
148048	19-mei	14-sep	-2.71	-2.643	20.6	20.6	0.067	3.9	https://app.bloc	Bildijkkade
148092	22-apr	10-sep	-3.448	-3.381	18.8	18.7	0.067	4.6	https://app.bloc	Nieuwe Herengracht 65 - 69
148084	18-apr	12-sep	-4.028	-4.095	18.3	18.3	0.067	4.8	https://app.bloc	Nieuwe Herengracht 95 - 105
148085	26-mei	16-sep	-4.01	-4.071	17.4	17.5	0.061	3.7	https://app.bloc	Oetewalerbrug
141436	23-apr	28-aug	-1.593	-1.532	18.4	18.4	0.061	4.2	https://app.bloc	Singel 426
148057	16-mei	9-sep	1.062	1.007	19.6	19.5	0.055	3.8	https://app.bloc	Kromboomsloot 36
147378	27-mrt	9-sep	2.484	2.429	18	18	0.055	5.4	https://app.bloc	Oranjebrug
148055	23-apr	6-sep	-2.405	-2.35	20.4	20.5	0.055	4.5	https://app.bloc	Da Costakade 118-122
148078	15-apr	16-sep	-2.802	-2.856	14.9	14.9	0.054	5.0	https://app.bloc	Nieuwe Herengracht 95 - 105

Figure 6.1: Monitored inclination change with SmartBricks

6.1.2. Online Dashboard

The data measured by SmartBrick is sent to the online platform BlockBax. In this platform, a dashboard can be made to create an overview of the SmartBricks per city area and per canal. The battery, inclination and the active status are monitored, figure 6.2. For each SmartBrick a 'trigger' can be set to monitor when the inclination exceeds the critical value. This means that a warning message is given when too much inclination is detected, more specific analysis on site is thereafter advised.

The map of Amsterdam with the placed SmartBricks is depicted in figure 6.3. This map shows SmartBricks with high inclination in red, other warnings in orange, and OK SmartBricks in green. The SmartBricks have been placed all around Amsterdam to give a complete picture of the potential critical quay walls. More specific SmartBricks are placed on quay walls where already a large horizontal displacement or wall tilt is seen, or where cracks are visible on the masonry wall.

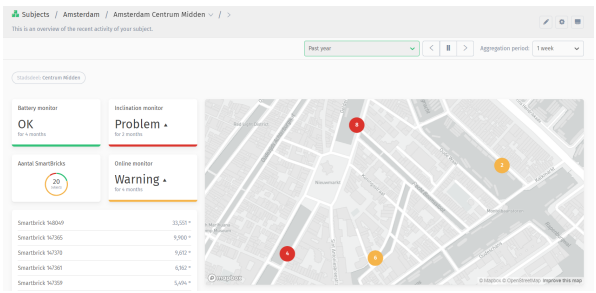

(a) Dashboard per city district

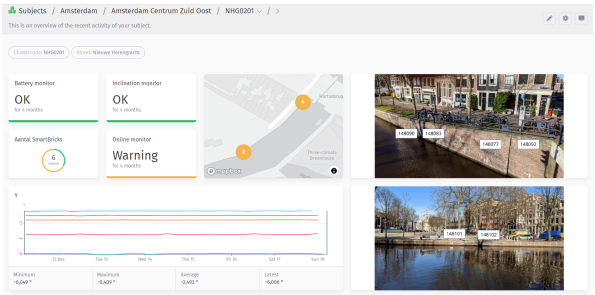

(b) Dashboard per canal

Figure 6.2: BlockBax monitoring dashboard

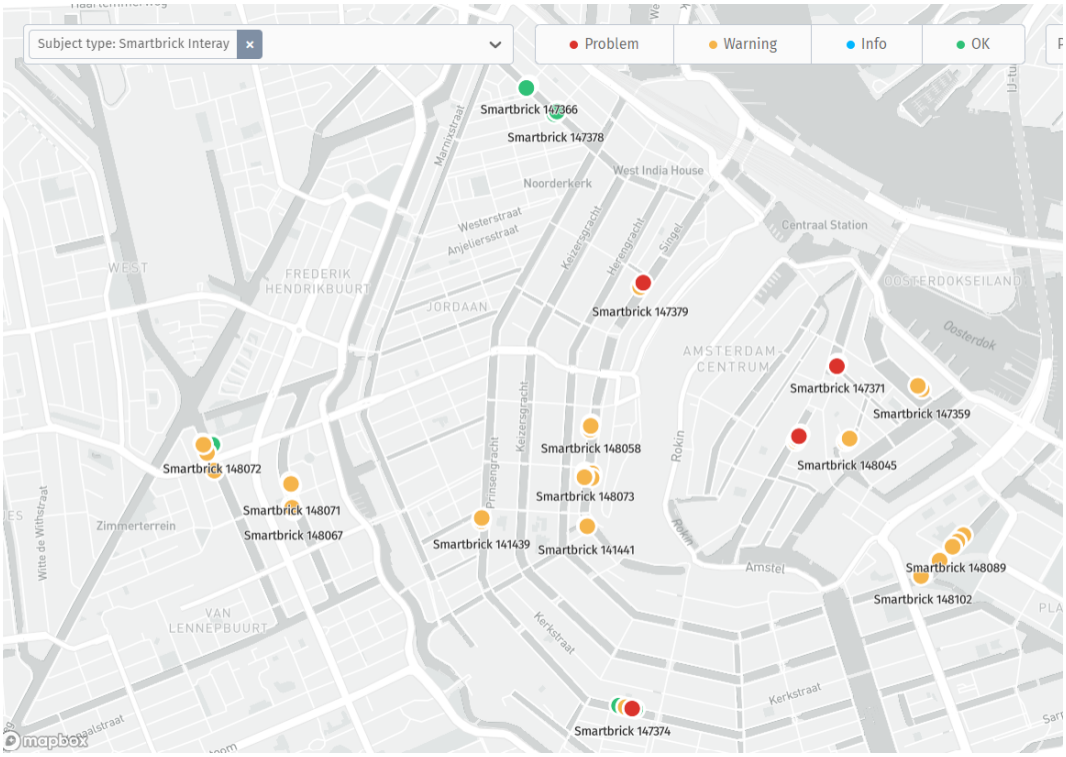

Figure 6.3: Amsterdam area with the placed SmartBricks

6.2. SmartBrick Case Study Data

Based on figure 6.1, a few locations show significant inclination with SmartBrick. The Nieuwe Herengracht, Singel and the Da Costakade show significant inclination differences over time. To make a relatable case-study of a quay wall, a location has to be picked which also has a lot of available data regarding its degradation and geometry, more about this in chapter 7, which provides more information about the chosen case-study. The Singel canal (SIN0401) has been chosen as case-study quay wall.

On the SIN0401 quay wall, two SmartBricks are placed, figure 6.4. Both bricks are on the historical quay walls with a masonry gravity wall and a wooden crossbeam and piles. The temperature dependent inclination data over the past year is shown in figure 6.5 and figure 6.6. From these graphs can be seen that the temperature is almost inversely proportional to the wall tilt. An increase in temperature gives a more negative tilt, which means more tilt towards the waterside. This temperature dependence can be caused by the behaviour of the sensor itself and/or partly due to the natural quay wall movement due to the temperature.

The temperature compensated inclination change over 4 months is shown in table 6.1. This gives an indication of the actual inclination change around this area. The canal erosion or pile degradation during this 4 months is not known, only during one diving inspection data within the last few years. Compared to available tachymetry data, an average tilt of 0.13 degrees in 7 months is measured. This gives an inclination rate of 0.019 degrees per month for tachymetry and 0.011 degrees per month for SmartBrick. However, it is difficult to compare both methods, due to limited data, different measurement frequencies, uncertain measurement accuracy for tachymetry and tachymetry measures only the horizontal displacement of the wall. However, high horizontal displacement measured by tachymetry also give high wall inclination values measured by SmartBrick.

Table 6.1: Wall inclination change over about 4 months

SmartBrick temperature compensated data: SIN0401							
SmartBrick	Date 1	Date 2	Wall angle 1 [°]	Wall angle 2 [°]	Temperature 1 [$C°$]	Temperature 2 [$C°$]	Inclination change [°]
147379	13-Dec	26-March	5.243	5.2	8.5	8.6	**0.043**
147376	8-Dec	10-April	-2.74	-2.704	5.9	5.8	**0.036**

Figure 6.4: Location of the two SmartBricks placed on the SIN0401 quay wall

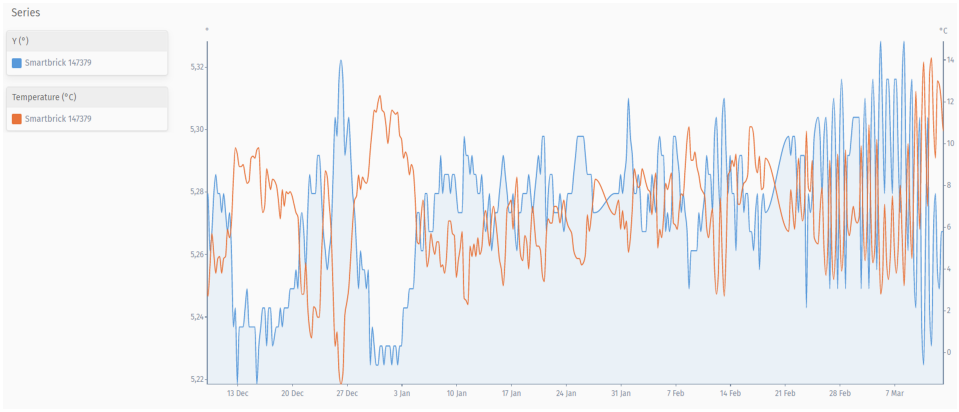

Figure 6.5: Wall tilt and temperature against the time for SmartBrick 147379

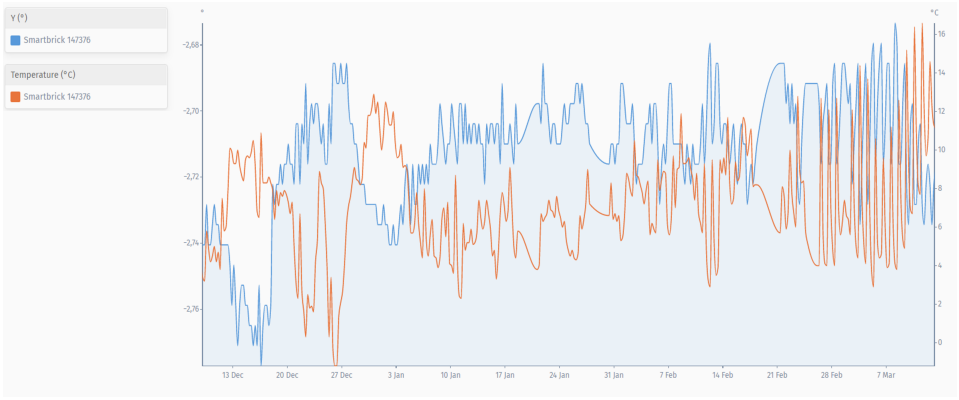

Figure 6.6: Wall tilt and temperature against the time for SmartBrick 147376

7

Case Study: Modelling Setup and Analysis

This chapter describes the results from the case study from a real quay wall in Amsterdam: the Singel quay wall (SIN0401). This case study will be compared with monitoring data from SmartBrick and with the sensitivity analysis.

7.1. Case Study Modelling Setup

For the Singel quay wall enough archive data about the specifications, diving inspections and damage analysis was available to create a representation of the quay wall in PLAXIS. Therefore, quay wall SIN0401 has been chosen as case study, the location is shown in figure 7.1. Two SmartBricks have been placed on this wall. One SmartBrick is placed on section B (figure 7.1) and one on section C. The dimensions of this quay wall are shown in table 7.2, based on figure 7.3 and archive documents. The detailed calculation and the sources of these values are shown in appendix C.4.

The quay wall has shown visual horizontal displacements of about 15 cm and a wall tilt around 4-5 degrees at some places, figure 7.2. This visual inspection shows that the quay wall is in critical condition. Therefore, a retaining structure has been placed since September 2022. The analysis of the quay wall in this project is done before this retaining structure is placed. The construction phases for implementing the model in PLAXIS are shown in figure 7.4 and table 7.1.

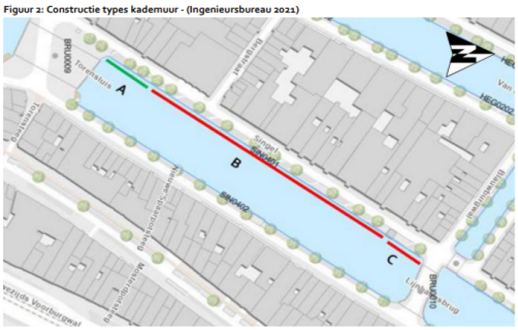

(a) Location SIN0401, part B consists out of the historic quay wall configuration

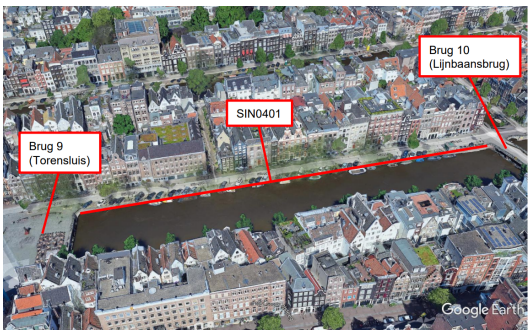

(b) Satellite image of the study location

Figure 7.1: Location of the canal and quay wall SIN0401 in Amsterdam

(a) Quay wall horizontal movement and tilt, a tilt between 4-5 degrees has been observed.

(b) Quay wall horizontal displacement, around 15 cm.

Figure 7.2: Quay wall damage observations, Gemeente Amsterdam (2021b)

.

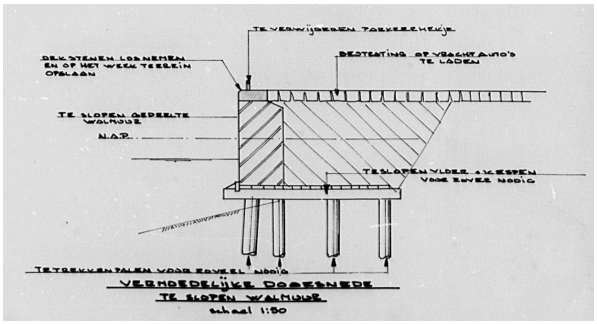

(a) Expected quay wall geometry according to Gemeente Amsterdam (2021a)

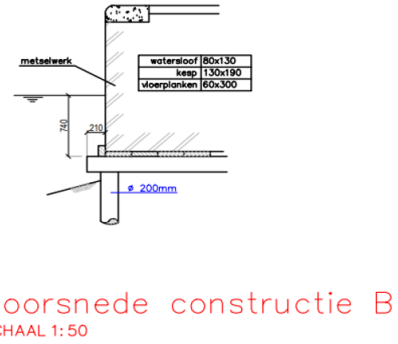

(b) Excepted initial dimensions of the quay wall according to Nebest Duikinspectie B.V. (2021a)

Figure 7.3: Expected initial geometry of the SIN0401 quay wall

Table 7.1: Staged construction phases for SIN0401

Phase 0	Initial phase (K0 procedure)
Phase 1	Lowering groundwater table
Phase 2	Excavating of the building pit and canal
Phase 3-4	Installation of the piles, wall, and the crossbeam
Phase 5-6	Final backfill and rising of the (ground)water table
Phase 7	Current canal erosion (3D laser scan)
Phase 8	Permanent loads (5 kPa)
Phase 9	Degradation of the pile(s)
Phase 8	Activation of the traffic loads (10 kPa)

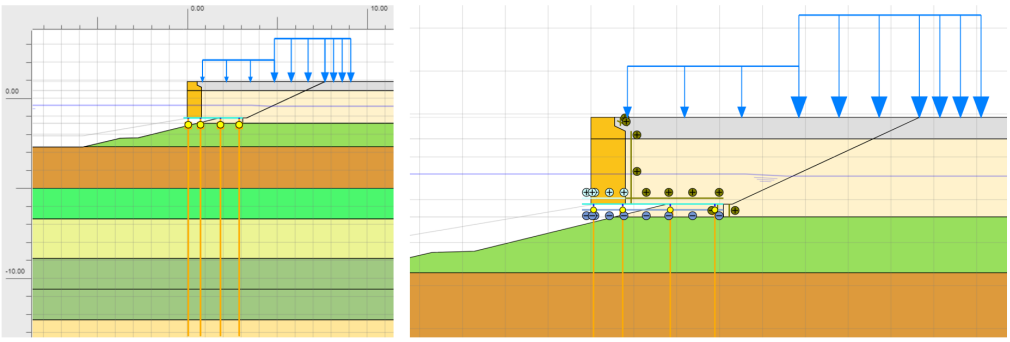

Figure 7.4: PLAXIS geometry of the SIN0401 quay wall, soil model based on a CPT near the quay wall, figure C.6

Table 7.2: SIN0401 geometry

SIN0401	
Dimension	Value
W_t (Wall thickness)	0.84 [m]
W_h (Wall height)	2.02 [m]
CB_l (Crossbeam length)	3.26 [m]
Z (Canal depth)	-2.72 [m]
P_d (Relevant pile diameter)	0.177 [m]
$P_{degraded}$ (Relevant degraded pile diameter)	0.083 [m]
Street level	+0.88 NAP [m]
Water level	-0.40 NAP [m]
Amount of piles	4 [-]
Pile spacing	0.74-1.07-1.04 [m]
Pile length	12.05 [m]
Parking load	5 [kPa] over 4 [m]
Traffic load	10 [kPa] over 4.2 [m]

7.1.1. Modelling time dependent factors

During the lifespan of the quay wall, surrounding factors could have been changed over the years. These are factors such as the water levels, the surcharge loads behind the wall, the degradation of the piles and the masonry wall and the erosion of the canal bottom. In this case-study, only the effect of the pile degradation and the deepening of the canal is taken into account as time-dependent factors.

This pile degradation can be done on all the piles (as done in 5.2.4) or by only degrading the front pile row, figure 7.5. To analyze the degraded pile diameters, a diving inspection has been done (Nebest Duikinspectie B.V., 2021a), the detailed results are shown in appendix C.4 and figure C.5. A 3D scan of the canal depth has been done using a multibeam echosounder, figure C.5.

7.1.2. Assumptions

- The volume of the wooden piles stays the same after degradation. The outer shell of the wooden piles becomes soft and loses its structural strength. Therefore, the reduction in diameter only has an impact on the moment of inertia of the wooden piles.
- Only the front pile rows have been inspected. It is assumed that all the piles degrade the same. An extra model is made where only the front pile diameter is reduced, which would cause the wall to tilt more.

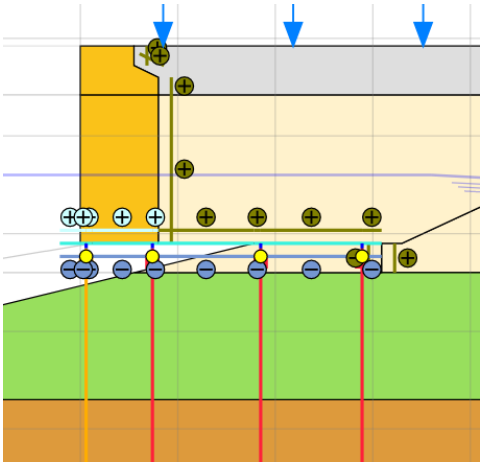

Figure 7.5: Front pile row degradation SIN0401

7.2. PLAXIS inclination behaviour SIN0401

This section analyses the output based on the PLAXIS model of the case study.

Figure 7.6 and figure 7.7 show the development of the wall tilt during the quay wall construction for a parking load of 5 kPa and a traffic load of 10 kPa. In this case, the pile degradation is compared for all piles and for only the front pile row. If only the front pile row degrades more wall tilt is seen. An increase in this parking load to 10 kPa, also increases the total inclination of the quay wall, as shown in appendix figure B.1.

As can be seen, the relation between the wall tilt and the horizontal wall displacement is linear, which corresponds to the models in the sensitivity analysis.

The structural output images, such as the crossbeam displacement, pile displacement and bending moments are shown in appendix B.2. The behaviour during the addition of the surface loads, the pile degradation and canal erosion is in line with the expected behaviour based on the geometry variations in the sensitivity analysis. An interesting addition is the variable traffic load, which is modelled as undrained. The traffic load occurs at a further distance from the wall than the parking loads. The accumulation of this surcharge load at this distance has as consequence that it has a smaller impact on the wall tilt, but a larger impact on the horizontal wall displacement. This is seen by comparing the green and orange parts of the curve in figure 7.6.

In the case where only the front pile row degrades, the wall tilt during this phase is 0.047 degrees. This inclination change is comparable with the inclination change measured by SmartBrick. However, this means that this pile degradation would have happened within 4 months, which is not expected. Therefore, this SmartBrick measured inclination is due to other external factors, which have not been modelled in PLAXIS, section 7.2.1.

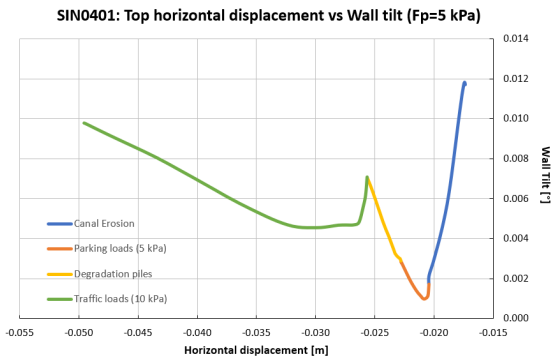

(a) Wall tilt against the horizontal top wall displacement for SIN0401

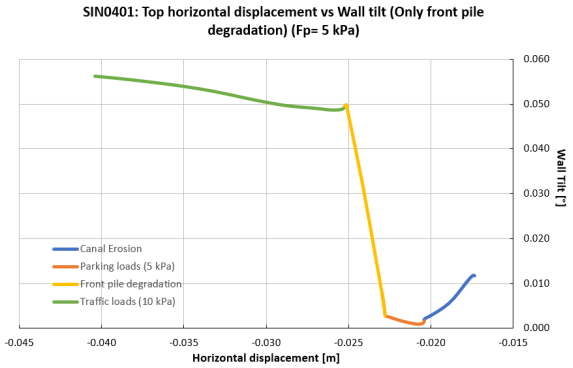

(b) Wall tilt against the horizontal top wall displacement for SIN0401, where only the front pile row is degraded

Figure 7.6: Inclination graphs for the quay wall: SIN0401

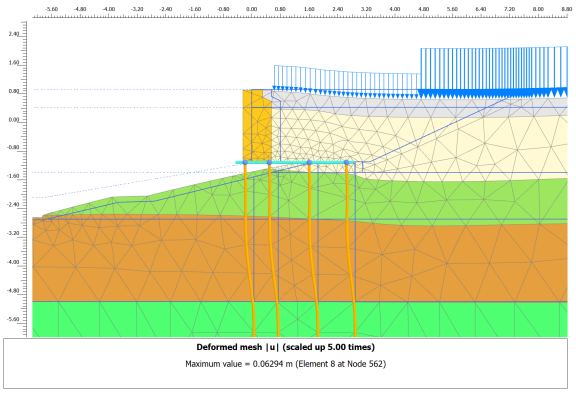

(a) Quay wall displacement after the traffic loads, all piles degrade

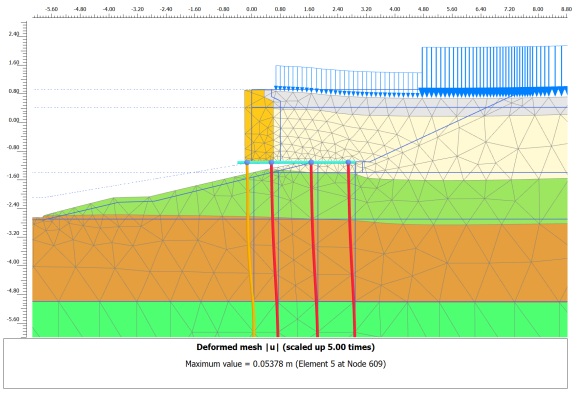

(b) Quay wall displacement after the traffic loads, only the front pile row degrades

Figure 7.7: Quay wall displacement after the traffic loads: SIN0401

7.2.1. Prescribed pile displacement

The diving inspection has observed significant damage to the wooden crossbeams and piles. The damage in the wooden crossbeams cause a downward axial force on the piles according to Nebest Duikinspectie B.V. (2021a). It is not possible to model this effect naturally in PLAXIS, therefore a manual prescribed displacement is set to see the effect of such an axial displacement on the quay structure, figure 7.8, representing a settlement due to axial loading of the piles. Figure 7.9 and figure 7.10 show the structural displacement in the floor and piles. It can be seen that a large downward movement of the crossbeam and the front pile is initiated underneath the wall. This causes the wall to settle and tilt forward. During this displacement, the bending moments are exceeded, however this is expected from the visual damage in the elements.

From manual tilt measurements the inclination of the quay wall is around 5 degrees. This tilt is achievable by setting a vertical displacement in the front pile of -7.25 cm and a displacement of -2 cm in the second pile, more about this in chapter 8. In this case, the crossbeam is already broken, the bending capacity is exceeded, so the effect after the damage (during failure) is simulated. The horizontal displacement is more in line with the measured displacement in figure 7.2. By introducing a vertical pile displacement larger than -20 cm the masonry wall will fall over at a tilt of 17 degrees and exceed the bending capacity in the second pile (figure B.9). In appendix B.3, a prescribed displacement onto the wall is introduced to simulate a potential structural loss due to cracks in the masonry wall.

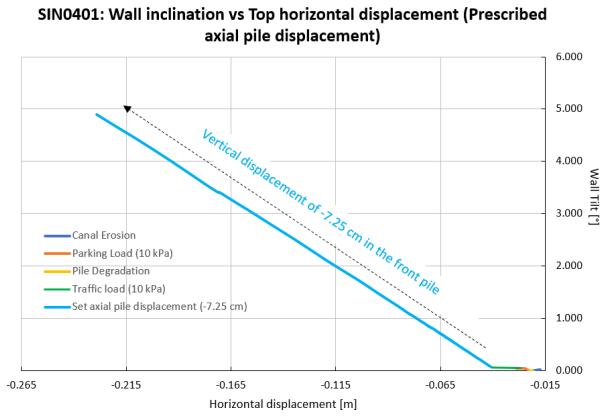

(a) Wall tilt against the horizontal top wall displacement for SIN0401 with the prescribed pile displacement

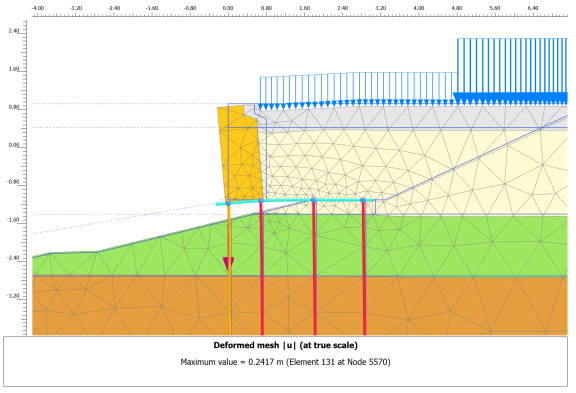

(b) Quay wall displacement with the prescribed pile displacement.

Figure 7.8: Quay wall tilt and displacement with the prescribed pile displacement of -7.25 cm and second pile axial displacement of -2 cm

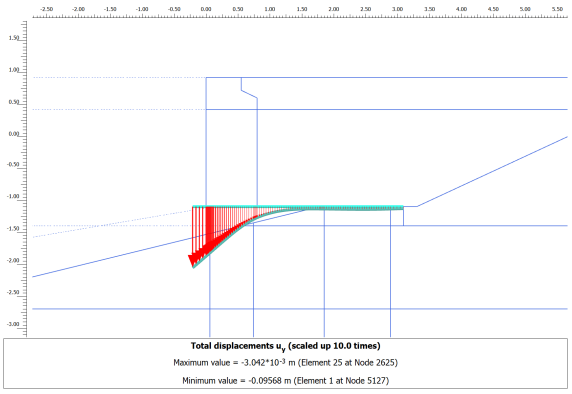

(a) Total vertical crossbeam displacement

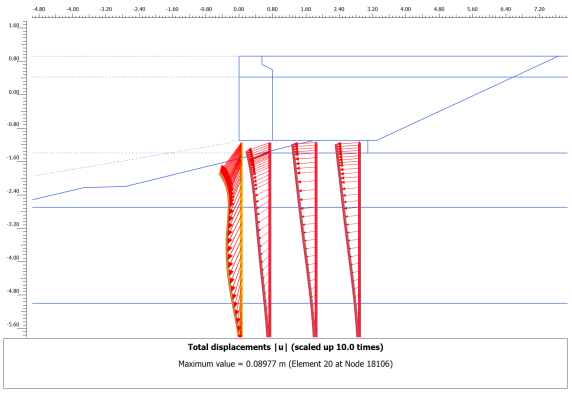

(b) Total pile displacement

Figure 7.9: Quay wall pile and crossbeam displacement with the prescribed pile displacement of -7.25 cm and second pile axial displacement of -2 cm

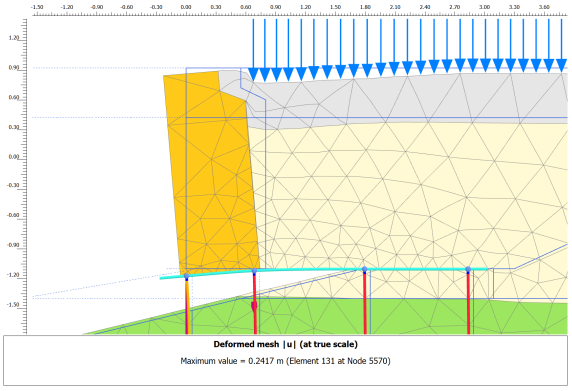

(a) Quay wall displacement with the prescribed pile displacement, close up indicating the tilt

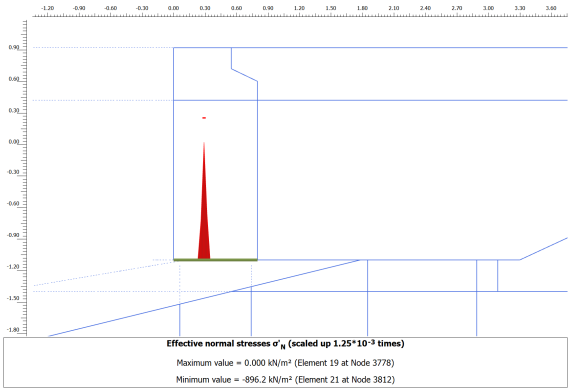

(b) Total normal stress distribution in underneath the wall, indication the contact area

Figure 7.10: Tilting behaviour of the wall with prescribed pile displacements of -7.25 cm in the front pile and -2 cm in the second pile

7.3. SmartBrick and Case-Study Conclusions

The following key findings have been gained from the case study analysis in PLAXIS and with SmartBrick:

- Horizontal displacement more than 15mm measured by tachymetry also resulted in detectable indications for wall inclination change measured by SmartBrick. A moving quay wall is often associated with wall tilt.
- The SmartBrick measurements have only gathered data for 6 months and have to be compensated for the temperature. This temperature dependence can be caused by the behaviour of the sensor itself and partly due to the natural quay wall movement due to the temperature.
- The behaviour and relationship between the wall inclination and the horizontal displacement in the case-study similar to the sensitively analysis.
- The simulated maximum wall tilt is not comparable with the monitored and measured quay wall tilt. The simulated wall tilt is an order of magnitude smaller than the tilt measured by SmartBrick. The horizontal displacement is more in line with the visual displacements of the quay wall. The SIN0401 quay wall showed a wall tilt of 5 degrees, while the numerical models only showed less than 1 degree wall tilt.
- Introducing only a degradation at the front row of piles, increases the maximum wall tilt significantly more, than by degrading all the piles.

- Adding a surcharge load further behind the quay wall mainly increases the horizontal wall displacement.
- Damage in the floor and the piles (seen by diving inspections) may cause the wall to tilt significantly more than simulated in the PLAXIS model. This can cause axial pile capacity loss and additional vertical displacements in the piles.
- An addition of a vertical prescribed displacement (representing a settlement due to axial loading of the piles) in the front pile can represent this damage and approach the measured wall tilt.

8

Discussion and Limitations

8.1. Evaluation of results

This section evaluates the results regarding the reliability of the numerical models and compares the indicators for failure with the standard failure mechanisms.

8.1.1. Failure indications from the sensitivity analysis

The sensitivity cases are edited from the initial base model. The base model shows that during the lifespan of the quay wall, the inclination of the wall predominately comes from the surcharge load on the street-side of the wall. This load gives an increase in the soil pressure behind the wall, along the wooden piles and the crossbeam. Therefore, these elements tend to approach instability and reach their structural capacity. In the base model, these limits have not been reached and the quay wall is stable. Therefore, this behaviour and the values of tilting are safe. The purpose of the sensitivity analysis is to approach an unstable quay wall configuration by changing the dimensions and properties of the elements and see what the impact is on the wall tilt and horizontal displacement. The results of the sensitivity analysis are compared to the failure mechanisms (figure 2.2). The most important failure mechanisms that have been observed during the analysis are presented in figure 8.1.

Figure 8.1: Relevant Failure Mechanisms, edited from figure 2.2

8.1.1.1. Case 1 (Wall height) and Case 5 (Wall thickness)

The results regarding the wall height show that an increase in wall height approximates a square root relationship with the maximum wall tilt. By increasing the wall height, the thickness of the backfill sand also increases. Together, this gives more downward pressure onto the crossbeam and piles and more lateral stress behind the wall. This causes the crossbeam to bend underneath the wall, partly initiating the wall rotation. These high pressures exceed the bending capacity in both the crossbeam and the piles, which will break. The simulations assume an elastic behaviour in the wooden elements, which allows the piles to keep bending past their capacity. Introducing a bending limit in the piles, figure A.5, shows that after reaching the limit, the inclination stays nearly constant, only the horizontal displacement of the wall increases rapidly. Assuming the elastic behaviour, around a wall height over wall thickness ratio of 4, the quay wall becomes unstable, and the tilt reaches values more than 1 degree.

By only changing the thickness of the wall (case 5), the pressure on the wooden elements do not exceed their capacity. The wall tilt is caused predominately as a reaction to the lateral soil pressure on the active side, causing it to tip over on the crossbeam and showing less settlement due to the deforming crossbeam. This ratio of wall height over wall thickness reaches 4.5 before failure at a wall tilt higher than 1 degree, which is roughly similar to case 1. However, these ratio's are not directly comparable since a wall height increase

also adds more sand backfill. The horizontal displacement of the wall is less sensitive to the wall thickness compared to the other sensitivity cases. Wall thickness is more sensitive to the wall tilt.

The failure mode in case 5, closely resembles to failure mechanism 5 (figure 8.1) and the failure mode in case 1 corresponds to a combination of failure mechanisms 10 and 1 (figure 8.1).

8.1.1.2. Case 2 (Crossbeam length)

In case 2, the tilt of the wall is approximately inversely proportional to the crossbeam length. The wall rapidly inclines around a crossbeam length of less than 2 meters ($CB_l/W_t < 2.71$), towards values higher than 1 degree and large horizontal displacements. A longer crossbeam length results in a more stable quay wall configuration, with less displacement and tilt. An important driving factor in these configurations is the amount of piles present. Longer crossbeams tend to have more pile rows, resulting in a more stable quay structure. The distribution of these piles underneath the crossbeam has an important impact on the tilt. If more piles are present directly underneath the wall, the tilt will be less. If the piles are asymmetrically distributed underneath the floor, the tilt will be more, and the structural limits will be reached.

Typically, a quay wall in Amsterdam has three or four pile rows, where the crossbeam is around 3 meters ($CB_l/W_t = 3.70$). Quay walls with only 2 piles rows always resulted in an exceedance of the bending capacity in both the crossbeam and the piles towards reaching a surcharge load of 20 kPa, no matter the pile spacing. By setting a limit on the bending capacity, the tilt becomes constant after the limit is reached and the quay wall only moves more towards the waterside until it reaches failure at a certain surcharge load.

For more than three pile rows, the piles tend to push the front of the crossbeam up in the phase before loading, this reduces the inclination towards the waterside. Within the PLAXIS models, stability failure has not been reached while keeping realistic dimensions. A crossbeam length less than 1.85 meters ($CB_l/W_t < 2.31$) would already fail during the construction of the wall. Compared to the failure mechanisms, case 2 would be close to failure mode 4 (figure 8.1), where the wall tilt is a consequence of the failure in piles.

8.1.1.3. Case 3 (Canal depth)

Deepening of the canal corresponds, in this case, also to less soil underneath the floor and more piles exposed. The relationship between the wall tilt and the canal depth is less apparent than in other cases, but it follows the expectation that a deeper canal is less stable while keeping the same quay structure geometry.

The soil displacement underneath the floor shows that for a shallow canal, more soil is pushed up than for a deeper canal. This upward movement also causes the piles to push up against the crossbeam, reducing its downward bending. Therefore, the wall also tilts less towards the waterside since it reacts with the moving crossbeam. For a shallow canal depth, this means that the inclination is negative, meaning the wall tilts towards the street, before the surcharge load is applied, during the erosion phase (figure 5.15). More erosion of the canal and the slope, causes the wall to tilt more towards the water. However, the tilt during erosion is very small compared to the total lifespan of the quay wall. Most of the inclination comes during applying the surcharge load, all variations are stable before this load is applied.

Soil body failure is reached at a depth of -4 meters ($Z/CB_l = 1.13[-]$) with a surcharge load of 17 kPa , where the entire crossbeam is not embedded anymore in the soil. In this case it only reaches a tilt around 0.4 degrees and a horizontal displacement of 47 centimeters. The canal depth does not clearly resemble a failure mechanism according to figure 8.1 with an indication of inclination. For shallow canals, with the slope ending at the front of the quay wall, a small indication of failure mechanism 6 (figure 8.1) can be seen, tilting the wall backwards (figure A.7). Furthermore, it can cause structural failure in the piles according to failure mechanism 4 (figure 8.1).

8.1.1.4. Case 4 (Pile degradation)

The pile diameter against the tilt behaves nearly linear until failure was reached. The difference in maximum tilt between each degraded pile diameter is very small, around 0.03 degrees and towards 0.09 degrees when 45% of its original diameter is left. A larger effect is seen in the horizontal displacement of the front wall, which reaches the most displacement towards the waterside compared to the other cases. A decrease in diameter, results in a higher horizontal wall displacement, until it reaches failure, around -1 meters. This horizontal displacement is caused by the lateral forces on the piles, they move horizontally towards the waterside. Therefore, the piles also cause the crossbeam and masonry wall to move. This reaction is recognized in failure mechanism 10 (figure 8.1), without showing much wall tilt. A larger effect from the pile degradation towards the tilt could be that only the front pile degrades, which is analyzed in the case study.

8.1.2. Comparison between the sensitivity analysis and the case study

The quay wall along the Singel consist out of four pile rows underneath the floor. For this floor length in case 2, usually three piles rows are enough for a stable configuration. As has been seen in case 2, adding an extra pile underneath the wall will reduce the maximum tilt of the masonry wall to under the 0.18 degrees at 20 kPa. The canal is shallow with a gentle slope, causing only the top of the front two piles to be exposed from the soil, which will result in less forward tilt, according to case 3. Moreover, the surcharge load is more realistic for the parking and traffic loads, which only reach 5 kPa next to the wall and 10 kPa on the street. The traffic load accumulation causes the wall to move horizontally towards the water. The combination of these factors results in the small wall tilt observed in the PLAXIS model. The inclination difference observed during the pile degradation phase is similar to the inclination measured by SmartBrick in 4 months, however it is not expected that this degradation occurs in just 4 months.

From the diving inspection, only the front piles rows could be reached and measured. It is uncertain how degraded the other pile rows are. For this reason, an additional configuration of SIN0401 was made, where only the front pile rows has degraded. This causes an increase in the wall tilt, since the front pile moves more downwards and forward than the rest of the piles, causing the crossbeam with the wall to bend towards the water.

In reality, a wall tilt around 4-5 degrees had been measured by hand. These values have not been reached in the case study model or the sensitivity models. The results from the diving inspection reported that the wooden foundations show signification damages. These damages consist out of cracked and severely displaced crossbeams and damage to the connection of the pile and the floor. These displaced crossbeams are reported (Nebest Duikinspectie B.V., 2021a) to compress the first and second foundation pile rows, which leads to the forward tilting of the quay wall. The cracks in the wooden elements are hard to model in PLAXIS. However, a prescribed axial displacement in the front two piles is set to simulate and amplify the effect of the damaged crossbeam and pile in the model (representing a settlement due to axial loading of the piles). To reach a wall tilt around 5 degrees, a vertical displacement of -7.25 cm in the first pile and a vertical displacement of the -2 cm in the second pile should be present. This results in a stable PLAXIS configuration with a settlement of the quay wall at the surface. However, this configuration is made by trail-and-error and is not a good predictive simulation of the quay wall, for this the actual axial displacement in the piles should be known.

Within the masonry wall, vertical cracks are also observed together with displacement along the horizontal axis. The wall is modelled as an uniform, solid soil element in PLAXIS which does not allow it to deform. As a response, the loss of structural capacity due to cracks in the masonry wall might cause that it tips over easier due to the lateral forces behind the wall. A simulation of this is made in PLAXIS by adding a prescribed horizontal displacement of -22 centimeters, causing the wall to rotate independently from the vertical crossbeam deformation towards a tilt of 5 degrees, B.8.

The SIN0401 quay wall has been chosen because it is currently being renovated due to critical damage to the wall. The damage in the wooden elements is large and the wall showed significant tilt. Geotechnically speaking this quay wall is representative for more quay walls in Amsterdam, but from structural point of view is does not represent all quay walls, it acts as an extreme case.

8.1.3. Comparison between modelling and monitoring

The SmartBrick inclination sensors are only reliable when measuring the change in tilt over time. The initial tilt value during placement depends on the orientation of the masonry brick it has been placed on, which could be different for each brick. Therefore, it is not possible to measure the total tilt from the masonry wall from construction until today, which is something that PLAXIS results indicate. The tilt over time is an important indicator for the prediction of the quay wall condition. It can predict how much inclination the wall can still manage based on the past measurements. This time-dependency is not directly modelled in PLAXIS 2D. Therefore, a direct comparison between SmartBrick and the FEM models would not be possible.

An indirect time-dependency is modelled in PLAXIS by introducing a degradation of the piles, an erosion of the canal and an increase in the surcharge load. As seen from case 3 (canal erosion), the canal deepening increases the wall tilt towards the waterside, but very little. The same behaviour is noticed during the pile degradation. An increase of the surcharge load has the largest effect on the wall inclination. For this reason, one of the first mitigated measures for quay failure is to close off the parking loads and reduce the amount of traffic. The inclination differences during the pile degradation steps and the canal erosion steps are in the same order of magnitude as inclination measured by SmartBrick in 4 months, however it is not expected that

this degradation and erosion occurs in only 4 months.

Another key phenomenon is the horizontal displacement of the quay wall. In all cases this shows significant values towards the waterside, where the wall tilt shows small angles. Measuring only the tilt with SmartBrick gives a linear relation with the horizontal displacement but does not always give the full extent of the of the quay wall condition. This horizontal displacement could be measured using InSAR or tachymetry. The inclination monitoring acts as a first order measurement system for failure, if high tilt is noticed, other methods can be applied for more detail.

The SmartBrick measurements for the SIN0401 quay wall showed a value around 0.040 degrees inclination over 4 months. Over the full lifespan, this quay wall tilt is five degrees. It is difficult to know where in the horizontal displacement-tilt graph the SmartBrick has been installed and what the pile conditions are at that point of placement. This should be known to compare the inclination seen in PLAXIS between those phases. The SmartBricks in the city center of Amsterdam have only been installed since December 2021, which is too recent to measure quay walls that have approached failure by tilting.

The purpose of quay wall inclination modelling in PLAXIS was to prove the concept and behaviour of inclination towards failure in inner-city quay walls, from which SmartBrick could be validated. The sensitivity cases have shown that wall tilt increases linearly with the top horizontal displacement of the wall when approaching several failure mechanisms.

8.1.3.1. Additional SmartBrick applications

From the PLAXIS simulations it is shown that the tilt of the quay wall is associated in most cases with the bending of the crossbeam and the piles. These displacements often reach their structural limit before the wall falls over during the accumulation of the surcharge load. This indicates that the quay structure is unstable and can fail according to failure mechanism 4. Therefore, this inclination of, for example, the first wooden foundation pile could also be monitored to assess the state of the quay wall.

The latest version of SmartBrick has been assessed for underwater connectivity. SmartBrick is able to measure the tilt up to 1 meters below the water level without using an external antenna. For deeper measurements, an external antenna can be used. For some quay walls the first pile is exposed from the soil underneath the floor. Consequently, SmartBrick could then be placed on the wooden pile to measure its inclination and gain data about the state of the quay wall. However, it is important to know the connection between the pile and floor, as these are easily damaged. This application could be investigated in further research.

During the testing phase of SmartBrick, the surcharge load values behind the quay wall have been increased at a remote location, Overamstel. These surcharge loads are not reached in the inner-city of Amsterdam. In the city center, there are more houses and variable loads near the quay wall. It could be useful to evaluate the effect of large trucks passing the quay wall on the wall displacement using the SmartBrick data.

8.1.3.2. SmartBrick and FEM Uncertainty

- The SmartBrick data sensor has to be compensated for the temperature. The raw data shows a near inversely proportional relationship between the temperature and the wall tilt. Higher temperature results in more tilt towards the waterside. For this project, a simple manual temperature compensation has been done, by looking for two or three points with the same temperature over a certain time period. More advanced algorithms are currently being developed by Althen to compensate for the temperature more effectively.
- The SmartBrick measures the inclination currently with an accuracy less than 0.05 degrees. This means that for the SIN0401 quay wall the inclination data approaches the background noise. More reliable measurements occur at quay walls with more inclination over time.
- During the degradation of the piles and the canal erosion, the wall tilt increases in steps smaller than 0.05 degrees, which makes it difficult to measure the change accurately with SmartBrick.
- From the PLAXIS models can be seen that by applying the surcharge load, the wall inclination change is simulated well within the 0.05 degrees accuracy of Smartbrick, most inclination changes are larger than 0.05 degrees.

- The order of magnitude of the horizontal displacement is higher than for the wall tilt, due to the entire wall also moving forward. The changes are simulated in centimeters, which therefore require a less precise monitoring device. For the inclination, a high-resolution sensor should be used.
- A medium mesh size is chosen in the PLAXIS models, with a finer mesh near the crucial elements. This gives a good balance between the computation time and the accuracy of the results.
- Best estimate values for the soil have been applied in the model. No design approaches or partial factors have been used, which could make the model more reliable.

8.2. Assumptions and Limitations

During the calculations in the models a number of limitations are observed based on assumptions made. These are described in the following list:

- The values for the wall tilt and horizontal displacement in the sensitivity cases are based on the dimensions of the base model. Not every dimension is changed in all the cases. This could mean that for other quay wall configurations, the maximum tilt before failure could be different. However, the behaviour should be the same according to the results.
- The maximum tilt is determined from the accumulation of 20 kPa surcharge load, which is reasonably high for Amsterdam. More representative values for the wall tilt can be found around 10 kPa, which can be determined from the surcharge load against wall tilt graphs. However, with this load, failure has not been reached in the cases.
- For the pile degradation, only the moment of inertia is reduced based on the reduction in the diameter. The surface area is kept constant in the degradation steps, because the soft, outer shell of the wooden piles is still present, but it has lost its structural value.
- Pile degradation and canal erosion are time-dependent processes, which happens over a long time period. In the models this degradation/erosion is instantly initiated in the next phase, while in reality it is more gradual. Also, the effect of creep in the foundations and soil has not been taken into account.
- The representative diameter of the piles has been based on the tapering tables, at a depth of 3/4 of the pile length. This depth could be different for different soil profiles.
- It has been assumed that the total bending capacity and axial capacity in the piles does not change during the degradation.
- The wooden elements are assumed to be linear elastic. This has been done to focus more on the total behaviour in the piles and the wall. In reality the elements reach their structural capacity, after which it breaks and behaves differently.
- The pile-floor connection resembles a hinge with a stiff spring constant of 400 kNm/m/rad. A looser connection behaves more as a hinged connection, causing a lower tilt and more horizontal displacement, figure A.3
- The masonry wall is modelled as a solid element on top of the wooden floor. In reality, the masonry wall can develop cracking, which may cause it to behave differently in the modelled cases.
- Damage in the wooden foundation and in the masonry wall is hard to model in PLAXIS. Still, these effects could have a significant impact on the wall tilt, as seen in the case study.
- In the PLAXIS models the geotechnical factors are more accurately modelled than potential structural factors, which causes differences with reality.
- This analysis is done in 2 dimensions. In 3D, when failure is reached or a pile breaks, the forces can redistribute over the quay structure, causing the wall to displace or tilt more before the entire structure eventually fails.
- PLAXIS 2D is more accurate for verification or feasibility calculations, with intact structural elements and variations in geotechnical factors, such as the soil thickness and amount of piles. Broken structural elements should be analyzed more in 3D.

9

Conclusion

9.1. Research questions

This section gives a summary of the most important findings and relate this to the research questions in order to give the best advice for quay wall inclination sensing in Amsterdam.

9.1.1. Sub-question 1

How can the link between quay wall tilt and failure mechanisms be predicted in finite element modelling as seen in Amsterdam's city center?

To answer this question, five sensitivity models have been made with different geometry configurations and pile properties. In addition, a case study has been modelled about an actual quay wall in Amsterdam, the Singel quay wall (SIN0401). The displacement and tilt patterns of the front quay wall are analyzed by these FEM models towards failure.

- Changing the height of the masonry wall and the thickness of the wall has a clear impact on the wall tilt. A higher wall, tilts increasingly more when adding surcharge loads. A thinner wall tips-over around a wall height/thickness ratio of 4.5. Both cases approach a combination of failure mechanism 1, 5 and 10 (figure 2.2).
- The dimension variations in most sensitivity cases give a significant change in horizontal displacement and in wall tilt. Only for the wall thickness this horizontal displacement stays roughly constant in the variations and shows more increase in wall tilt.
- The amount of piles underneath the floor has an important impact on the stability and structural capacity of the structure. Shortening the crossbeam and removing piles underneath the masonry wall increases the wall tilt. However, high tilt corresponds to an already other activated failure mechanism where the crossbeam or piles break, failure mechanism 4 (figure 2.2).
- Erosion in the canal can cause the soil underneath the crossbeam to also erode away, exposing the piles. Shallow canals tend to tilt the quay wall slightly towards the street-side, deeper canals tilt the wall towards the canal.
- A degradation of all piles underneath the floor, does not result in high wall tilt values. The more important failure feature is the horizontal displacement of the front wall towards the canal, indicating failure mode 10 (figure 2.2). Degradation of just the front pile row gives more wall tilt, as seen in the case study.
- The case study showed that it is important to know the damage of the foundation elements such as the masonry wall and wooden beams. These damages can cause the foundation piles to move downwards (representing a settlement due to axial loading of the piles), which therefore activate the tilt in the wall. However, not all these effects can be modelled correctly in PLAXIS 2D. This could explain why the monitored wall tilt over the full lifespan of the structure is sometimes five times higher than the 1 degree predicted in the numerical models.

- The activation of the surcharge load has the largest effect on the wall tilt, causing it to move towards the canal.
- When reaching failure in the sensitivity analysis, both the wall tilt and the horizontal displacement increase significantly and show a more plastic behaviour.

Therefore, to answer sub-question 1, to predict the link between failure mechanisms and the wall tilt in finite element modelling, a sensitivity analysis based on several quay wall geometry variations should be made. The most sensitive variations towards inclination are the change in the masonry wall height and thickness, the pile distribution underneath the floor and the addition of a surcharge load directly behind the masonry wall.

The displacement pattern before reaching failure where the wall falls over or the structure collapses, gives a linear correlation between the wall tilt and the top horizontal wall displacement. Adding a surcharge load exponentially increases the wall tilt in unstable quay walls. This relationship is seen in all sensitivity analysis. The resulting tilt can be explained by the behaviour of all elements in the quay wall in combination with failure mechanism 4, 5 and 10.

9.1.2. Sub-question 2

To what extent is inclination monitoring using SmartBrick able to give insight and recommendations to predict the state of the quay wall?

To answer this question, the SmartBrick data is assessed on its feasibility for quay wall tilt in the inner-city of Amsterdam. Moreover, it is compared to the finite element models to validate the concept of tilting as failure indication.

- The measurements of the SmartBrick quay wall tilt values are not monitored long enough yet to show failure. The highest inclination is around 0.5 degrees over 5 months.Pile degradation should occur over a longer time period.
- In stable quay walls (not approaching failure), the tilt caused by degradation is approximately equal to the measurement background noise. SmartBrick should be installed on quay walls with visible cracks, horizontal displacements and/or a subsided street to monitor the inclination rate.
- High inclination values from SmartBrick over time, are predominately caused by the high surcharge load. This is seen by the effect of surcharge load on the wall tilt in the PLAXIS models. This load should be reduced as first mitigation measure.
- The time-dependency of monitoring methods is not as effectively feasible in PLAXIS. The moving quay wall over time is difficult to model PLAXIS. It is not always known what the initial and latest quay structure conditions are between monitoring measurements. Extra factors such as creep, consolidation and different loading conditions could also play a key role in this. The exact lifespan of the quay wall structure with the wood degradation, canal erosion and surface loads are difficult to determine. For a future prediction, only assumptions can be made based on past inspections, which are limited. An indirect comparison with pile degradation and erosion steps has to be modelled, which shows only small wall inclination intervals.
- The SmartBrick senor for quay wall tilt is inversely proportional to the temperature, for which it has to be compensated.
- A combination of quay wall tilt sensing with SmartBrick and horizontal displacement measuring with another method (InSAR) could give a more complete picture of potential failure.

Therefore, to answer sub-question 2, inclination sensing using SmartBrick can give insight into the state of the quay wall. Due to the linear relationship between the wall tilt and the horizontal displacement during time-dependent factors such as the degradation of the piles and the erosion of the canal, an increase in wall tilt also is associated with further displacement until failure, normally measured by other monitoring methods.

However, the extend of this displacement is difficult to predict by only measuring the wall tilt, a high accuracy is needed to measure this inclination change. A direct comparison between SmartBrick and FEM was not possible, but the FEM results can be interpreted to predict the behaviour of the wall reaching failure, which can be compared to the behaviour seen in SmartBrick. Therefore, inclination monitoring can be used as an extra first order monitoring technique to locate potential quay wall failures using clear and easy routine measurements in Amsterdam or potential other cities.

The uncertainty in SmartBrick is due to its measurement precision of 0.05 degrees. The wall inclination change due to the parking or traffic loads in PLAXIS is well within this accuracy. However, during the pile degradation, the simulated wall tilt approaches the noise level of SmartBrick. It is advised to respond to the changes an order of magnitude larger than the 0.05 degrees.

9.1.3. Main question

What is the relationship between the tilt of the masonry quay wall and the state of the quay wall structure approaching failure?

To answer the main research question, the relationship between the tilt of the masonry wall and the state of the quay wall structure approaching failure, is that a linear correlation between the wall tilt and the top horizontal wall displacement is seen approaching failure. By changing the geometry of the quay wall and by increasing the surcharge load, the wall tilt becomes exponentially larger for more unstable structure configurations. Therefore, approaching certain failure mechanisms, show that wall tilt in combination with horizontal displacement is expected. Reaching the maximum tilt values give that the quay wall often is already failing, due to exceeding bending capacities in the wooden elements. The structural elements in the quay structure reach their capacity first before the quay wall falls over.

Inclination sensing is a good first order monitoring technique to automatically check the state of the quay wall. When large tilt is observed, also high horizontal displacements are seen.

Failure where only the masonry wall tilts separately from the crossbeam, does not occur often in the models. The wall typically moves and rotates due to the vertical deformation in the crossbeam, causing the tilt. Only with an increase in lateral pressure behind the wall (or a decrease in lateral resistance of the wall), tipping-over is observed.

9.2. Recommendations

The value of wall tilt monitoring for the assessment of quay wall failure has not been done to a great extent before. It has been shown that the wall tilt behaves linearly with the horizontal wall displacement. Therefore, measuring the wall tilt can give insight into the state of the quay wall, which could be used as additional knowledge in the current 'Programma Bruggen en Kademuren'.

Amsterdam contains a lot of different quay wall configurations, some are concrete L-walls, others are masonry gravity walls. It is not possible to make one general model which can be applied for Amsterdam. Using monitoring methods such as SmartBrick, a large amount of walls can be monitored easily, and the most critical areas can be selected. From this, a detailed numerical verification and future feasibility model can be made, using available archive data and inspections. This gives information about the amount and the condition of the piles and the masonry wall dimensions, which gives insight into the expected tilt behaviour.

SmartBrick can be placed on several places on the quay structures, not only the masonry walls, but also the wooden piles or floors to measure their inclination. These places are often the driving factors for the wall tilt and the state of the quay wall.

In SmartBrick, a wall inclination change over 0.2 degrees in a week has been set as inspection trigger. This trigger could be due to the addition of the surcharge load behind the wall or by damage in the structural

elements. Further inspection can be done with other monitoring techniques after this trigger is active in SmartBrick so that preventative measures can be taken.

9.2.1. Future work

- More research towards the geometry and structural properties of the quay wall should be done before a SmartBrick is installed so that the inclination behaviour towards failure can be predicted more accurately. For example, the connection types between the floor and the piles can be an important factor in amount of wall displacement and tilt.
- The inclination changes predicted by PLAXIS are very small, which would need a very sensitive sensor to measure. In reality, higher wall tilts are measured and observed. Therefore, it is recommended to do more analysis towards the behaviour of the quay structure over time and the effect of the damaged structural elements in quay walls, also including creep and partial factors.
- 3D analysis towards the effect of pile failure, crossbeam cracks and masonry wall cracks on the stability of the quay wall, can improve the tilt behaviour, to be more comparable with SmartBrick. A 2D study about this is done by Voortman (2021).
- A quay wall reaching a tilt of 1 degree, usually results in quay wall failure based on the numerical models. It is not certain in which time span this maximum tilt is achieved. It can be useful to do an additional true time-dependent analysis in PLAXIS or in another software.
- A SmartBrick combination with satellite images can be explored to monitor both the tilt and the horizontal displacement and is advised for a full safety assessment. By measuring only the tilt, it is difficult to predict the order of magnitude for the horizontal displacement and the damage in the foundation.
- Revisiting the SmartBrick data after a few years of monitoring in Amsterdam can be helpful to check if some quay walls approached failure, and if this data can be compared the sensitively simulations or with a different model.

References

AHN (2019). Actueel hoogtebestand nederland. https://www.ahn.nl/ahn-viewer. Accessed: 2022–10-20.

Althen Sensors and Controls (2022). Smartbrick early failure detection system (sefd). Unpublished.

AlthenSensors (2022). Smartbrick IoT sensoroplossing. https://www.althensensors.com/nl/custom-oplossingen/iiot-custom-sensor-oplossingen/smartbrick/. Accessed: 5-09-2022.

Bentley (2022). *Material Models Manual V22*. PLAXIS.

Blum, H. (1931). Einspannungsverhältnisse bei bohlwerken. *Berlin, Germany: Wil. Ernst und Sohn (in German)*.

Brinkgreve, R. (2019). Hardening soil model. Lecture Slides Behaviour of Soils And Rocks TU Delft. Accessed: 2022–07-09.

Brinkgreve, R. (2021). Possibilities and limitations of models. Lecture Slides Behaviour of Soils And Rocks TU Delft. Accessed: 2022–07-09.

CURNET (2008). CUR166 Damwandconstructies. *CROW*.

De Boer, R., Özdemir, R., Wensveen, P., and Wesstein, R. (2022). TCVK - Recht Boomssloot RBS0101-A. Unpublished - Draft report Arcadis.

de Cleen, M. (2021). The decay of amsterdam's quays. https://mforamsterdam.com/the-decay-of-amsterdams-quays/. Accessed: 2022–10-15.

de Gans, W. (2011). De bodem onder Amsterdam: Een geologische stadswandeling. *TNO*.

DINOloket (2022a). Subsurface data. https://www.dinoloket.nl/en/subsurface-data. Accessed: 2022–05-15.

DINOloket (2022b). Subsurface models. https://www.dinoloket.nl/en/subsurface-models. Accessed: 2022–05-15.

EAU (2004). Empfehlungen des arbeitsausschusses 'ufereinfassungen' hafen und wasserstrassen. *Hafenbautechnischen Gesellschaft e.v. und der Deutschen Gesellschaft fur geotechnik e. V. 10*.

Frankenmolen, S. (2006). Analyse noord/zuidlijn monitoringsdata: Effecten van de beinvloeding van de holocene laag op het zettingsgedrag van vooroorlogse panden. Master's thesis, Delft University of Technology. http://resolver.tudelft.nl/uuid:85cf8739-d477-4b69-bfb3-ab53f62c2883.

Gemeente Amsterdam (1887). Bestek en voorwaarden het bouwen van stenen en houten wallen. Unpublished - Bestek Amsterdam.

Gemeente Amsterdam (1902). Bestek voor het uitvoeren van onderhoudswerken, herstellingen en vernieuwingen aan: gebouwen, bruggen, wallen, riolen, openbare waterplaatsen, enz. Unpublished - Bestek Amsterdam.

Gemeente Amsterdam (1988). Bestek tekening, nieuwmarktbuurt, het vernieuwen van walmuren langs de recht boomssloot extra te vervangen walmuren. Unpublished - Bestek Amsterdam.

Gemeente Amsterdam (2020). Aanpak bruggen en kademuren. https://www.amsterdam.nl/parkeren-verkeer/bruggen-kademuren/uitleg-programma/. Accessed: 2022–10-15.

Gemeente Amsterdam (2021a). Historisch bodemonderzoek singel 110-168. Technical report, Gemeente Amsterdam Stadsarchief.

Gemeente Amsterdam (2021b). Sin0401 technisch advies light kademuur singel. Unpublished.

Gemeente Amsterdam (2021c). Toetskader Amsterdamse Kademuren 3.0. Unpublished - Concept V1.0 Gemeente Amsterdam TCVK-TAK3.0.

Hemel, M.-J., Korff, M., and Peters, D. J. (2022). Analytical model for laterally loaded pile groups in layered sloping soil. *Marine Structures*, 84:103229.

Hetényi, M. and Hetbenyi, M. I. (1946). *Beams on elastic foundation: theory with applications in the fields of civil and mechanical engineering*, volume 16. University of Michigan press Ann Arbor, MI.

Jaeger, Y. (2020). Levensduurverlengende maatregelen voor kademuurconstructies - een paalmatras en maaiveldverlaging als duurzame innovatieve levensduurverlengende maatregelen voor kademuurconstructies in de binnenstad van amsterdam. Master's thesis, Hanzehogeschool Groningen. In cooperation with Gemeente Amsterdam.

Korff, M. (2018). *Reader Deep Excavations*. Lecture material CIE4363 - TU Delft.

Korff, M., Hemel, M., and Esposito, R. (2021). Bezwijken grimburgwal: Leerpunten voor het Amsterdamse areaal. *Delft University of Technology*.

Korff, M., Hemel, M.-J., and Peters, D. J. (2022). Collapse of the grimburgwal, a historic quay in amsterdam, the netherlands. *Proceedings of the Institution of Civil Engineers-Forensic Engineering*, 40(XXXX):1–10.

Korff, M., Mair, R. J., and Van Tol, F. A. (2016). Pile-soil interaction and settlement effects induced by deep excavations. *Journal of Geotechnical and Geoenvironmental Engineering*, 142(8):04016034.

Kuiper, M., Peters, D., and Hemel, M. (2020). Proef kade overamstel voorbereidingsrapport. Unpublished - Draft report between TUDelft and AMS.

Ma, J., Berggren, B., Bengtsson, P.-E., Stille, H., and Hintze, S. (2006). Back analysis on a deep excavation in stockholm with finite element method. In *Proc. 6th European Conference on Numerical Methods in Geotechnical Engineering, Graz, Austria*, pages 423–429.

Mourillon, N. K., De Gijt, J., Bakker, K. J., Brassinga, H., and Broos, E. (2017). Stability analysis quay wall at the amazonehaven, port of rotterdam. In *MATEC Web of Conferences*, volume 138, page 06001. EDP Sciences.

Nebest Duikinspectie B.V. (2021a). Bepaling houtsoort en toestand funderingshout:SIN0401. Unpublished.

Nebest Duikinspectie B.V. (2021b). Houtmonstername en visuele inspectie fundering recht boomssloot: Rbs0101, kenmerk: Rbs0101 houtmonstername en visueleinspectiev1.1. Unpublished.

NEN (2017). NEN9997-1 Geotechnical design of structures.

NEN-EN-1912 (2012). Hout voor constructieve toepassingen sterkteklassen toewijzing van visuele sorteringsklassen en houtsoorten. *Technical Report*.

Roubos, A. (2019). *Enhancing reliability-based assessments of quay walls*. PhD thesis, Delft University of Technology. `https://doi.org/10.4233/uuid:40632b7a-970e-433d-9b4e-ff2d2249b156`.

Sas, F. (2006). De houten paalfundering doorgezaagd. Technical report, Tech. Rep. F3O.

SBRCURnet (2012). Handboek funderingsherstel op palen en op staal. *KCAF*.

SBRCURnet (2013). *Handbook of Quay walls - CUR211E*. CROW.

SBRCURnet (2014). *Binnenstedelijke kademuren*. CROW.

SkyGEO (2022). Wat is InSAR? `https://skygeo.com/nl/insar-monitoring/`. Accessed: 5-09-2022.

Sluis, J., Besseling, F., Stuurwold, P., and Lengkeek, A. (2013). Validation and application of the embedded pile row-feature in plaxis 2d. *Plaxis Bulletin*, 34:10–13.

Spannenburg, T. (2020). Timber creep of historic urban quay walls: The influence of timber creep on the assessment of inner-city quay walls. Master's thesis, TU Delft.

Vakili, K., Barciaga, T., Lavasan, A., and Schanz, T. (2013). A practical approach to constitutive models for the analysis of geotechnical problems. In *The Third International Symposium On Computational Geomechanics (ComGeo III), at Krakow, Poland*, volume 1, pages 738–749.

van Hulten, C. (2021). Recognizing critically damaged quay wall structures using a three-dimensional numerical model. Master's thesis, Delft University of Technology. http://resolver.tudelft.nl/uuid:1f59c348-1c14-43b4-881d-d4c81cffd65d.

Van Tilborg, R. (2016). Quay walls in urban areas: A method to predict the remaining life span. Master's thesis, Delft University of Technology. http://resolver.tudelft.nl/uuid:a6c3e595-b295-4106-b2c2-da12201c14e1.

Venmans, A. A., de Jong, J., Korff, M., Houtepen, M., et al. (2020). Reliability of insar satellite monitoring of buildings near inner city quay walls. *Proceedings of the International Association of Hydrological Sciences*, 382:195–199.

Voortman, R. (2021). The historic quay walls of amsterdam. Master's thesis, Delft University of Technology. http://resolver.tudelft.nl/uuid:a0fdfa81-9fbb-47cb-b5a0-4ca999ca8121.

Wang, Y. (2019). The impact of micro-tunnelling on adjacent pile foundations: Numerical modelling of micro-tunnel excavation in plaxis. *TU Delft*.

Waternet (2005). Stijghoogte 1e wvp agv-gebied, gemiddelde stijghoogte over het jaar 2005. https://www.planviewer.nl/imro/files/NL.IMRO.0363.E1701BPGST-VO01/b_NL.IMRO.0363.E1701BPGST-VO01_tb7.pdf. Accessed: 2022–10-20.

Waternet (2022). Peilbuizen Waternet. https://maps.waternet.nl/kaarten/peilbuizen.html. Accessed: 2022–10-20.

Wolfert, H. (2019). Innovation collabs for future-proof bridges and quay walls of amsterdam. https://www.ams-institute.org/news/innovation-collabs-future-proof-bridges-and-quay-walls-amsterdam/. Accessed: 2022–11-05.

Appendices

A

Additional Sensitivity Analysis

This appendix gives additional graphs and simulations from the sensitivity analysis to further support the inclination behaviour described in the main text.

A.1. Base model

The following output images, figure A.1, give more information about the behaviour of the soil and the wall tilt during the addition of the surcharge load. In Figure A.1a, the effective stress distribution along the interface between the masonry wall and the crossbeam is shown. It can be seen that due to the tension cut-off, no tension occurs (compression is negative). This stress distribution shows the area of the wall that is still in contact with the crossbeam, over which the wall tilts.

In figure A.1b, the development of a shear strain zone behind the wall is depicted. This zone shows a potential sliding or failure plane of the quay structure during the accumulation of the surcharge load.

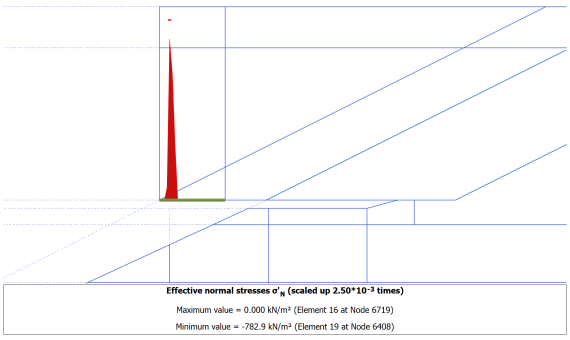

(a) Effective stress development near between the wall and the crossbeam, no tension occurs due to the tension cut-off, meaning the wall tips over along the shown stress zone

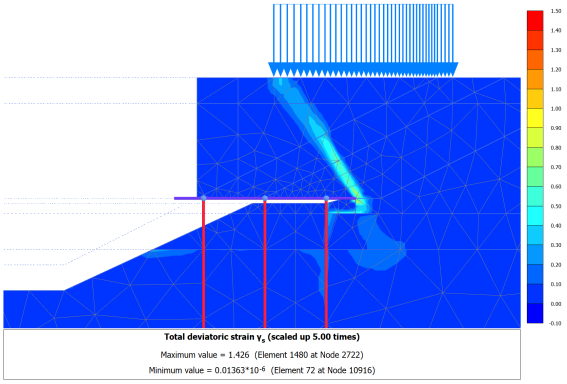

(b) Deviatoric strain along the quay wall structure

Figure A.1: PLAXIS output of the base model for the effective stress and strain

A.1.1. Front pile row removal

In figure A.2 the output is shown when the front pile row is completely removed from the base model. This situation could represent a broken pile or a failed connection between the pile and the floor. In this phase, the bending moments in the second and third pile are exceeding their capacities. Therefore, the maximum wall tilt value is not very representative for the real-life situation. It does show that the front pile row has an important effect on the amount of tilt of the masonry wall.

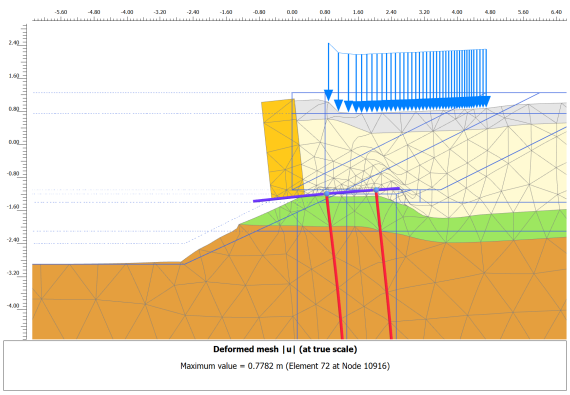

(a) PLAXIS wall displacement plot which shows the inclined masonry wall

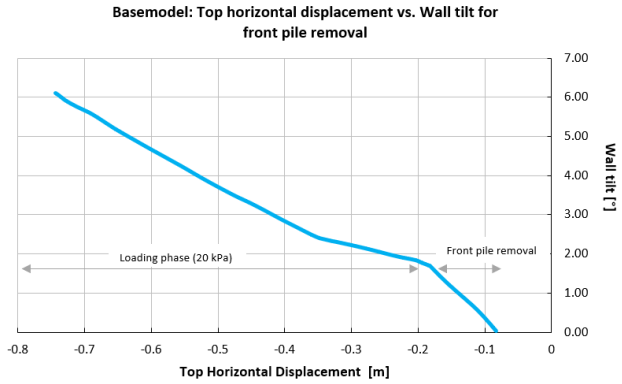

(b) Maximum wall tilt against the horizontal wall displacement during the pile row removal phase and the succeeding loading phase

Figure A.2: PLAXIS output of the base model during the removal of the front pile row

A.2. Pile-floor connection effect

For the connection between the piles and the floor, a hinge connection with a spring constant is used. A higher value of this spring constant results in a more fixed connection. Figure A.3 shows that changing the connection to a more hinged connection, it decreases the wall tilt and increases the horizontal displacement. A more fixed/rigid connection gives higher maximum wall tilt (more bending moments at the tip of the pile) and lower horizontal wall displacement.

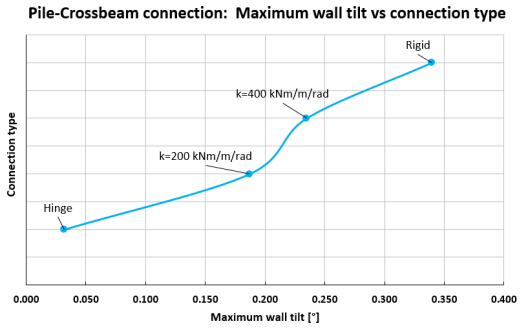

(a) Effect of on the maximum wall tilt for different pile-floor connections

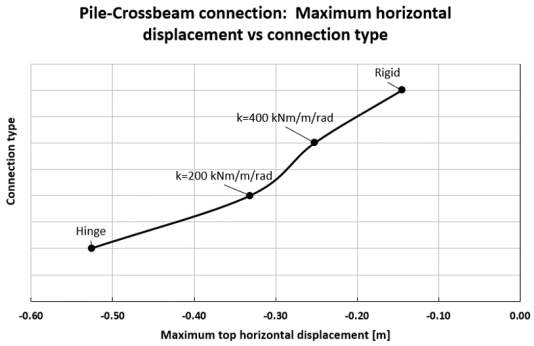

(b) Effect of on the maximum wall horizontal displacement for different pile-floor connections

Figure A.3: Connection type behaviour after the loading phase (20 kPa)

A.3. Elastic behaviour in the piles

The material model in the embedded beam rows is modelled as elastic. In reality there is a maximum and minimum bending capacity for each pile. This bending capacity for C24 wood is 24 kN m/m. In order to check if this capacity has been exceeded in the loading phase, the development of the bending moment is plotted, figure A.4. In these plots can be seen at which surcharge load value the bending capacity is exceeded.

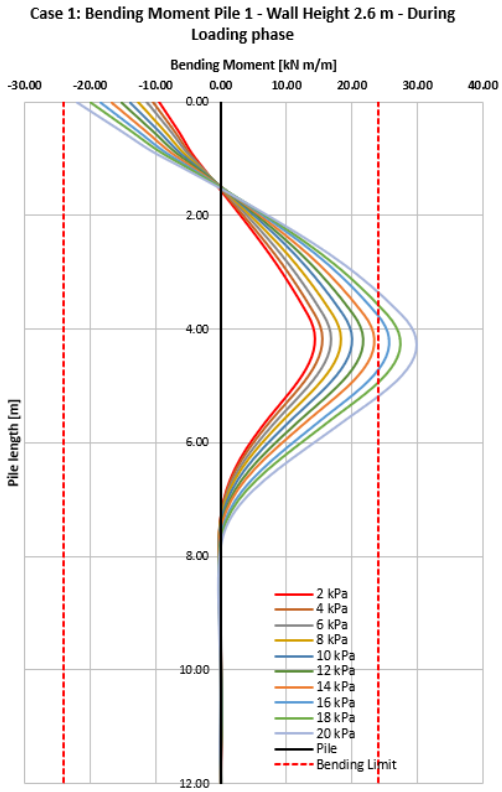

(a) Bending moment development in the front pile during loading, wall height 2.6 meters

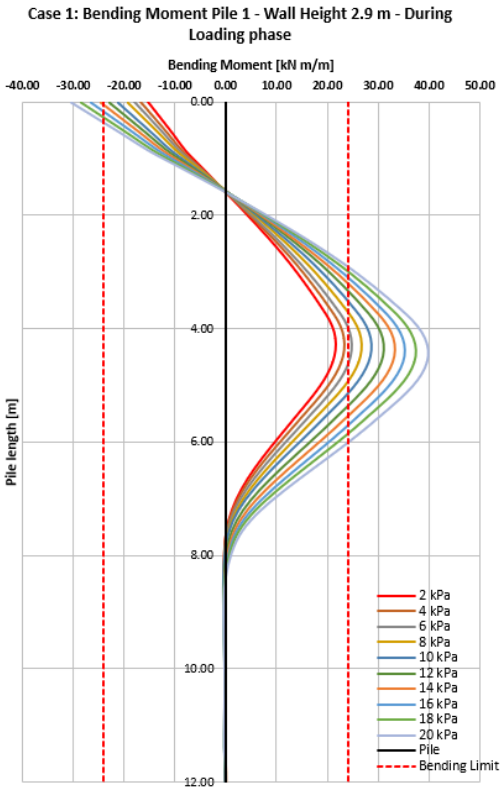

(b) Bending moment development in the front pile during loading, wall height 2.9 meters

Figure A.4: Elastic bending moment development in the front piles during the surcharge loading phase, case 1. When the amount of surcharge loads exceeds the bending capacity, the pile breaks

A.3.1. Elastoplastic behaviour in the piles

The material model in the embedded beam rows can also be modelled as elastoplastic. This allows to set the bending capacity in the piles. This material model has not been used in the analysis since the running time is very long and only plotting the behaviour until failure is the most useful. Setting the piles to elastoplastic results in the same linear behaviour between the horizontal displacement and the wall tilt until a certain surcharge load value, after that, the wall tilt becomes nearly constant, and the wall only displaces horizontally, figure A.5.

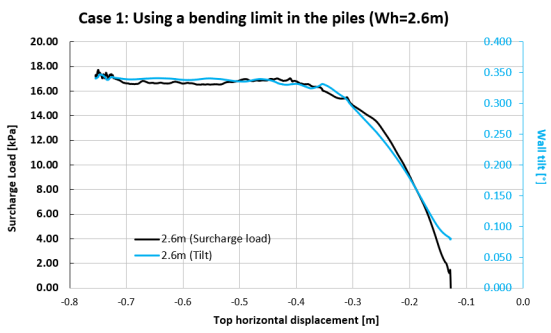

(a) Quay wall behaviour using a bending capacity of 24 kPa in the piles, for a wall height of 2.6 meters

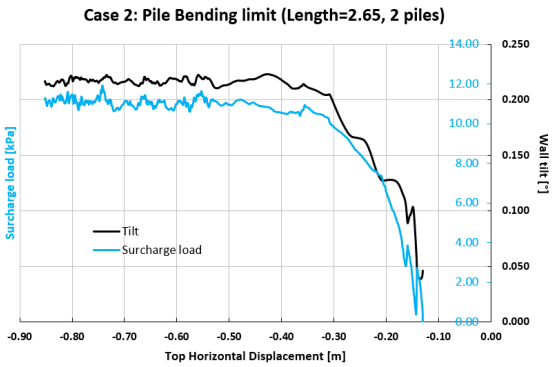

(b) Quay wall behaviour using a bending capacity of 24 kPa in the piles, for a crossbeam length of 2.65 meters with two piles

Figure A.5: Inclination and displacement behaviour using elastoplastic behaviour with a bending capacity of 24 kPa in the wooden piles

A.4. Case 1: Wall Height

In the sensitivity analysis for the wall height, the quay wall fell over at a height of 3.2 meters (or a (W_h/W_t) ratio of 4.0). In that section only a small part of that full curve has been shown. In figure A.6 the entire development of this curve during failure is shown. These graphs indicate that at a certain surcharge load, the tilt rapidly increases, and the horizontal displacement approaches a constant value, indicating that the wall falls over.

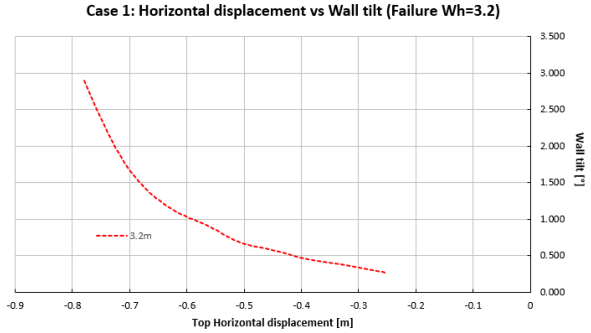

(a) Wall tilt versus the horizontal displacement for a wall height of 3.2 meters, (W_h/W_t) ratio of 4.0, indicating failure

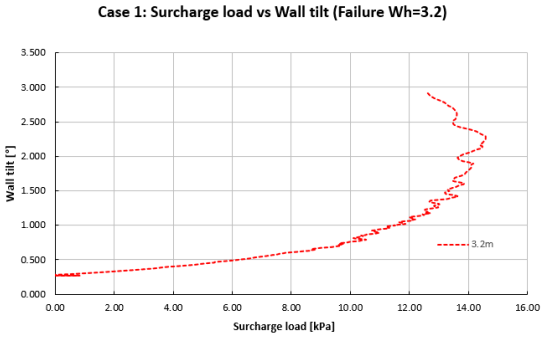

(b) Wall tilt versus the surcharge load for a wall height of 3.2 meters, (W_h/W_t) ratio of 4.0, indicating failure

Figure A.6: Wall tilt development curves for a wall height 3.2 meters, (W_h/W_t) ratio of 4.0, indicating failure

A.5. Case 3: Canal Depth

During shallow canal depths, the strain development in the soil begins to show a circular sliding plane exceeding the general stability, this tends to tilt the structure towards the street (negative tilt), figure A.7.

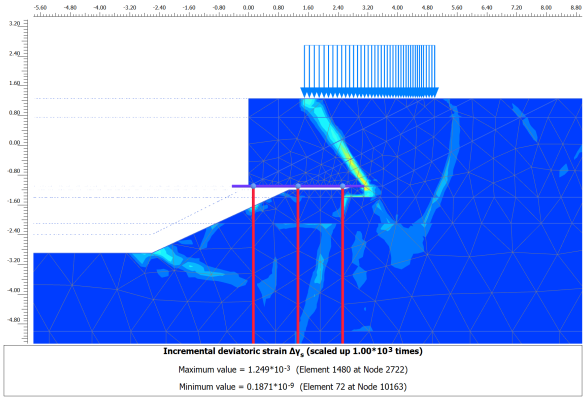

Figure A.7: Incremental deviatoric strain development during loading, canal depth -2.4 meters

A.6. Case 5: Normal Stress distribution underneath the wall

By reducing the wall thickness, the wall rotates on the wooden floor, initiating the wall tilt. For a thin wall, the tilt is high, the wall rotates at the edge of the masonry wall and the compression normal stress is high, figure A.8. For a thicker wall, this compression zone is wider, more centered underneath the wall and results in lower normal stresses, which gives less wall tilt.

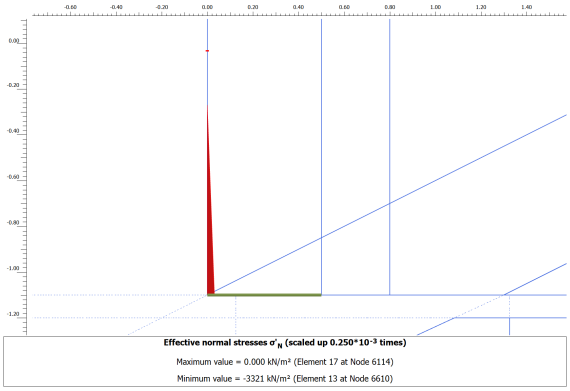

(a) Smaller stress area, indication of a higher wall rotation around this zone for a 0.5 meters thin wall

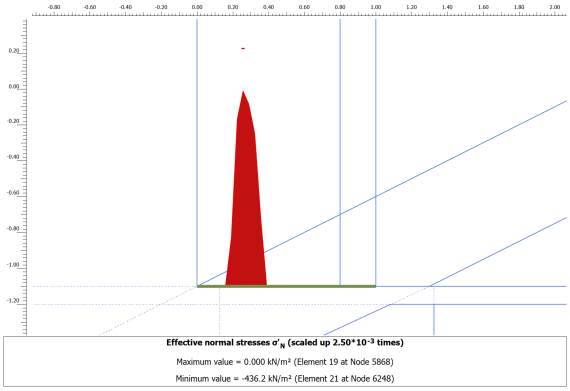

(b) Wider stress area, indication of a lower wall rotation around this zone for 1 meters thick wall

Figure A.8: Normal effective stress distribution underneath the wall, indicating the wall rotation zone

B

Additional Case-Study Analysis

This appendix gives additional graphs and simulations from the case-study to further support the inclination behaviour described in the main text.

B.1. Inclination behaviour case-study SIN0401

Figure B.1 shows the behaviour of the wall tilt and horizontal wall displacement during the construction of the quay wall. In this case, a higher parking load is applied (10 kPa). This results in more wall tilt during the accumulation of this parking load and therefore a higher maximum wall inclination after applying the traffic loads.

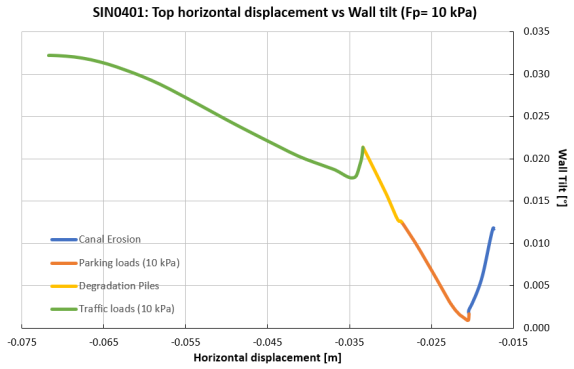

(a) Wall tilt against the horizontal top wall displacement for SIN0401

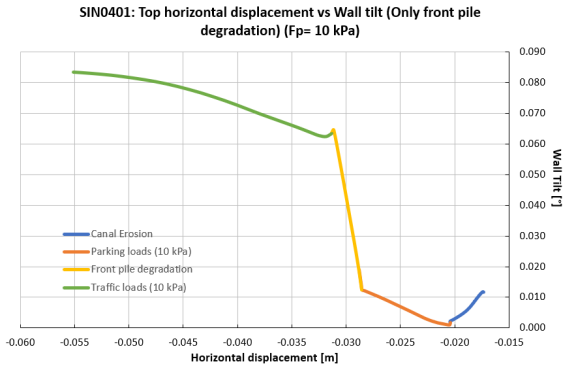

(b) Wall tilt against the horizontal top wall displacement for SIN0401, where only the front pile is degraded

Figure B.1: Inclination graphs for the quay wall: SIN0401 with a parking load of 10 kPa

B.2. SIN0401 Structural output images

In this section additional output images for the SIN0401 quay wall are presented, these are the bending moments and displacements in the piles and in the crossbeam.

In figure B.2 the maximum bending moments in the piles are shown after the addition of the traffic load. It can be seen that for degraded piles the bending moments are lower. The capacity is not exceeded due to the stable distribution underneath the floor and low surcharge loads.

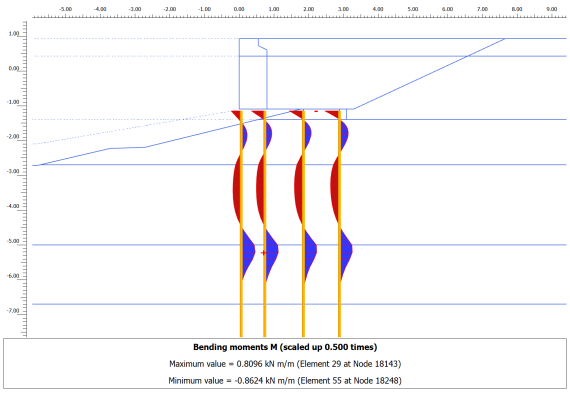

(a) Bending moment distribution, all piles degraded

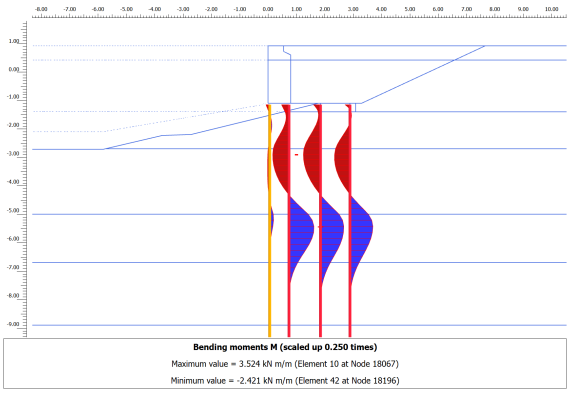

(b) Bending moment distribution, only front pile degraded

Figure B.2: Bending moment distribution for SIN0401

In figure B.3a can be seen that the piles all move with the same magnitude left and down, giving a small tilt in the piles. In figure B.3b can be seen that with one degraded pile, the displacement angle in the piles is steeper, resulting in more wall inclination. The result of this effect in the piles is seen in figure B.4, in the crossbeam. A steeper angle of the crossbeam underneath the masonry wall is created when only the front pile diameter is reduced.

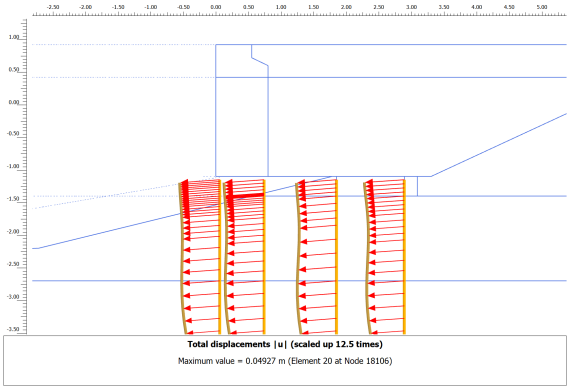

(a) Pile displacement, all piles degraded

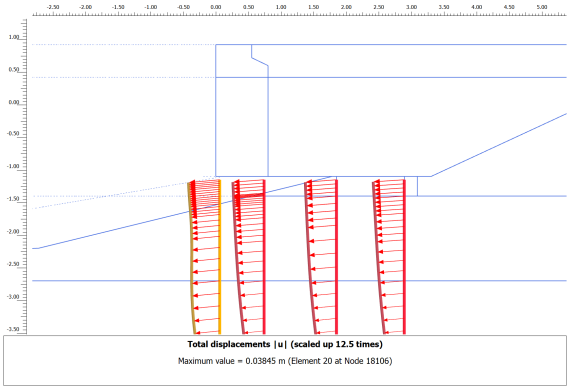

(b) Pile displacement, only front pile degraded

Figure B.3: Pile displacement for SIN0401

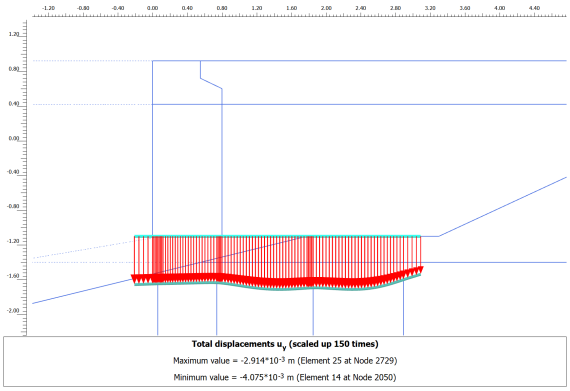

(a) Crossbeam vertical displacement, all piles degraded

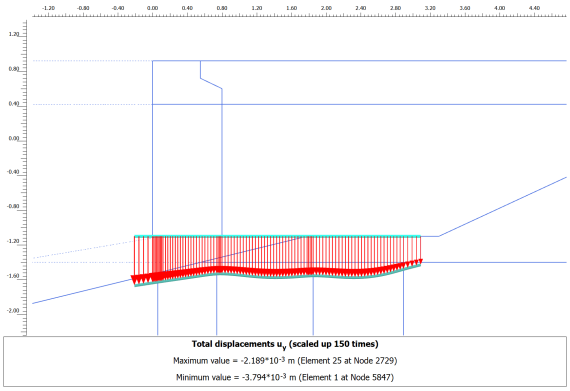

(b) Crossbeam vertical displacement, only front pile degraded

Figure B.4: Crossbeam vertical displacement for SIN0401

The distribution of the normal stress in the interface between the masonry wall and the crossbeam is shown in figure B.5. The compressive stress is low compared to the base model and the sensitivity analysis. Moreover, the stress zone is very wide, almost the entire width of the masonry wall, which indicates that it does not rotate independently from the crossbeam, and the inclination is mainly due to the bending of this crossbeam, so low wall tilt values are expected.

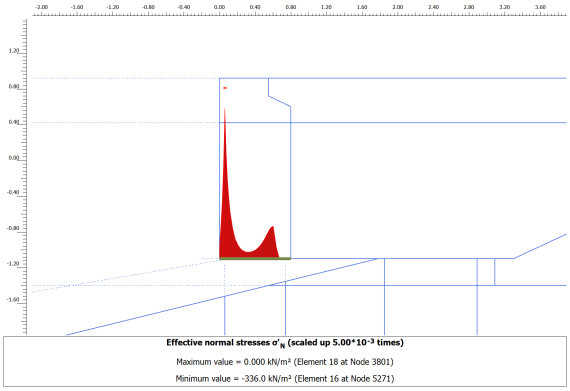

(a) Normal stress distribution underneath the wall, all piles degraded

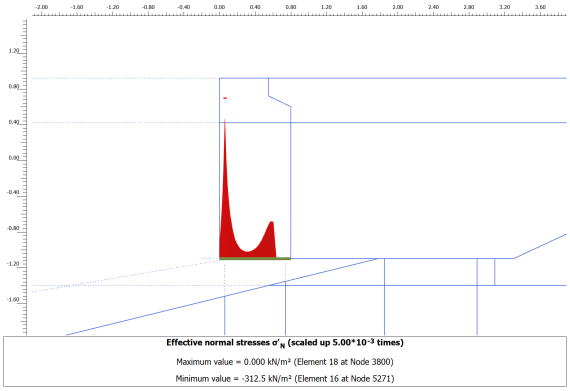

(b) Normal stress distribution underneath the wall, only front pile degraded

Figure B.5: Normal stress distribution underneath the wall for SIN0401, indication of the area of rotation, no tension occurs

B.3. SIN0401 Prescribed wall displacement

An extra prescribed wall displacement is introduced in the case-study. In figure B.6, a situation is created where a horizontal force is pulling at the front of the quay wall or pushing behind the quay wall. This force could be due to damage in the masonry wall, tree and wind loads or mooring forces. A displacement of -22.5 cm gives a wall tilt around 5 degrees, which is measured in reality. Figure B.8 shows that in this case the wall rotates freely on the crossbeam.

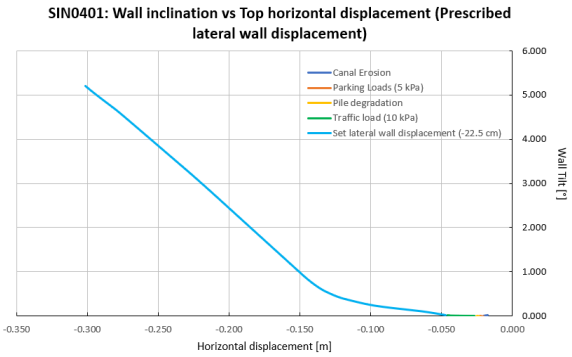

(a) Wall tilt against the horizontal top wall displacement for SIN0401 with the prescribed wall displacement

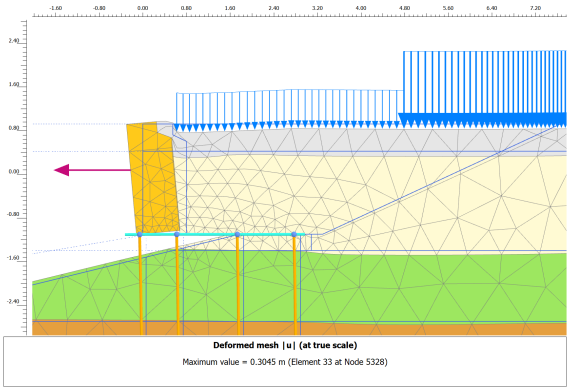

(b) Quay wall displacement with the prescribed wall displacement

Figure B.6: Quay wall tilt and displacement with the prescribed wall displacement of -22.5 cm

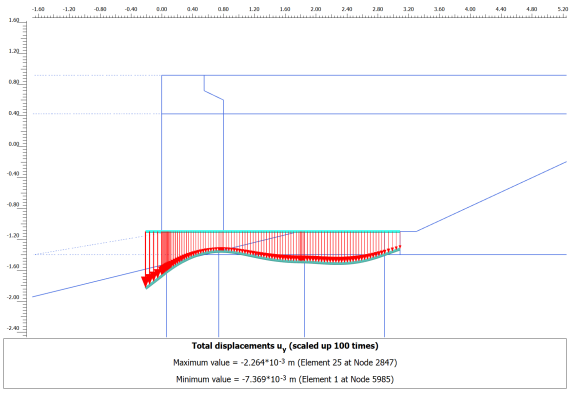

(a) Total vertical crossbeam displacement

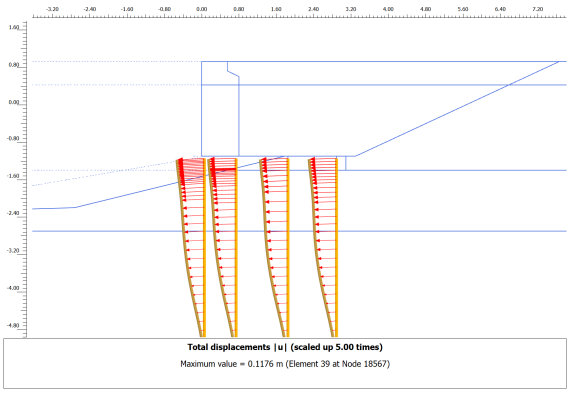

(b) Total pile displacement

Figure B.7: Quay wall pile and crossbeam displacement with the prescribed pile displacement of -22.5 cm

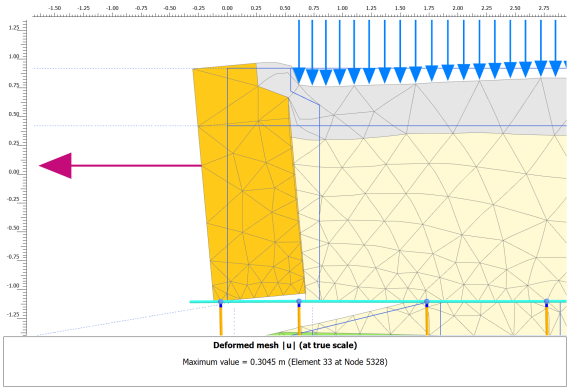

(a) Quay wall displacement with the prescribed wall displacement, close-up indicating the tilt

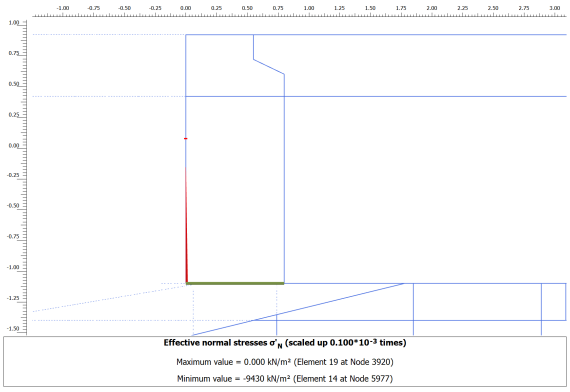

(b) Total normal stress distribution in underneath the wall, indication the contact area

Figure B.8: Tilting behaviour of the wall with prescribed wall displacement of -22.5 cm, no tension occurs

B.3.1. Prescribed displacement until failure

By adding a vertical displacement of -20 cm in the front pile, the wall tilts towards an angle of 17 degrees. In figure B.9 can be seen that this creates an unrealistic situation where the wall will fall over. Additionally, the bending moments in the piles and crossbeam are exceeded. However, this is expected because the displacement is simulated due to the damage observed in the diving inspections.

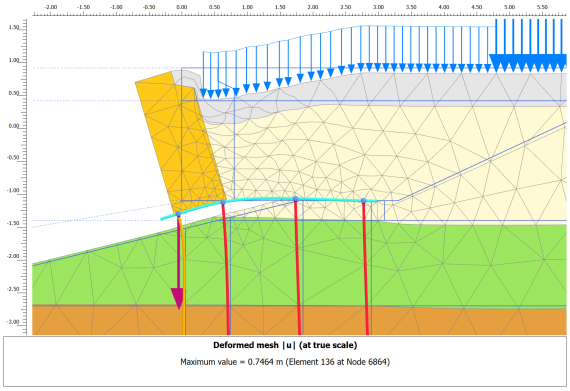

(a) Wall displacement

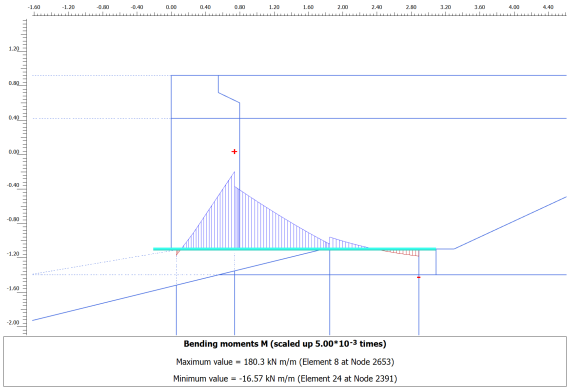

(b) Crossbeam bending moments

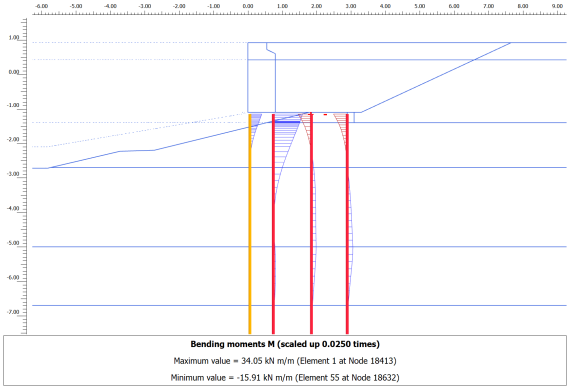

(c) Pile bending moments

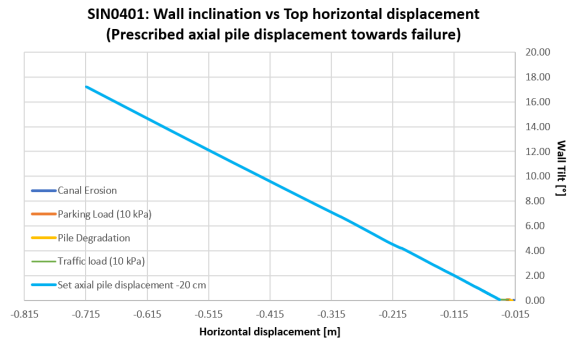

(d) Wall tilt against the horizontal wall displacement

Figure B.9: Prescribed displacement of -20 cm, where the wall will fall over at 17 degrees

C

Input parameters and calculations

This appendix gives the source of some input parameters and the detailed calculations made for the implementation into PLAXIS 2D.

C.1. Characteristic soil parameters

Using table 2b from the NEN9997 (figure C.1), the soil parameters are evaluated based on the findings by Frankenmolen (2006). This table shows the characteristic soil parameters used for geotechnical purposes.

Grondsoort			Karakteristieke waarde[a] van grondeigenschap																					
Hoofd-naam	Bijmengsel	Consis-tentie [b]	γ [c] kN/m³		γ_{sat} kN/m³		q_c [d] [g] MPa		C'_p [g]		C'_s		$C_c/(1+e_0)$ [g] [-]		C_α [f] [-]		$C_{sw}/(1+e_0)$ [g] [-]		E_{100} [g] [h] MPa		φ' [g] Graden		c' kPa		c_u kPa	
Grind	Zwak siltig	Los	17		19		15		500		∞		0,0046		0		0,0015		45		32,5		0			
		Matig	18		20		25		1000		∞		0,0023		0		0,0008		75		35,0		0		n.v.t.	
		Vast	19	20	21	22	30		1200	1400	∞		0,0019	0,0016	0		0,0006	0,0005	90	105	37,5	40,0	0			
	Sterk siltig	Los	18		20		10		400		∞		0,0058		0		0,0019		30		30,0		0			
		Matig	19		21		15		600		∞		0,0038		0		0,0013		45		32,5		0		n.v.t.	
		Vast	20	21	22	22,5	25		1000	1500	∞		0,0023	0,0015	0		0,0008	0,0005	75	110	35,0	40,0	0			
Zand	Schoon	Los	17		19		5		200		∞		0,0115		0		0,0038		15		30,0		0			
		Matig	18		20		15		600		∞		0,0038		0		0,0013		45		32,5		0		n.v.t.	
		Vast	19	20	21	22	25		1000	1500	∞		0,0023	0,0015	0		0,0008	0,0005	75	110	35,0	40,0	0			
	Zwak siltig, kleiig		18	19	20	21	12		450	650	∞		0,0051	0,0035	0		0,0017	0,0012	35	50	27,0	32,5	0		n.v.t.	
	Sterk siltig, kleiig		18	19	20	21	8		200	400	∞		0,0115	0,0058	0		0,0038	0,0019	15	30	25,0	30,0	0		n.v.t.	
Leem [e]	Zwak zandig	Slap	19		19		1		25		650		0,0920		0,0037		0,0307		2		27,5	30,0	0		50	
		Matig	20		20		2		45		1300		0,0511		0,0020		0,0170		3		27,5	32,5	1		100	
		Vast	21	22	21	22	3		70	100	1900	2500	0,0329	0,0230	0,0013	0,0009	0,0110	0,0077	5	7	27,5	35,0	2,5	3,8	200	300
	Sterk zandig		19	20	19	20	2		45	70	1300	2000	0,0511	0,0329	0,0020	0,0013	0,0170	0,0110	3	5	27,5	35,0	0	1	50	100
Klei	Schoon	Slap	14		14		0,5		7		80		0,3286		0,0131		0,1095		1		17,5		0		25	
		Matig	17		17		1,0		15		160		0,1533		0,0061		0,0511		2		17,5		5		50	
		Vast	19	20	19	20	2,0		25	30	320	500	0,0920	0,0767	0,0037	0,0031	0,0307	0,0256	4	10	17,5	25,0	13	15	100	200
	Zwak zandig	Slap	15		15		0,7		10		110		0,2300		0,0092		0,0767		1,5		22,5		0		40	
		Matig	18		18		1,5		20		240		0,1150		0,0046		0,0383		3		22,5		5		80	
		Vast	20	21	20	21	2,5		30	50	400	600	0,0767	0,0460	0,0031	0,0018	0,0256	0,0153	5	10	22,5	27,5	13	15	120	170
	Sterk zandig	-	18	20	18	20	1,0		25	140	320	1680	0,0920	0,0164	0,0037	0,0007	0,0307	0,0055	2	5	27,5	32,5	0	1	0	10
	Organisch	Slap	13		13		0,2		7,5		30		0,3067		0,0153		0,1022		0,5		15,0		0	1	10	
		Matig	15	16	15	16	0,5		10	15	40	60	0,2300	0,1533	0,0115	0,0077	0,0767	0,0511	1,0	2,0	15,0		0	1	25	30
Veen	Niet voorbelast	Slap	10	12	10	12	0,1		5	7,5	20	30	0,4600	0,3067	0,0230	0,0153	0,1533	0,1022	0,2	0,5	15,0		1	2,5	10	20
	Matig voorbelast	Matig	12	13	12	13	0,2		7,5	10	30	40	0,3067	0,2300	0,0153	0,0115	0,1022	0,0767	0,5	1,0	15,0		2,5	5	20	30
Variatiecoëfficiënt v			0,05				–		0,25										0,10				0,20			

Figure C.1: General soil parameters, table2b NEN9997 (NEN, 2017)

C.2. Characteristic timber parameters

The table in figure C.2, helps to gain insight into the properties for the wooden piles and the wooden crossbeam, namely their bending capacity, density and young's modulus.

Karakteristieke eigenschappen en sterkteklassen van gezaagd naaldhout													
Eigenschap	**C14**	**C16**	**C18**	**C20**	**C22**	**C24**	**C27**	**C30**	**C35**	**C40**	**C45**	**C50**	**Eenheid**
$f_{m,k}$	14	16	18	20	22	24	27	30	35	40	45	50	N/mm^2
$E_{0,mean}$	7	8	9	9,5	10	11	11,5	12	13	14	15	16	kN/mm^2
ρ_{mean}	350	370	380	400	410	420	430	460	470	480	520	520	kg/m^3
ρ_k	290	310	320	330	340	350	360	380	390	400	440	430	kg/m^3
$f_{t,0,k}$	7,2	8,5	10	11,5	13	14,5	16,5	19	22,5	26	30	33,5	N/mm^2
$f_{t,90,k}$	0,4	0,4	0,4	0,4	0,4	0,4	0,4	0,4	0,4	0,4	0,4	0,4	N/mm^2
$f_{c,0,k}$	16	17	18	19	20	21	22	24	25	27	29	30	N/mm^2
$f_{c,90,k}$	2,0	2,2	2,2	2,3	2,4	2,5	2,5	2,7	2,7	2,8	2,9	3,0	N/mm^2
$f_{v,k}$	3,0	3,2	3,4	3,6	3,8	4,0	4,0	4,0	4,0	4,0	4,0	4,0	N/mm^2
$E_{0,05}$	4,7	5,4	6,0	6,4	6,7	7,4	7,7	8,0	8,7	9,4	10,1	10,7	kN/mm^2
$E_{90,mean}$	0,23	0,27	0,30	0,32	0,33	0,37	0,38	0,40	0,43	0,47	0,50	0,53	kN/mm^2
G_{mean}	0,44	0,50	0,56	0,59	0,63	0,69	0,72	0,75	0,81	0,88	0,94	1,00	kN/mm^2
$G_{0,05}$	0,29	0,34	0,38	0,40	0,42	0,46	0,48	0,50	0,54	0,59	0,63	0,67	kN/mm^2
Tabel 1. Karakteristieke eigenschappen en sterkteklassen van gezaagd naaldhout													

Figure C.2: Timber material properties. (NEN-EN-1912, 2012)

C.3. Axial/lateral resistance

The calculations for the axial and lateral resistances in the piles are done in Excel, figure C.3, with a template from Arcadis. This is done for the base model and the case-study. It also calculates the degraded pile diameter and moment of inertia based on the pile tapering values.

Axial, Lateral and base resistance (Arcadis)
SIN0401

Houten palen

Jaar van inspectie	2022	-
Gemiddelde aantasting tijdens inspectie	54	mm/zijde
Tapsheid	8.6	mm/m1
Paalkopniveau	-1.15	m NAP
Inklemmingsniveau	-7.2	m NAP
Paalpuntniveau	-13.2	m NAP
Lengte paal	12.05	m
alpha s	0.012	-
qc;z;a	1.00E+04	[kN/m2]

	Oorspronkelijk	
	0	2022
D_kop [m]	0.203	0.095
D_voet [m]	0.099	0.045
D_gem [m]	0.151	0.070
A_gem [m2]	1.795E-02	3.869E-03
I_gem [m4]	2.565E-05	1.191E-06
D_inklemming [m]	0.151	0.070
D_gem_boven_inklemming [m]	0.177	0.083
A_gem_boven_inklemming [m2]	2.460E-02	5.351E-03
I_gem_boven_inklemming [m4]	4.816E-05	2.279E-06
Relatieve capaciteit paal [%]	100%	5%
O_voet [m]	0.312	
T_skin_voet [kN/m]	37.5	
Axial skin resistance table	[0, 0, -1.16, 0, -1.15, 37.5, 12.05, 37.5]	

Maximale laterale weerstand (Brinch Hansen)

Nummer	Geologische naam	Omschrijving	gdr [kN/m3]	gnat [kN/m3]	phi'-kar. [grad]	c'-kar. [kPa]	b.k. laag [m NAP]	o.k. laag [m NAP]	σ-vert (b.k [kPa]	P (b.k. laag) [kPa]	σ'-vert (b [kPa]	Diameter p [m]	Kq0 [-]
GWS							-0.40						
01A	Ophoogzand	Zand, los	17.0	19.0	30	0.1	-1.15	-1.4	7.5	7.5	0.0	0.203	4.8
07A	Geulse klei	Humeuse klei (klei, slap)	13.9	13.9	20	7.1	-1.4	-2.1	12.3	10.0	2.3	0.201	2.3
08	Hollandveen	Veen, slap	10.5	10.5	18	3.6	-2.1	-5	22.0	17.0	5.0	0.195	1.9
09	Oude Zeeklei	Klei, matig	16.5	16.5	26	5.0	-5	-6.7	52.4	46.0	6.4	0.170	3.4
10	Wadzand	Zand, sterk siltig, kleiig	17.9	17.9	27	1.4	-6.7	-8.9	80.5	63.0	17.5	0.155	3.8
11	Hydrobiaklei	Klei, matig	15.2	15.2	27	5.7	-8.9	-12.3	119.9	85.0	34.9	0.136	3.8
12	Basisveen	Veen, matig	11.7	11.7	18	4.3	-12.3	-12.3	171.5	119.0	52.5	0.107	1.95
13	1e zandlaag	Zand, matig	16.6	19.7	33	0.1	-12.3	-13.2	171.5	119.0	52.5	0.107	6
							-13.2		189.3	128.0	61.3	0.099	

Kq-oneind. [-]	Kc0 [-]	Kc-oneind. [-]	K0 [-]	αq [-]	αc [-]	Kq (b.k. la	Kc (b.k. la	σ'p (b.k. la	σ'p (b.k. l	Kq (o.k. laag) [-]	Kc (o.k. l [-]	σ'p (o.k. laa [kPa]	σ'p (o.k. l [kN/m]
17.7	7	61.3	0.50	0.11	0.22	9.68	37.33	4	1	10.32	40	27	5
5.9	4.7	24.5	0.66	0.18	0.39	4.28	19.16	146	29	4.66	21	170	33
4.5	4.3	20.6	0.69	0.19	0.43	3.66	17.69	81	16	4.11	19	95	16
11.5	5.8	40	0.56	0.12	0.29	9.73	36.39	243	41	10.21	37	365	57
12.3	6	43	0.55	0.13	0.28	11.01	40.14	250	39	11.40	41	456	62
12.3	6	43	0.55	0.13	0.28	11.40	41.06	631	86	11.77	42	856	92
4.7	4.4	21	0.69	0.19	0.43	4.58	20.67	329	35	4.58	21	329	35
27	8.1	88	0.46	0.08	0.18	24.95	84.28	1319	141				

Afstand vanaf paalkop [m]	Laterale weerstand p [kN/m]
0	1
0.25	5
0.25	29
0.95	33
0.95	16
3.85	16
3.85	41
5.55	57
5.55	39
7.75	62
7.75	86
11.15	92
11.15	35
11.15	35
11.15	141
12.05	141

Figure C.3: Excel sheet with axial and lateral resistance calculations, both for the base model and SIN0401

C.4. SIN0401 geometry calculations

The detailed geometry values and calculations have been done based on available archive documents and visual inspections. The calculations are done in Excel and an overview of all the dimensions and the results from the diving inspections towards the pile diameters is shown in figure C.4.

Dimensions SIN0401

Crossbeam Initial

	Value	Unit	Source
In front of wall	**0.21**	m	Diving Inspection
Length	**3.26**	m	Sketch
Thickness	**0.2**	m	Archive
Width	**0.25**	m	Archive
Area	5.00E-02	m^2	
Intertia	1.67E-04	m^4	
EI	1.83E+03	kNm^2/m	
EA	5.50E+05	kN/m^2	
E	11000000	kN/m^2	Standard value
Amount	7		Archive

Masonry wall

	Value	Unit	Source
Height (with top)	**2.02**	m	ANH, Sketch
Height (without top)	**1.82**	m	ANH, Sketch
Height (underwater)	**0.74**	m	Diving Inspection
Thickness (bottom)	**0.84**	m	Diving inspection and TAK
Thickness (top)	**0.51**	m	Diving Inspection
Height cut	**0.175**	m	Sketch

Piles

			Source
3D h.t.h	**1.00**	m	Diving inspection
Start naar 1	**0.210**	m	Diving inspection
1 naar 2	**0.74**	m	Archive Sketch
2 naar 3	**1.07**	m	Archive Sketch
3 naar 4	**1.04**	m	Archive Sketch
4 naar eind	**0.20**	m	Archive Sketch
Amount of piles	28.00		Archive
Piles per crossbeams	**4**		Archive
Diameter (taps)	**0.177**	m	Na Tapsheid, Archive
A	0.024682067	m^2	
I	4.8479E-05	m^4	

Surface/canal profile

	Value	Unit	Source
Street level	**0.88**	m NAP+	AHN, average
Waterstand	-0.4	m NAP-	Monitoring well
Grondwaterstand	-0.45	m NAP-	Monitoring well
Diepte kesp	-1.11	m NAP-	Point cloud, diving inspection
Pijlhoogte zandlaag	-2.15	m NAP-	Isomap
Dredge margin	0.5	m	TAK

Load

	Value	Unit	Source
Parking load	5	kPa	TAK, CUR
Parking load distance	4	m	Google maps
Traffic load	10	kPa	TAK, CUR
Traffic load distance	4.2	m	Google maps

Degradation

Crossbeam	**Value**	**Source**
Thickness	**0.13**	Diving inspection
Width	**0.19**	Diving inspection
EA	2.717E+05	
EI	3.826E+02	
I	3.47858E-05	
A	0.0247	
E	11000000	

Piles	**Value**	**Source**
Diameter	**0.08150**	Diving inspection, average, Na tapsheid
A	0.024682067	0.005216913
I	2.16579E-06	

Diving Inspection SIN0401 (Construction B)

Piles	Diameter original [[mm]		Degraded (ra	Degraded total [mm]	Intact diameter [mm]
P.153	0.2	200	71	142	58
P.163	0.15	150	49	98	52
P.174	0.2	200	71	142	58
P.197	0.21	210	61	122	88
P.112	0.205	205	51	102	103
P.122	0.17	170	51	102	68
P.132	0.21	210	38	76	134
P.147	0.18	180	25	50	130
P.161	0.23	230	65	130	100
P.280	0.24	240	54	108	132
P.297	0.24	240	62	124	116
Average	0.203	m			**94.45454545** mm
					0.0945 m

Figure C.4: Excel sheet with the geometry calculations and values for SIN0401

C.5. SIN0401 Diving inspections

The analysis towards the pile degradation is done based on diving inspections and measuring the intact pile diameter. Figure C.5a, shows a typical result of a degraded pile. In this case, it can be seen that the light green material is still intact, the dark green part has been degraded. The current underwater canal profile is scanned using a multibeam echosounder, figure C.5b. This profile is recreated in PLAXIS to make the SIN0401 model.

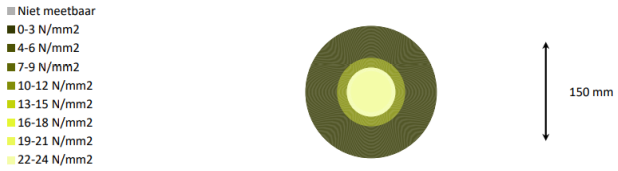

(a) One of the degraded piles according to the diving inspection of the front pile of the SIN0401 quay wall

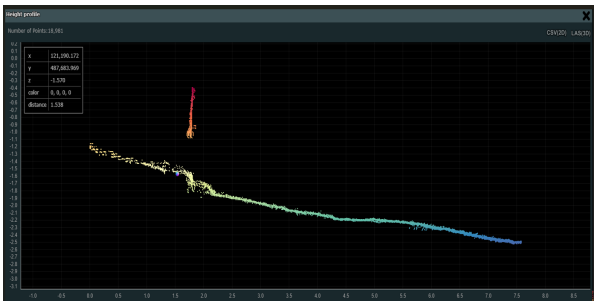

(b) Underwater canal profile, done with a multibeam echosounder

Figure C.5: Diving inspection and 3D point cloud - SIN0401

C.6. SIN0401 CPT

The following CPT is obtained from Dinoloket, near the Singel quay wall. The soil profile obtained from this CPT almost similar to the soil profile used in the base model. Figure C.6 also shows the depth of the second sand layer, at 20 meters depth. This layer is not taken into account in the PLAXIS models.

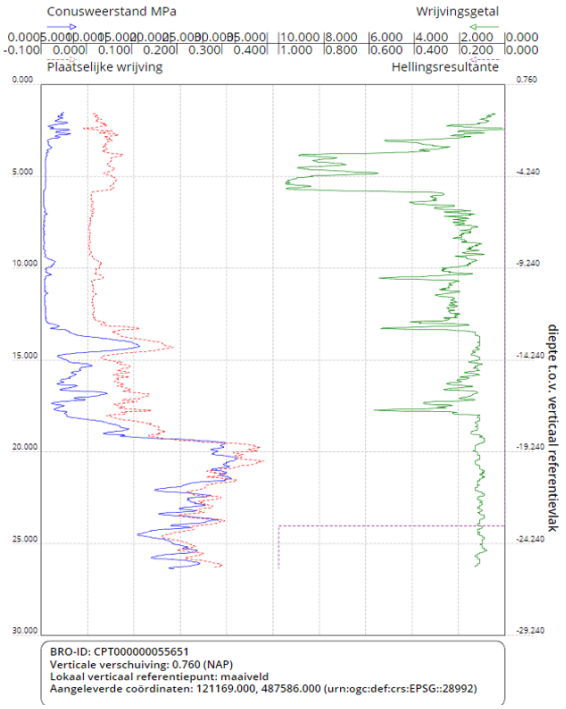

Figure C.6: CPT near SIN0401 (DINOloket, 2022a)


TU Delft
Delft
University of
Technology

ALTHEN
SENSORS & CONTROLS

ARCADIS